Accepted for publication in *Nature* published by Springer Nature.

Accurate compound-specific ^{14}C dating of archaeological pottery vessels

Emmanuelle Casanova[1], Timothy D.J. Knowles[1,2], Alex Bayliss[3,4], Julie Dunne[1], Marek Z. Barański[5], Anthony Denaire[6], Philippe Lefranc[7], Savino di Lernia[8,9], Mélanie Roffet-Salque[1], Jessica Smyth[1,10], Alistair Barclay[11], Toby Gillard[1], Erich Claβen[12], Bryony Coles[13], Michael Ilett[14], Christian Jeunesse[15], Marta Krueger[16], Arkadiusz Marciniak[16], Steve Minnitt[17], Rocco Rotunno[8], Pieter van de Velde[18], Ivo van Wijk[19], Jonathan Cotton[20], Andy Daykin[20] and Richard P. Evershed[1,2]

[1]Organic Geochemistry unit, School of chemistry, University of Bristol, Cantock's Close Bristol BS8 1TS, UK

[2] Bristol Radiocarbon Accelerator Mass Spectrometer, 43 Woodland Road, University of Bristol, Bristol BS8 1UU, UK

[3]Scientific Dating, Historic England, Cannon Bridge House, 25 Dowgate Hill, London, EC4R 2YA, UK

[4]Biological & Environmental Sciences, University of Stirling, FK9 4LA, Stirling, UK

[5]Academy of Fine Arts in Gdańsk, Faculty of Architecture and Design, ul. Targ Węglowy 6, Gdańsk, Poland

[6]University of Burgundy/UMR 6298 ARTEHIS, Bâtiment Sciences Gabriel, 6 Boulevard Gabriel, 21000 Dijon, France

[7]University of Strasbourg UMR 7044/INRAP, 10 rue Altkirch, 67100 Strasbourg, France

[8]Dipartimento di Scienze dell'Antichità, Sapienza, Università di Roma, Via dei Volsci, 122 – 00185 Roma, Italy

[9]GAES, University of the Witwatersrand, Johannesburg, South Africa

[10]School of Archaeology, University College Dublin, Belfield, D04F6X4, Ireland

[11]Cotswold Archaeology, Building 11, Keble Enterprise Park, Kemble, Cirencester GL7 6BQ, UK

[12]LVR-State Service for Archaeological Heritage, Endenicher Str. 133, 53115 Bonn, Germany

[13]Department of Archaeology, University of Exeter, Laver Building, North Park Road, Exeter, Devon, 27 EX4 4QE, UK

[14]Université Paris 1 Panthéon-Sorbonne, UMR 8215 TRAJECTOIRES, 21 allée de l'université, 92023 Nanterre, France

[15]University of Strasbourg, UMR7044, Misha, 5 allé du général Rouvillois, 67083 Strasbourg, France

[16]Institute of Archaeology, Adam Mickiewicz University, 61-614 Poznan, Poland

[17]Somerset County Museum, Taunton Castle, Castle Green, Taunton, TA1 1AA, UK

[18]Archaeological Research Leiden, Einsteinweg 2, 2333 CC Leiden, The Netherlands

[19]Faculty of Archaeology, Leiden University, Einsteinweg 2, 2333 CC Leiden, The Netherlands
[20]MOLA (Museum of London Archaeology), 46 Eagle Wharf Road, London N1 7ED

Pottery is one of the most commonly recovered artefacts from archaeological sites. Despite more than a century of relative dating based on typology and seriation[1], accurate dating of pottery by the radiocarbon method has proven extremely challenging due to the limited survival of organic temper and unreliability of visible residues[2-4]. We report here a new method of dating directly archaeological pottery based on accelerator mass spectrometry (AMS) analysis of ^{14}C in absorbed food residues: palmitic ($C_{16:0}$) and stearic ($C_{18:0}$) fatty acids purified by preparative gas chromatography (pcGC)[5-8]. We present the first accurate compound-specific radiocarbon determinations of lipids extracted from pottery vessels, which were rigorously evaluated by comparison with dendrochronological dates[9,10] and inclusion in site and regional chronologies containing suites of radiocarbon dates on other materials[11-15]. Critically, the compound-specific dates from each of the $C_{16:0}$ and $C_{18:0}$ fatty acids in pottery vessels provide an internal quality control of the results[6] and, are entirely compatible with dates for other commonly dated materials. Accurate radiocarbon dating of pottery vessels can reveal: (i) the period of use of pottery; (ii) the antiquity of organic residues including when specific foodstuffs were exploited; (iii) sites chronologies in the absence of traditionally datable materials and (iv) direct verification of pottery typochronologies. As exemplars, the method was applied to the dating of dairy and carcass product exploitation in Neolithic vessels, from Britain, Anatolia, central and western Europe, and Saharan Africa.

Chronology lies at the very heart of archaeology[16]. Radiocarbon dating by accelerator mass spectrometry (AMS) is the most widely used method for providing calendrical chronologies for past human activity over the last 50,000 years[17], most commonly using samples of charred plant remains and bone[17]. Radiocarbon dates can be used alongside relative sequences, such as those derived from stratigraphy or the typological analysis or seriation of artefact-types, to build chronological models. Applying Bayes' theorem allows radiocarbon dating to provide calendar age estimates with uncertainties as low as a few decades[18].

The invention of pottery in the late Pleistocene was likely a significant driver for developments in food processing[19,20]. Pottery vessels can often be placed in robust relative chronological sequences using typology and seriation, although obtaining precise and accurate radiocarbon dates from pottery is extremely challenging[2,3,21]. All sources of carbon associated with pottery vessels have been considered for dating[4,5], including organic temper, which occasionally survives firing, and surficial food crusts, although these are rare and prone to contamination due to their exposed nature[22]. In contrast, the lipidic components of food residues absorbed into, and protected by, the clay matrix during cooking occur very commonly[8], often in high concentrations (mg per g clay fabric). These offer an untapped resource for radiocarbon dating. The most common absorbed residues correspond to degraded animal fats characterised by their high abundances of $C_{16:0}$ and $C_{18:0}$ fatty acids[7,8]. More than 20 years ago we recognised the possibility of using preparative capillary gas chromatography (pcGC) to isolate chemically pure fatty acids from such residues for compound-specific radiocarbon analysis (CSRA)[21,23,24]. Although initial attempts to date pottery vessels were promising, the accuracy and precision demanded by archaeology could not be achieved due to unidentified technical difficulties, leading to highly variable results[21,23].

We have brought together the latest technologies for radiocarbon measurement, including automated graphitisation and MICADAS compact AMS, in conjunction with high-field 700 MHz NMR, to undertake systematic investigations of the pcGC protocol[5,6]. Rigorous assessment of contamination in compounds purified by pcGC was undertaken for the first time, leading to our invention of a solventless pcGC trap and implementation of cleaning procedures to avoid between run carryover[5,6]. These advances reduce exogenous contamination of fatty acids previously associated with the pcGC to below concentrations that would significantly affect measured radiocarbon ages. For archaeological animal fats we demonstrated that two fatty acids isolated from the same matrix giving the same radiocarbon age (i.e. statistically consistent at the 95% significance level), provides an internal quality control for archaeological dating[6]. In this work we aim to extend this method to archaeological pot lipids. We selected pottery rich in animal fats from our database of lipid residues built up over the last three decades. Pottery vessels from chronologically well-characterised settings and different burial environments were analysed and the compatibility of pot lipid dates with these existing chronologies was evaluated by statistical comparison of posterior density estimates for the key parameters and the use of indices of agreement with inclusion in these known frameworks (Fig. 1, extended data (ED) Table 1, Supplementary information (SI) 1).

We initially focused on Neolithic pottery from the Sweet Track, an impressive elevated wooden trackway discovered in a wetland area of the Somerset Levels (UK; SI 2)[9,10,25]. This site is critical because its construction has been precisely dated by dendrochronology to the winter/early spring of 3807/6 BC (Fig. 2a) and it was used and maintained for approximately ten years[10]. We had previously dated lipids from pots found alongside the trackway and likely contemporaneous to its construction and use, but the measured dates were a century later than the trackway's construction[23]. Re-analysis of the two vessels (Fig. 2b) using our new approach produced radiocarbon ages of 5110 ± 25 BP (SW1) and 5092 ± 26 BP (SW2), which are statistically indistinguishable ($T'=9.0$, $T'(5\%)=9.5$, $\nu=4$) from the measurements on tree rings included in IntCal13 calibration curve for the relevant decade (Fig. 2c)[26]. The calibrated dates of these ages are clearly compatible with the tree-ring dates for the construction of the trackway.

Extending our approach to Anatolia, the Neolithic tell of Çatalhöyük East was a locus for the emergence and development of pottery production. A 21 m-deep stratigraphic sequence provides strong archaeological prior information for a Bayesian chronological model covering the upper parts of the mound (TP Area)[11]. The sequence of houses, middens, and burial structures has been combined with 50 radiocarbon dates revealing a Neolithic sequence occupied from the mid-64th to the mid-60th centuries cal BC[11]. Our compound-specific radiocarbon ages on adipose lipids[27] from four pottery vessels from four different contexts (TP.M17: 7382 ± 31 BP; TP.N10: 7348 ± 25 BP; TP.O23: 7340 ± 27 BP, and TP.P13: 7364 ± 25 BP) were incorporated into the Bayesian chronological model for this part of the site (SI 3, ED Figs. 1 & 2). The revised model for the Neolithic deposits in the TP Area shows posterior distributions for the key parameters almost identical to those from the original model[11]. Their median values vary by an average of 4 years and a maximum of 10 years, confirming the compatibility of the radiocarbon ages on fatty acids with the site stratigraphy. Based on sensitivity analyses (SI 3) this well-constrained model is at least as sensitive as measurements on paired materials to detect inaccuracies. In this case, the CSRA dates not only provide direct dating for the importance of ruminant carcass products (Fig. 1c) to the inhabitants of Çatalhöyük at this time (derived from $\delta^{13}C$ values of preserved fats), but also provide direct dating evidence for the climatic changes associated with the global 8.2 kyr event (derived from compound-specific deuterium isotope analyses on the same fats)[27].

The next exemplar tests the accuracy of our new dating approach using a classic pottery seriation study relating to Neolithic ceramics from Lower Alsace (France) that spans the second quarter of the fifth millennium cal BC (SI 4)[12]. The regional correspondence analysis clearly separates the Hinkelstein, Grossgartach, Planig-Friedberg, and Rössen Middle Neolithic ceramic groups. We focused on vessels from three pits, all of which can be assigned to the Grossgartach phase (Fig. 3a,b). The sequence of ceramic phases was combined with the existing assemblage of 95 radiocarbon dates, largely on articulated bones, along with four CSRA on fatty acids (ROS-C-4596: 5804 ± 25 BP; ROS-C-4600: 5904 ± 28 BP; ROS-C-4644: 5931 ± 26 BP, and ROS-C-4657: 5912 ± 28 BP) from the Grossgartach sherds in a model using Bayesian statistics. The phase boundaries in this revised model are very similar to those produced by the original analysis[12], as median values differ by an average of 6 years and a maximum of 15 years (Fig. 3c). The sensitivity analyses (SI 4) demonstrate the model to be particularly sensitive to small biases, and likely more sensitive than measurements on paired materials. The CSRAs are clearly compatible with the attribution of these pottery vessels to the Grossgartach ceramic phase based on their decorative motifs, and with the other radiocarbon dates for this group.

We then explored the introduction of a new food product, i.e. milk, into Neolithic Europe by undertaking radiocarbon dating of animal fat residues, including dairy fats, recovered from early farming settlements of the *Linearbandkeramik* (LBK) pottery (Fig. 1). These communities settled in Central Europe from the early 54th century BC[13]. Animal fats in twelve potsherds from the earliest LBK contexts at six sites, in Poland, France, Germany and the Netherlands, produced radiocarbon dates that were modelled and shown to be compatible with the currency of LBK ceramics in Northern and Western Europe (SI 5, ED Figs. 3 & 4)[12,13]. Sensitivity analyses (SI 5, ED Fig. 4) demonstrate this model to be more sensitive to older biases as we focused on early settlements, illustrating the direct dating of a new food commodity. The radiocarbon dates on the earliest dairying residues suggest that the practice began in 5385–5225 cal BC (95% probability; start LBK lipid; ED Fig. 3), and probably arrived with the earliest farmers in these areas. Thus, the linking of fatty acid structures with compound-specific carbon isotope values and CSRA provides a powerful means of directly dating prehistoric foodways and their introduction.

Our investigations then moved to pottery from the Sahara Desert to provide a test of the methodology for a region where depositional conditions are very different from the temperate climes of Northern Europe. The Takarkori rock shelter, located in the hyper-arid area of the Acacus Mountains, SW Libya, demonstrates evidence of animal exploitation based on rock art and archaeological finds[14] (ED Figs 5 & 6). Our previous work revealed abundant carcass and dairy fat residues in fragments of the pottery vessels[28]. Stratigraphy and radiocarbon dating of a range of materials (bone collagen, charred plant remains, dung, skin, and enamel bioapatite) placed deposits associated with Middle Pastoral pottery in the sixth-fifth millennia cal BC[14,28,29]. The fatty acids from five potsherds, containing dairy fat (ED Fig. 6b), produced uncalibrated radiocarbon ages of 5993 ± 28 BP (TAK443), 5979 ± 28 BP (TAK120), 5493 ± 28 BP (TAK420), 5348 ± 24 BP (TAK21) and 5085 ± 24 BP (TAK1572). The CSRA dates were proven entirely compatible with the currency of Middle Pastoral Neolithic ceramics (SI 6, ED Fig. 6d), and the direct radiocarbon dating of dairy residues confirms that dairying in North Africa began as early as the end of the 6th millennium cal BC[14,28,29]. While, the model sensitivity is weak based on the small number of reference dates it includes (SI 6, ED Fig. 7), it demonstrates the possibility of dating potsherds from extremely arid burial conditions. In addition, direct dating of pottery lipids represents a major contribution to ascertain the correct cultural attribution of materials found in loose sediments (organic sands), which are typical of desert environments and frequently found in highly disturbed sequences[14].

Finally, archaeological excavations of several pits by Museum of London Archaeology in advance of building works at Principal Place, London (PPL11) revealed the largest assemblage of Neolithic pottery recovered so far from the City of London or its immediate environs.

Critically, the only finds other than pottery recovered from this deposit (lithics, bones and charred plant remains) were compromised by later disturbance and truncation. The assemblage comprised Neolithic Plain and Decorated Bowls, consisting of thin-walled medium-sized open/neutral bowls, together with several smaller open bowls/cups[30]. Similar material has been found elsewhere in the Thames Valley and beyond. Lipid residue analyses revealed high concentrations of degraded animal fats in several sherds, which were shown by compound-specific $\delta^{13}C$ values to derive from dairy and carcass fats (Fig. 1c). Radiocarbon measurements of fatty acids from four plain sherds yielded uncalibrated ages of 4911 ± 27 BP (PPL012), 4742 ± 22 BP (PPL015), 4652 ± 26 BP (PPL020) and 4733 ± 22 BP (PPL021). A new statistical model confirms that the pottery dates fit well within the currency of Plain Bowl in southern Britain (SI 7, ED Fig. 8)[15]. The sensitivity analyses (SI 7, ED Fig. 9) are weaker in this case, but demonstrates the value of dating absorbed lipid residues in situations where no other datable material exists. Our new ability to undertake accurate radiocarbon dating of compound-specific fatty acids from pottery was invaluable in affording a, previously impossible, temporal insight into some of the earliest traces of human activity in what is now the City of London.

In summary, the radiocarbon determinations of lipid residues from Neolithic pottery vessels presented above, modelled against site chronologies, unequivocally establish CSRA of fatty acids as a robust new tool for archaeological dating. Significantly, our method and findings bring pottery vessels within the range of other archaeological materials routinely dated by radiocarbon. The importance of this advance to the archaeological community cannot be overstated. Pottery typology is the most widely used dating technique in the discipline, and so the opportunity to anchor different kinds of pottery securely to the calendrical timescale will be of utmost practical significance. Critically, pottery often survives in circumstances where other organic materials often do not, and so archaeological questions relating to chronology that are currently intractable will come within the scope of our technologies.

References

1 Orton, C. & Hughes, M. *Pottery in Archaeology.* 2nd edition (Cambridge University Press, Cambridge, 2014).

2 Evin, J., Gabasio, M. & Lefevre, J. C. Preparation techniques for radiocarbon dating of potsherds. *Radiocarbon*. **31**, 276-283 (1989).

3 Hedges, R. M., Tiemei, C. & Housley, R. A. Results and methods in the radiocarbon dating of pottery. *Radiocarbon*. **34**, 906-915 (1992).

4 Gabasio, M., Evin, J., Arnal, G. B. & Andrieux, P. Origins of carbon in potsherds. *Radiocarbon*. **28**, 711-718 (1986).

5 Casanova, E., Knowles, T. D. J., Williams, C., Crump, M. P. & Evershed, R. P. Use of a 700 MHz NMR microcryoprobe for the identification and quantification of exogenous carbon in compounds purified by preparative capillary gas chromatography for radiocarbon determinations. *Anal. Chem.* **89**, 7090-7098 (2017).

6 Casanova, E., Knowles, T. D. J., Williams, C., Crump, M. P. & Evershed, R. P. Practical considerations in high precision compound-specific radiocarbon dating: Eliminating the effects of solvent and sample cross-contamination on accuracy and precision. *Anal. Chem.* **90**, 11025-11032 (2018).

7 Evershed, R. P. et al. Chemistry of archaeological animal fats. *Accounts Chem. Res.* **35**, 660-668 (2002).

8 Roffet-Salque, M. et al. From the inside out: Upscaling organic residue analyses of archaeological ceramics. *J. Archaeol. Sci. Rep.* **16**, 627-640 (2017).

9 Coles, J. M. & Orme, B. J. Ten excavations along the Sweet Track (3200 BC). *Somerset Lev. Pap.* **10**, 45 (1984).

10 Hillam, J. et al. Dendrochronology of the English Neolithic. *Antiquity* **64**, 210-220 (1990).

11 Marciniak, A. et al. Fragmenting times: Interpreting a Bayesian chronology for the late Neolithic occupation of Çatalhöyük East, Turkey. *Antiquity*. **89**, 154-176 (2015).

12 Denaire, A. et al. The cultural project: Formal chronological modelling of the early and middle Neolithic sequence in Lower Alsace. *J. Archaeol. Method Th.* **24**, 1072-1149 (2017).

13 Jakucs, J. et al. Between the Vinča and Linearbandkeramik worlds: The diversity of practices and identities in the 54th–53rd centuries cal BC in Southwest Hungary and beyond. *J. World Prehist.* **29**, 267-336 (2016).

14 Biagetti, S. & di Lernia, S. Holocene deposits of Saharan Rock Shelters: The case of Takarkori and other sites from the Tadrart Acacus Mountains (southwest Libya). *Afr. Archaeol. Review.* **30**, 305-338 (2013).

15 Whittle, A. W. R., Healy, F. M. A. & Bayliss, A. *Gathering Time: dating the early Neolithic Enclosures of Southern Britain and Ireland.* (Oxbow Books, Oxford, 2011).

16 Wheeler, R. E. M. *Archaeology from the Earth*. (Penguin, Baltimore, 1956).

17 Taylor, R. E. *Radiocarbon Dating, An Archaeological Perspective.* (Academic press, London, 1987).

18 Bronk Ramsey, C. Bayesian analysis of radiocarbon dates. *Radiocarbon* **51**, 337-360 (2009).

19 Barnett, W. & Hoopes, J. W. *The Emergence of Pottery: Technology and Innovation in Ancient Societies.* (Smithsonian Institution Press, Washington DC, 1995).

20 Kuzmin, Y. The origins of pottery in East Asia: Updated analysis (the 2015 state-of-the-art). *Doc. Praehist.* **42**, 1-11 (2015).

21 Stott, A. W. et al. Radiocarbon dating of single compounds isolated from pottery cooking vessel residues. *Radiocarbon*. **43**, 191-197 (2001).

22 Evershed, R. P. Biomolecular archaeology and lipids. *World Archaeol.* **25**, 74-93 (1993).

23 Berstan, R. et al. Direct dating of pottery from its organic residues: new precision using compound-specific carbon isotopes. *Antiquity*. **82**, 702-713 (2008).

24 Eglinton, T. I., Aluwihare, L. I., Bauer, J. E., Druffel, E. R. M. & McNichol, A. P. Gas chromatographic isolation of individual compounds from complex matrices for radiocarbon dating. *Anal. Chem.* **68**, 904-912 (1996).

25 Coles, B. J. & Coles, J. M. *Sweet Track to Glastonbury: the Somerset Levels in Prehistory*. 163-169 (Oxbow, Oxford,1986).

26 Reimer, P. J. et al. IntCal13 and Marine13 radiocarbon age calibration curves 0–50,000 years cal BP. *Radiocarbon*. **55**, 1869-1887 (2013).

27 Roffet-Salque, M. et al. Evidence for the impact of the 8.2-kyBP climate event on Near Eastern early farmers. *Proc. Natl. Acad. Sci. USA.* **115**, 8705-8709 (2018).

28 Dunne, J. et al. First dairying in green Saharan Africa in the fifth millennium BC. *Nature.* **486**, 390-394 (2012).

29 Cherkinsky, A. & di Lernia, S. Bayesian approach to ^{14}C dates for estimation of long-term archaeological sequences in arid environments: The Holocene site of Takarkori Rockshelter, Southwest Libya. *Radiocarbon.* **55**, 771-782 (2013).

30 Cotton, J. et al. Early Neolithic pits and pottery at Principal Place, Shoreditch, Hackney. *In prep.*

Figure captions

Figure 1: Site location map, partial gas chromatograms and stable isotope determination of compound-specific radiocarbon dated lipid residues preserved in Neolithic pottery vessels. (a) Map showing the location of the archaeological sites where CSRA was applied in this study. (b) Partial gas chromatograms of a selection of potsherds showing $C_{16:0}$ and $C_{18:0}$ FA abundances and (c) Scatter plots of $\Delta^{13}C$ (= $\delta^{13}C_{18:0}$ - $\delta^{13}C_{16:0}$) values plotted against $\delta^{13}C_{16:0}$ values for all the sherds dated (n = 31), ranges on the left denote the mean ± 1 SD of modern reference fats.

Figure 2: Sweet Track timbers, pottery vessel and calibrated radiocarbon dates. (a) Picture of Sweet Track timbers. (b) Picture of a pottery vessel (SW2) recovered alongside the Sweet Track. (c) Probability distributions of dates from pots deposited next to the Sweet Track (in green), and from oaks trees (in black) included in IntCal13[26] that include the tree-ring for 3807 BC. Each distribution represents the relative probability that an event occurs at a particular time. For each of the dates two distributions have been plotted: one in outline, which is the simple radiocarbon calibration, and a solid one, based on the model used. The square bracket down the left-hand side along with the OxCal keywords define the overall model exactly.

Figure 3: Drawings, correspondence analysis and radiocarbon dates of Neolithic vessels from Alsace (France) modelled using Bayesian statistics. (a) Drawings of decorated pottery vessels from the Grossgartach group from pits 122 (1-2), 50 (4-5) and 63 (3, 6-7) from which the undecorated potsherds dated in the model were recovered. (b) Revised correspondence analysis on the cultural assemblages (axis 1) and horizontal decorative motifs (axis 2), including features which contained the dated sherds from the Alsatian Neolithic groups. (c) Revised statistical model of the Middle Neolithic with radiocarbon dates on pot lipids included in grey. Format is as Fig. 1.

Methods

Lipid extractions and isolation

Potsherds were selected based on the presence of terrestrial animal fats (dairy and ruminant carcass fats) in the lipid residue in order to avoid any possible reservoir effect caused by aquatic products processing in pots. A piece of 1 to 10 g of the potsherd was sampled, according to the lipid concentration. The sherds were extracted in a glass culture tube using H_2SO_4/MeOH (4

% *v/v*, 3 x 8 mL, 70ºC, 1 h). The supernatants were centrifuged (2500 rpm, 10 min) and combined into new culture tubes containing double-distilled water (5 mL). The lipids were extracted with *n*-hexane (4 x 5 mL), transferred into 3.5 mL vials and blown down to dryness at room temperature under a gentle nitrogen stream. Then ~180 µL of *n*-hexane was added to obtain a concentration of fatty acid methyl esters (FAMEs) at 5 µg of C.μL^{-1} before transfer to an autosampler vial for isolation by pcGC.

The pcGC consisted of a Hewlett Packard 5890 series II gas chromatograph coupled to a Gerstel Preparative Fraction Collector by a heated transfer line. The pcGC was equipped with a column with a 100% poly(dimethyl siloxane) stationary phase (Rxi-1ms, 30 m x 0.53 mm i.d., 1.5 µm film thickness, Restek,). Helium was used as the carrier gas at a constant pressure of 10 psi. The GC temperature programme started with an isothermal hold at 50 °C for 2 min, increased to 200 °C at 40 °C.min^{-1}, then to 270 °C at 10 °C.min^{-1} and finally increased to 300 °C at 20 °C.min^{-1} and held for 8.75 min. The $C_{16:0}$ and $C_{18:0}$ FAMEs were injected (1 µL per run), separated and trapped 40 times per trapping sequence. One percent of the GC column effluent flows to the flame ionization detector (FID), whilst the remaining 99% passes via a transfer line into the fraction collector, both heated to 300 °C. Compounds were isolated based on their retention times[6]. The stationary phase degradation of the pcGC column and other sources of exogenous carbonaceous contamination were monitored on a Brucker Avance III HD 700 MHz NMR instrument following our recently published procedure[5,6].

Radiocarbon determinations and statistical analysis

PCGC isolated compounds were transferred into Al capsules then combusted and graphitised in a Vario Microcube Elemental Analyser linked to an Automated Graphitisation System (AGE 3, IonPlus). All the radiocarbon measurements were performed by the Bristol Accelerator Mass Spectrometer (BRAMS) facility at the University of Bristol. Data reduction was performed using the software BATS[31] (v4.07). Radiocarbon dates obtained for FAMEs were corrected for the presence of added methyl C using a mass balance approach[5,6,21] and reported as the conventional radiocarbon ages[32] (SI 1).

Two contemporaneous compounds ($C_{16:0}$ and $C_{18:0}$ FAs) were dated and every pair of statistically indistinguishable measurements (at the 95% significance level)[33] were combined as a weighted average prior to Bayesian chronological modelling using OxCal v4.2 and v4.3[18,34] and the currently internationally agreed radiocarbon calibration curve for the northern hemisphere, IntCal13[26]. The compatibility of the radiocarbon dates on absorbed fatty residues with existing sites/regional chronologies was assessed by including the lipid radiocarbon dates into existing statistical frameworks in a position defined by archaeological information (e.g. stratigraphy, seriation). Their compatibility with the existing chronologies were achieved by: (i) comparison of posterior density estimates for key modelled parameters with equivalent date estimate or known age by dendrochronology, (ii) using the individual and model agreement indices[18,34] in models containing FA dates, and (iii) comparing posterior density estimates for key parameters from models which includes the FA dates to one that does not include them (SI 1). The sensitivity of existing chronological models to the addition of the new radiocarbon measurements was evaluated as above, after deliberately biasing the radiocarbon dates on pottery vessels to varying degrees while assessing the effect on posterior density estimates for the key parameters and indices of agreements (SI 1-7).

Additional references

31 Wacker, L, et al. Bats: A new tool for AMS data reduction, *Nucl. Instrum. Meth. B*, **268**, 976–979 (2010).

32 Stuiver, M., Polach, H.A., Discussion reporting of ^{14}C data, *Radiocarbon,* **19**, 355-363 (1977).

33 Ward, G K, and Wilson, S R. Procedures for comparing and combining radiocarbon age determinations: a critique, *Archaeometry*, **20**, 19–31 (1978).

34 Bronk Ramsey, C, Radiocarbon calibration and analysis of stratigraphy: the OxCal program, *Radiocarbon*, **36**, 425–30 (1995).

35 Stuiver, M, and Reimer, P J. Extended ^{14}C data base and revised CALIB 3.0 ^{14}C age calibration program, *Radiocarbon*, **35**, 215–230 (1993).

Data availability statement

All data generated during this study are included in the main article, extended data and supplementary information.

Code availability statement

The codes used in OxCal for statistical modelling are provided in the supplementary information.

Extended data

Extended Data Table 1: Summary of radiocarbon dates of lipids preserved in pottery vessels. Vessel descriptions, lipid concentrations and conventional radiocarbon ages (as defined by Stuiver and Polach[32] and calculated according to Wacker *et al.*[31]) of $C_{16:0}$ and $C_{18:0}$ fatty acids (which passed the internal quality control) extracted from pottery vessels.

Extended Data Figure 1. **Schematic diagram showing the stratigraphic information of the Neolithic occupation of the TP area at Çatalhöyük (Turkey) included in the chronological model** (defined in ED Fig. 1). Contexts containing potsherds dated in this study are highlighted in green.

Extended Data Figure 2. Probability distributions of dates from Neolithic deposits in the TP Area at Çatalhöyük, Turkey (including the results on absorbed fatty acids in pottery sherds listed in ED Table 1). Each distribution represents the relative probability that an event occurs at a particular time. For each date, two distributions are plotted: one in outline, which is the result of a simple radiocarbon calibration, and a solid one, based on the chronological model used. The distributions in green correspond to the potsherds, in black to the pre-existing chronology. Distributions other than those relating to particular samples correspond to aspects of the model. For example, the distribution *'end East Mound occupation'* is the estimated date when Neolithic occupation of the East Mound ended at Çatalhöyük. Measurements followed by a question mark and shown in outline have been excluded from the model for reasons described by Marciniak *et al.*[11] (table 1) and are simple calibrated dates (Stuiver and Reimer[35]). The large square brackets down the left-hand side, along with the OxCal keywords, define the overall model exactly.

Extended Data Figure 3. Probability distributions of radiocarbon dates from absorbed fatty acids in LBK ceramics (listed in ED Table 1, black: dairy, blue: ruminant, red: non-ruminant). Format as ED Fig. 2.

Extended Data Figure 4. Sensitivity analyses of radiocarbon dates on LBK ceramics. Key parameters for the start of the use of LBK ceramics (blue distribution), derived from the models defined in Figures ED 3, Denaire *et al.*[12] (fig 8), and Jakucs *et al.*[13] (Model 1, figs 18–19; Model 2, figs 20–1; Model 3, figs 22–3) compared to the start of LBK lipids presented in ED Fig. 4 (red distributions) then deliberately biased by 1, 2, 3, 4 and 8 σ to younger (orange distributions) and older (pink distributions) values. Some distributions may have been truncated.

Extended Data Figure 5. **The Tadrart Acacus Mountains in SW Libya.** (a) The Wadi Takarkori area (dashed rectangle), (b) Schematic plan of the excavated areas (c). All sampled sherds come from the Main Sector.

Extended Data Figure 6: Site stratigraphy, pictures and radiocarbon dates of Middle Pastoral pottery vessels from Takarkori (Libya) modelled using Bayesian statistics. (a) Stratigraphic context of sampled potsherds from Takarkori East-West profile of the southern wall of the TK-NS (see ED Fig. 5), key: i); aeolian sand; ii) sand rich in organic matter; iii) lenses of undecomposed plant remains; iv) ash; v) charcoal; vi) slurry deposit; vii) eroded sand from the wall; viii) bedrock. (b) The five potsherds analysed showing typical Middle Pastoral decorative patterns. (c) Example of temporally and spatially wide deposit of organic sands (detail of Layer 25-Takarkori-Main Sector). (d) Statistical model of the Middle Pastoral period showing the comparison of pot lipid dates (in green) with previous radiocarbon measurements. Format is as ED Fig. 2.

Extended Data Figure 7. Sensitivity analyses of radiocarbon dates on vessels from Takarkory rockshelter, Lybia. Probability distributions for the beginning and end Middle Pastoral period ceramics from Takarkori rockshelter, Libya (no pot lipid dates) compared with those of the model shown in the ED Fig. 6d and deliberately biased by 1, 2, 4, 8, 20 and 40 σ**.** Format as ED Fig. 4.

Extended Data Figure 8. Probability distributions of dates associated with the use of early Neolithic Plain Bowl pottery in southern Britain. Prior distributions have been taken from the models described in the text. Format as ED Fig. 2.

Extended Data Figure 9. Sensitivity analyses of radiocarbon dates on vessels from Principal Place, London. Probability distributions of the start and end of early Neolithic Plain Bowl pottery in southern Britain compared with those of the model shown in ED Fig. 8 and deliberately biased by 2, 4, 8 and 16 σ. Format as ED Fig. 4.

Supplementary information is linked to the online version of the paper at

www.nature.com/nature

Acknowledgements

We thank the European Research Council for funding an advanced grant (NeoMilk, FP7-IDEAS-ERC/324202) and a proof of concept grant (LipDat, H2020 ERC-2018-PoC/812917) to RPE, financing a PhD to ECa and postdoctoral contract to MRS and JS, and a postdoctoral contract to ECa, respectively. We acknowledge the BRAMS facility for the radiocarbon measurements, establishment of which was jointly funded by the NERC, BBSRC and University of Bristol. We thank P. Monaghan for his help with the radiocarbon sample preparation. We thank the Polish National Science Centre (decision DEC-2012/06/M/H3/00286) for financing the work in the upper levels at Çatalhöyük and the Department of Antiquities in Tripoli, Libya for permits and Sapienza University of Rome and Italian Ministry of Foreign Affairs for funding the fieldwork in Libya. We thank MOLA (Museum of London Archaeology) for excavating and providing potsherds from Principal Place (PPL11), London EC2/E1. We acknowledge B. Schnitzler from the Palais Rohan for accessing the material from Rosheim, A. Mulot from the Achéologie Alsace (Centre of conservation and study) for accessing the material from Ensisheim, R.W. Schmitz from the LVR-Landes Museum Bonn for accessing the material from Königshoven 14 and R. Brunning from the South West Heritage Trust for sharing excavations pictures of the Sweet Track.

Author Contributions

RPE conceived the project. ECa, RPE and ABay wrote the paper. ECa, TDJK and RPE developed the method for dating lipids. ECa, JD and TG performed the preparation of pottery vessels for radiocarbon analysis. ECa and TDJK generated the radiocarbon measurements and performed data analysis. ABay undertook the statistical modelling of the radiocarbon dates.

MZB advised on the stratigraphic sequence of the TP Area of Çatalhöyük East. AM performed the stratigraphic analysis of the TP Area of Çatalhöyük East and chronological analysis of the LBK from the Polish lowlands and MK helped the selection and provided the pottery vessels from these sites. CJ and PL excavated the Alsatian sites. ADe and PL performed the correspondence analysis of the Alsace region. SDL advised on the stratigraphic sequence and pottery analysis of Takarkori and RR studied the pottery assemblage. ECa, MRS and JS sampled the LBK sites. MRS coordinated and processed the analyses of sherds from the LBK culture and from Çatalhöyük East. ABar advised on the project design. SM provided pottery vessels from the Sweet Track. ECl analysed the material and advised sampling for Königshoven 14. MI excavated and provided vessels from Cuiry-lès-Chaudardes. IVW excavated and advised sampling from the Netherlands and PVDV analysed the material. ADa excavated the site of Principal Place, London EC2/E1 as project manager and JC studied the pottery material.

Author Information Reprints and permissions information are available at www.nature.com/reprints. The authors declare no competing financial interests. Correspondence and requests for materials should be addressed to r.p.evershed@bristol.ac.uk.

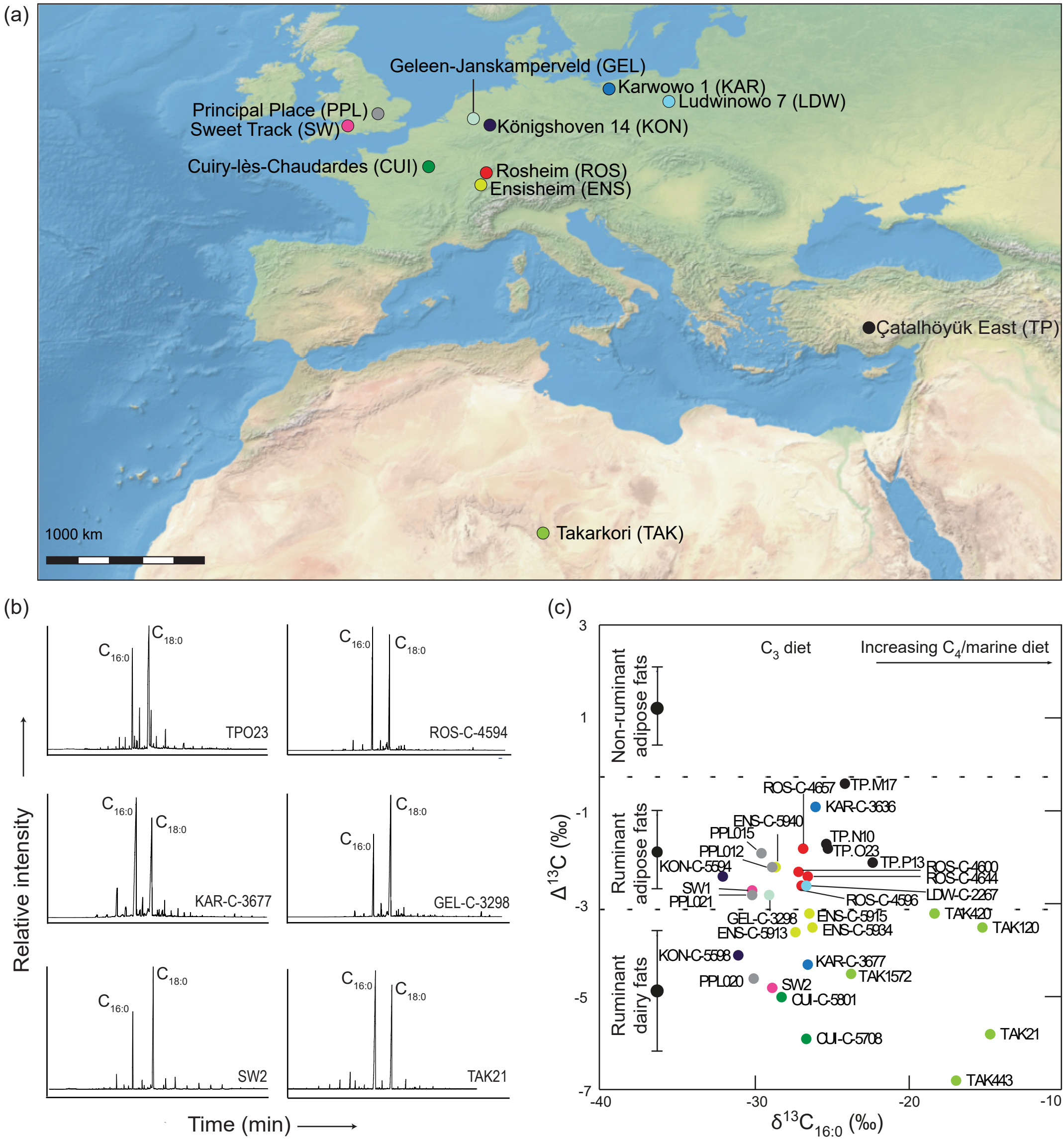
(a)
Geleen-Janskamperveld (GEL)
Karwowo 1 (KAR)
Ludwinowo 7 (LDW)
Principal Place (PPL)
Sweet Track (SW)
Königshoven 14 (KON)
Cuiry-lès-Chaudardes (CUI)
Rosheim (ROS)
Ensisheim (ENS)
Çatalhöyük East (TP)
Takarkori (TAK)
1000 km
(b)
Relative intensity
Time (min)
TPO23
ROS-C-4594
KAR-C-3677
GEL-C-3298
SW2
TAK21
$C_{16:0}$
$C_{18:0}$
(c)
C_3 diet
Increasing C_4/marine diet
Non-ruminant adipose fats
Ruminant adipose fats
Ruminant dairy fats
$\Delta^{13}C$ (‰)
$\delta^{13}C_{16:0}$ (‰)
ROS-C-4657
TP.M17
KAR-C-3636
ENS-C-5940
PPL015
TP.N10
TP.O23
PPL012
TP.P13
ROS-C-4600
ROS-C-4644
KON-C-5594
SW1
PPL021
ROS-C-4596
LDW-C-2267
GEL-C-3298
ENS-C-5915
TAK420
TAK120
ENS-C-5913
ENS-C-5934
KON-C-5598
KAR-C-3677
TAK1572
PPL020
SW2
CUI-C-5801
CUI-C-5708
TAK21
TAK443

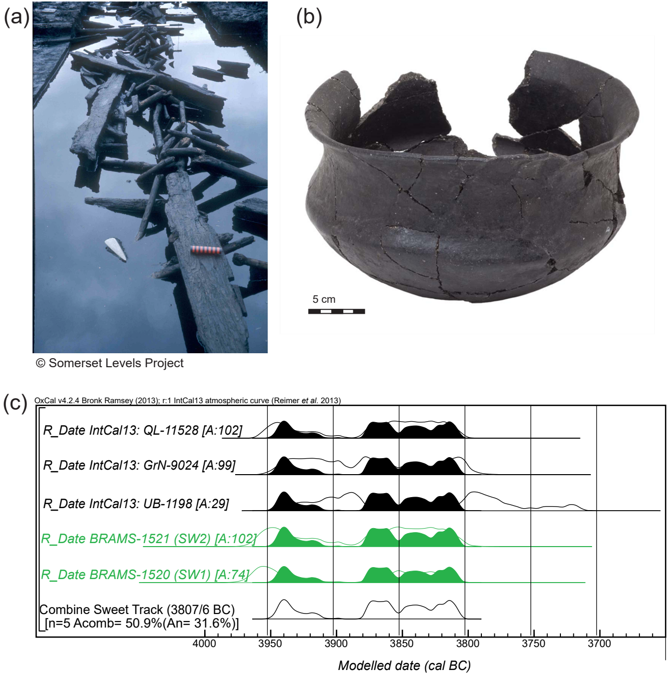
(a)
© Somerset Levels Project
(b)
5 cm
(c)
OxCal v4.2.4 Bronk Ramsey (2013); r:1 IntCal13 atmospheric curve (Reimer et al. 2013)
R_Date IntCal13: QL-11528 [A:102]
R_Date IntCal13: GrN-9024 [A:99]
R_Date IntCal13: UB-1198 [A:29]
R_Date BRAMS-1521 (SW2) [A:102]
R_Date BRAMS-1520 (SW1) [A:74]
Combine Sweet Track (3807/6 BC)
[n=5 Acomb= 50.9%(An= 31.6%)]
4000
3950
3900
3850
3800
3750
3700
Modelled date (cal BC)

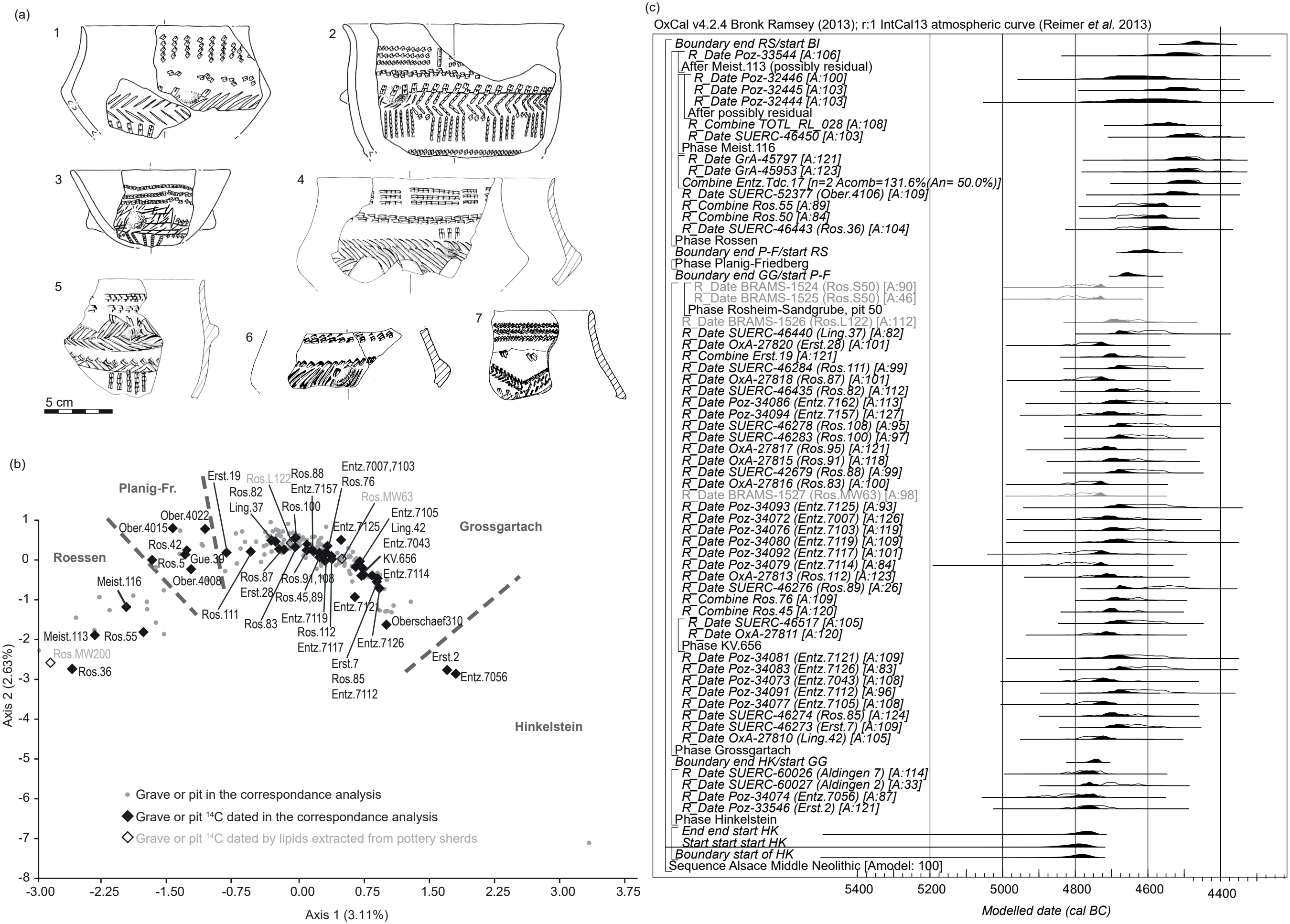

(a)
1
2
3
4
5
6
7
5 cm
(b)
Planig-Fr.
Roessen
Grossgartach
Hinkelstein
Erst.19
Ros.L122
Ros.88
Entz.7157
Entz.7007,7103
Ros.76
Ros.MW63
Ros.82
Ling.37
Ros.100
Entz.7125
Entz.7105
Ling.42
Entz.7043
KV.656
Entz.7114
Ober.4022
Ober.4015
Ros.42
Ros.5
Gue.39
Ober.4008
Ros.87
Erst.28
Ros.91,108
Ros.45,89
Meist.116
Ros.111
Ros.83
Entz.7119
Ros.112
Entz.7117
Entz.7121
Oberschaef310
Entz.7126
Erst.7
Ros.85
Entz.7112
Meist.113
Ros.55
Ros.MW200
Ros.36
Erst.2
Entz.7056
Axis 2 (2.63%)
Axis 1 (3.11%)
1
0
-1
-2
-3
-4
-5
-6
-7
-8
-3.00
-2.25
-1.50
-0.75
0.00
0.75
1.50
2.25
3.00
3.75
Grave or pit in the correspondance analysis
Grave or pit ^{14}C dated in the correspondance analysis
Grave or pit ^{14}C dated by lipids extracted from pottery sherds
(c)
OxCal v4.2.4 Bronk Ramsey (2013); r:1 IntCal13 atmospheric curve (Reimer *et al.* 2013)
Boundary end RS/start BI
R_Date Poz-33544 [A:106]
After Meist.113 (possibly residual)
R_Date Poz-32446 [A:100]
R_Date Poz-32445 [A:103]
R_Date Poz-32444 [A:103]
After possibly residual
R_Combine TOTL_RL_028 [A:108]
R_Date SUERC-46450 [A:103]
Phase Meist.116
R_Date GrA-45797 [A:121]
R_Date GrA-45953 [A:123]
Combine Entz.Tdc.17 [n=2 Acomb=131.6%(An= 50.0%)]
R_Date SUERC-52377 (Ober.4106) [A:109]
R_Combine Ros.55 [A:89]
R_Combine Ros.50 [A:84]
R_Date SUERC-46443 (Ros.36) [A:104]
Phase Rossen
Boundary end P-F/start RS
Phase Planig-Friedberg
Boundary end GG/start P-F
R_Date BRAMS-1524 (Ros.S50) [A:90]
R_Date BRAMS-1525 (Ros.S50) [A:46]
Phase Rosheim-Sandgrube, pit 50
R_Date BRAMS-1526 (Ros.L122) [A:112]
R_Date SUERC-46440 (Ling.37) [A:82]
R_Date OxA-27820 (Erst.28) [A:101]
R_Combine Erst.19 [A:121]
R_Date SUERC-46284 (Ros.111) [A:99]
R_Date OxA-27818 (Ros.87) [A:101]
R_Date SUERC-46435 (Ros.82) [A:112]
R_Date Poz-34086 (Entz.7162) [A:113]
R_Date Poz-34094 (Entz.7157) [A:127]
R_Date SUERC-46278 (Ros.108) [A:95]
R_Date SUERC-46283 (Ros.100) [A:97]
R_Date OxA-27817 (Ros.95) [A:121]
R_Date OxA-27815 (Ros.91) [A:118]
R_Date SUERC-42679 (Ros.88) [A:99]
R_Date OxA-27816 (Ros.83) [A:100]
R_Date BRAMS-1527 (Ros.MW63) [A:98]
R_Date Poz-34093 (Entz.7125) [A:93]
R_Date Poz-34072 (Entz.7007) [A:126]
R_Date Poz-34076 (Entz.7103) [A:119]
R_Date Poz-34080 (Entz.7119) [A:109]
R_Date Poz-34092 (Entz.7117) [A:101]
R_Date Poz-34079 (Entz.7114) [A:84]
R_Date OxA-27813 (Ros.112) [A:123]
R_Date SUERC-46276 (Ros.89) [A:26]
R_Combine Ros.76 [A:109]
R_Combine Ros.45 [A:120]
R_Date SUERC-46517 [A:105]
R_Date OxA-27811 [A:120]
Phase KV.656
R_Date Poz-34081 (Entz.7121) [A:109]
R_Date Poz-34083 (Entz.7126) [A:83]
R_Date Poz-34073 (Entz.7043) [A:108]
R_Date Poz-34091 (Entz.7112) [A:96]
R_Date Poz-34077 (Entz.7105) [A:108]
R_Date SUERC-46274 (Ros.85) [A:124]
R_Date SUERC-46273 (Erst.7) [A:109]
R_Date OxA-27810 (Ling.42) [A:105]
Phase Grossgartach
Boundary end HK/start GG
R_Date SUERC-60026 (Aldingen 7) [A:114]
R_Date SUERC-60027 (Aldingen 2) [A:33]
R_Date Poz-34074 (Entz.7056) [A:87]
R_Date Poz-33546 (Erst.2) [A:121]
Phase Hinkelstein
End end start HK
Start start start HK
Boundary start of HK
Sequence Alsace Middle Neolithic [Amodel: 100]
5400
5200
5000
4800
4600
4400
Modelled date (cal BC)

Site	Location	Potsherd #	Description	Cº (µg/g)	Laboratory#	$C_{16:0}$ age	$C_{18:0}$ age	Combined age	Reference
Sweet Track	Somerset levels, England	SW1	Carinated bowl, refitted sherd	13,806	BRAMS-1520	5,105 ± 33	5,114 ± 32	5,110 ± 25	9, 10, 25
		SW2	Carinated bowl, refitted sherd	4,900	BRAMS-1521	5,089 ± 38	5,094 ± 32	5,092 ± 26	
Çatalhöyük East 'TP Area'	Turkey	TP.M17	Holemouth jar, single sherd	393	BRAMS-1654	7,338 ± 42	7,416 ± 39	7,382 ± 31	11, 27
		TP.N10	Holemouth jar, refitted sherd	575	BRAMS-1699	7,318 ± 29	7,378 ± 30	7,348 ± 25	
		TP.O23	Holemouth jar, refitted sherd	1,390	BRAMS-1546	7,290 ± 36	7,375 ± 32	7,340 ± 27	
		TP.P13	Holemouth jar, single sherd	362	BRAMS-1703	7,328 ± 36	7,394 ± 29	7,364 ± 25	
Rosheim 'Sandgrube'	Lower Alsace, France	ROS-C-4596	Coarse kumpf, single sherd	973	BRAMS-1526	5,810 ± 30	5,798 ± 30	5,804 ± 25	12
		ROS-C-4600	Coarse kumpf, refitted sherd	4,163	BRAMS-1527	5,897 ± 36	5,909 ± 35	5,904 ± 28	
		ROS-C-4644	Fine kumpf, single sherd	6,064	BRAMS-1525	5,937 ± 33	5,926 ± 30	5,931 ± 26	
		ROS-C-4657	Coarse kumpf, single sherd	1,914	BRAMS-1524	5,885 ± 37	5,934 ± 34	5,912 ± 28	
Ensisheim 'Ratfeld'	Upper Alsace, France	ENS-C-5913	Coarse kumpf, single sherd	1,177	BRAMS-1915	6,345 ± 31	6,303 ± 31	6,324 ± 26	12, 13
		ENS-C-5915	Coarse kumpf, single sherd	771	BRAMS-1916	6,383 ± 32	6,314 ± 33	6,348 ± 26	
		ENS-C-5934	Coarse kumpf, single sherd	1,645	BRAMS-1958	6,282 ± 30	6,258 ± 30	6,270 ± 25	
		ENS-C-5940	Coarse kumpf, single sherd	2,082	BRAMS-2031	6,162 ± 33	6,239 ± 30	6,206 ± 26	
Cuiry-lès-Chaudardes	Aisne, France	CUI-C-5708	Coarse kumpf, single sherd	881	BRAMS-1917	6,252 ± 34	6,218 ± 36	6,236 ± 27	12, 13
		CUI-C-5801	Coarse kumpf, single sherd	9,886	BRAMS-2021	6,138 ± 30	6,134 ± 30	6,136 ± 25	
Königshoven 14	Rhineland, Germany	KON-C-5594	Coarse kumpf, single sherd	531	BRAMS-2029	6,253 ± 29	6,298 ± 29	6,276 ± 24	12, 13
		KON-C-5598	Coarse kumpf, single sherd	1,023	BRAMS-2026	6,106 ± 34	6,139 ± 34	6,123 ± 27	
Geleen-Janskamperveld	Graetheide, The Netherlands	GEL-C-3298	Coarse kumpf, single sherd	577	BRAMS-2032	6,188 ± 31	6,253 ± 29	6,224 ± 25	12, 13
Karwowo 1	Pomeriania, Poland	KAR-C-3636	Coarse kumpf, single sherd	3,316	BRAMS-2028	6,176 ± 30	6,230 ± 30	6,204 ± 25	12, 13
		KAR-C-3677	Coarse kumpf, single sherd	1,900	BRAMS-2025	6,255 ± 30	6,214 ± 32	6,236 ± 26	
Ludwinowo 7	Kuyavia, Poland	LDW-C-2267	Coarse kumpf, single sherd	323	BRAMS-2024	6,173 ± 36	6,179 ± 30	6,177 ± 26	12, 13
Takarkori Rockshelter	Acacus mountains, Libya	TAK 21	Decorated, single sherd	9,503	BRAMS-1522	5,362 ± 33	5,331 ± 32	5,348 ± 24	14, 28, 29
		TAK1572	Decorated, single sherd	3,558	BRAMS-1523	5,099 ± 38	5,071 ± 32	5,085 ± 24	
		TAK 120	Decorated, single sherd	5,593	BRAMS-2608	6,008 ± 35	5,949 ±3 5	5,979 ± 28	
		TAK 420	Decorated, single sherd	1,119	BRAMS-2609	5,487 ± 34	5,498 ± 35	5,493 ± 28	
		TAK 443	Decorated, single sherd	1,7217	BRAMS-2610	6,021 ± 35	5,962 ± 35	5,992 ± 28	
Principal Place	London, England	PPL012 (<1814>)	Plain bowl, single sherd	713	BRAMS-2618	4,894 ± 34	4,928 ± 33	4,911 ± 27	15, 30
		PPL015 (<1845>)	Plain bowl, refitted sherd	1,999	BRAMS-2479	4,708 ± 33	4,771 ± 30	4,742 ± 22	
		PPL020 (<1850>)	Plain bowl, refitted sherd	3,660	BRAMS-2483	4,628 ± 40	4,670 ± 34	4,652 ± 26	
		PPL021 (<1819>)	Plain cup, single sherd	2,985	BRAMS-2485	4,732 ± 32	4,734 ± 30	4,733 ± 22	

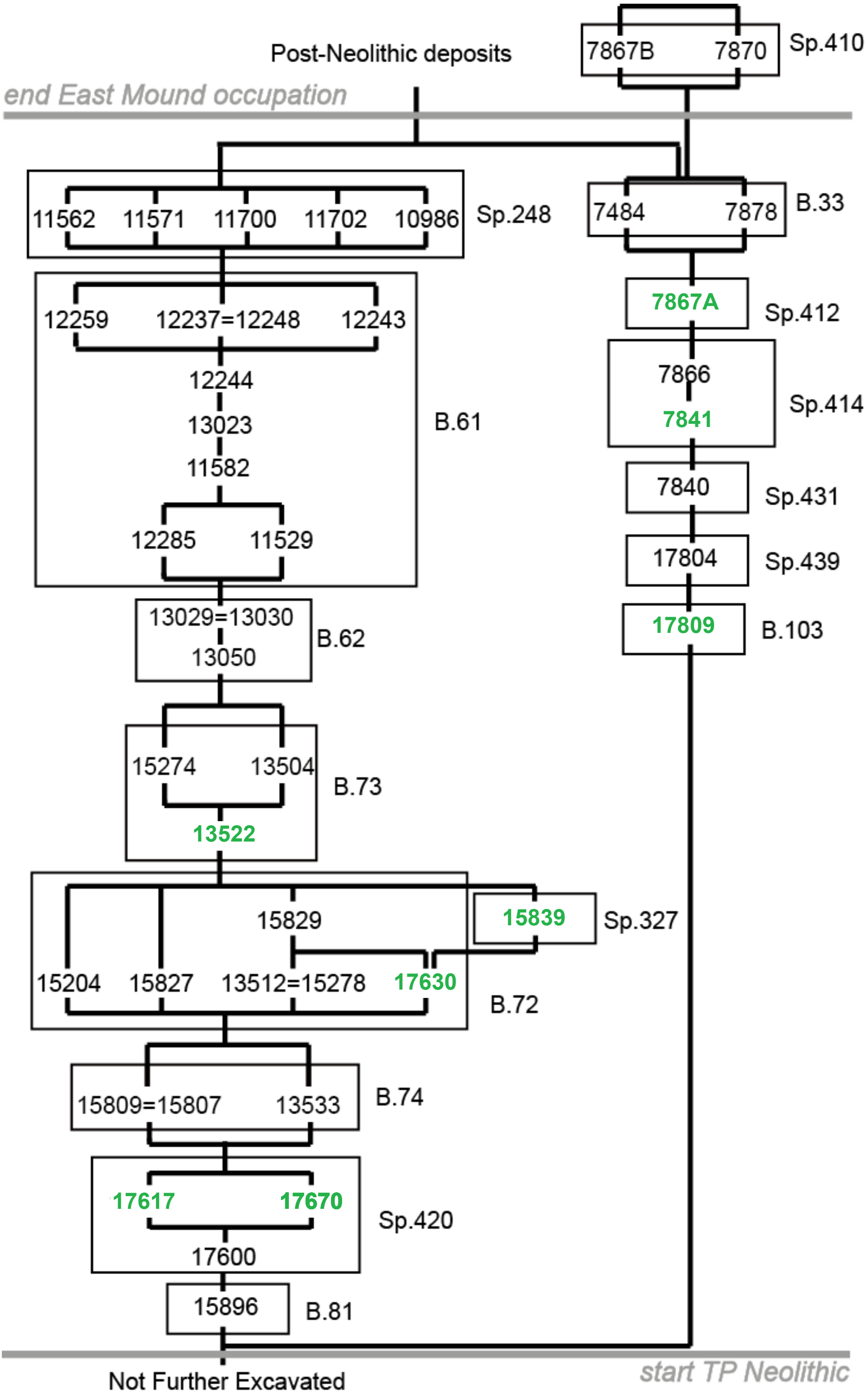

Post-Neolithic deposits
end East Mound occupation
7867B
7870
Sp.410
11562
11571
11700
11702
10986
Sp.248
7484
7878
B.33
12259
12237=12248
12243
7867A
Sp.412
12244
7866
13023
7841
Sp.414
B.61
11582
7840
Sp.431
12285
11529
17804
Sp.439
13029=13030
13050
B.62
17809
B.103
15274
13504
B.73
13522
15829
15839
Sp.327
15204
15827
13512=15278
17630
B.72
15809=15807
13533
B.74
17617
17670
Sp.420
17600
15896
B.81
start TP Neolithic
Not Further Excavated

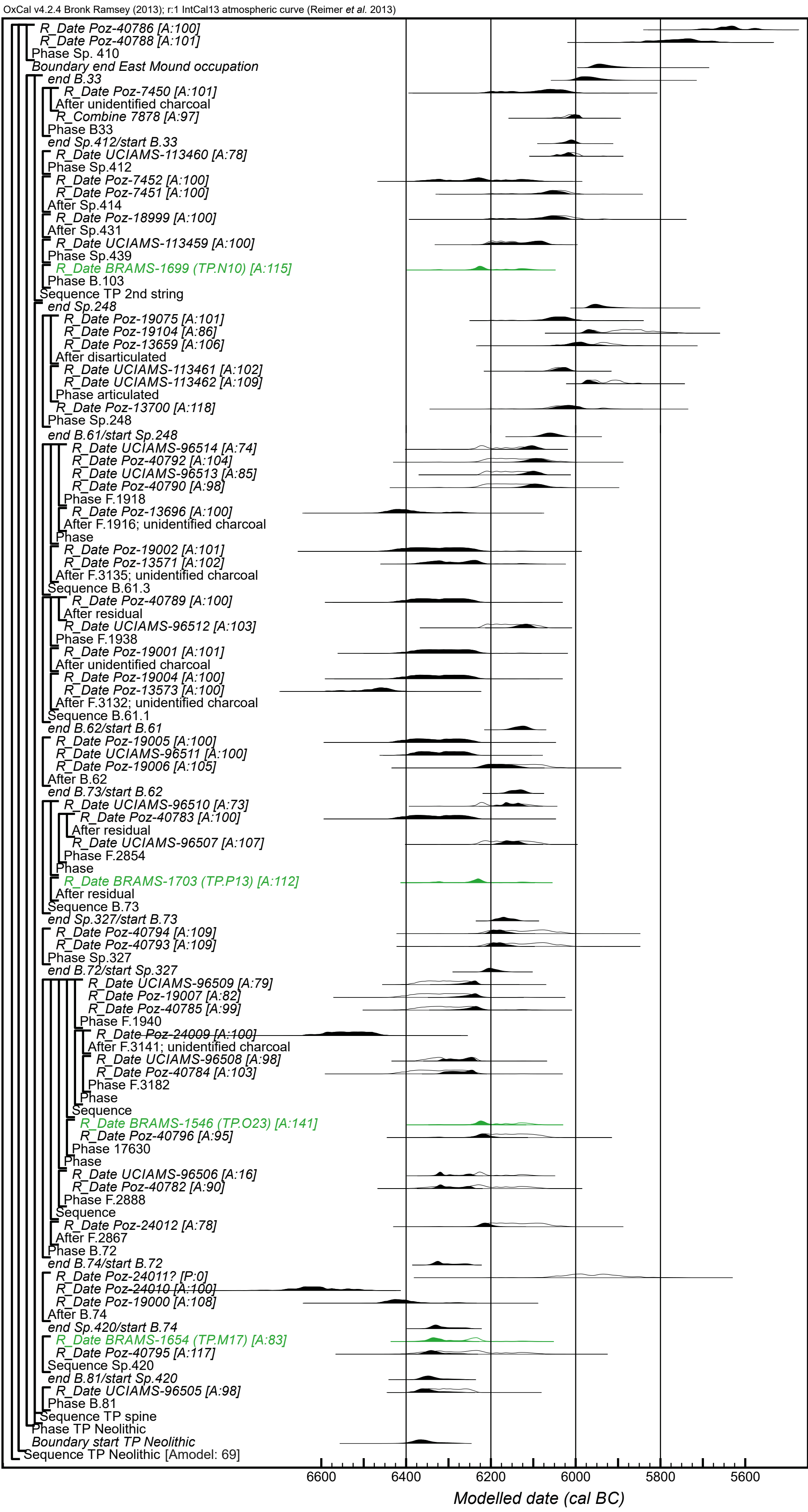
OxCal v4.2.4 Bronk Ramsey (2013); r:1 IntCal13 atmospheric curve (Reimer et al. 2013)
R_Date Poz-40786 [A:100]
R_Date Poz-40788 [A:101]
Phase Sp. 410
Boundary end East Mound occupation
end B.33
R_Date Poz-7450 [A:101]
After unidentified charcoal
R_Combine 7878 [A:97]
Phase B33
end Sp.412/start B.33
R_Date UCIAMS-113460 [A:78]
Phase Sp.412
R_Date Poz-7452 [A:100]
R_Date Poz-7451 [A:100]
After Sp.414
R_Date Poz-18999 [A:100]
After Sp.431
R_Date UCIAMS-113459 [A:100]
Phase Sp.439
R_Date BRAMS-1699 (TP.N10) [A:115]
Phase B.103
Sequence TP 2nd string
end Sp.248
R_Date Poz-19075 [A:101]
R_Date Poz-19104 [A:86]
R_Date Poz-13659 [A:106]
After disarticulated
R_Date UCIAMS-113461 [A:102]
R_Date UCIAMS-113462 [A:109]
Phase articulated
R_Date Poz-13700 [A:118]
Phase Sp.248
end B.61/start Sp.248
R_Date UCIAMS-96514 [A:74]
R_Date Poz-40792 [A:104]
R_Date UCIAMS-96513 [A:85]
R_Date Poz-40790 [A:98]
Phase F.1918
R_Date Poz-13696 [A:100]
After F.1916; unidentified charcoal
Phase
R_Date Poz-19002 [A:101]
R_Date Poz-13571 [A:102]
After F.3135; unidentified charcoal
Sequence B.61.3
R_Date Poz-40789 [A:100]
After residual
R_Date UCIAMS-96512 [A:103]
Phase F.1938
R_Date Poz-19001 [A:101]
After unidentified charcoal
R_Date Poz-19004 [A:100]
R_Date Poz-13573 [A:100]
After F.3132; unidentified charcoal
Sequence B.61.1
end B.62/start B.61
R_Date Poz-19005 [A:100]
R_Date UCIAMS-96511 [A:100]
R_Date Poz-19006 [A:105]
After B.62
end B.73/start B.62
R_Date UCIAMS-96510 [A:73]
R_Date Poz-40783 [A:100]
After residual
R_Date UCIAMS-96507 [A:107]
Phase F.2854
Phase
R_Date BRAMS-1703 (TP.P13) [A:112]
After residual
Sequence B.73
end Sp.327/start B.73
R_Date Poz-40794 [A:109]
R_Date Poz-40793 [A:109]
Phase Sp.327
end B.72/start Sp.327
R_Date UCIAMS-96509 [A:79]
R_Date Poz-19007 [A:82]
R_Date Poz-40785 [A:99]
Phase F.1940
R_Date Poz-24009 [A:100]
After F.3141; unidentified charcoal
R_Date UCIAMS-96508 [A:98]
R_Date Poz-40784 [A:103]
Phase F.3182
Phase
Sequence
R_Date BRAMS-1546 (TP.O23) [A:141]
R_Date Poz-40796 [A:95]
Phase 17630
Phase
R_Date UCIAMS-96506 [A:16]
R_Date Poz-40782 [A:90]
Phase F.2888
Sequence
R_Date Poz-24012 [A:78]
After F.2867
Phase B.72
end B.74/start B.72
R_Date Poz-24011? [P:0]
R_Date Poz-24010 [A:100]
R_Date Poz-19000 [A:108]
After B.74
end Sp.420/start B.74
R_Date BRAMS-1654 (TP.M17) [A:83]
R_Date Poz-40795 [A:117]
Sequence Sp.420
end B.81/start Sp.420
R_Date UCIAMS-96505 [A:98]
Phase B.81
Sequence TP spine
Phase TP Neolithic
Boundary start TP Neolithic
Sequence TP Neolithic [Amodel: 69]
6600
6400
6200
6000
5800
5600
Modelled date (cal BC)

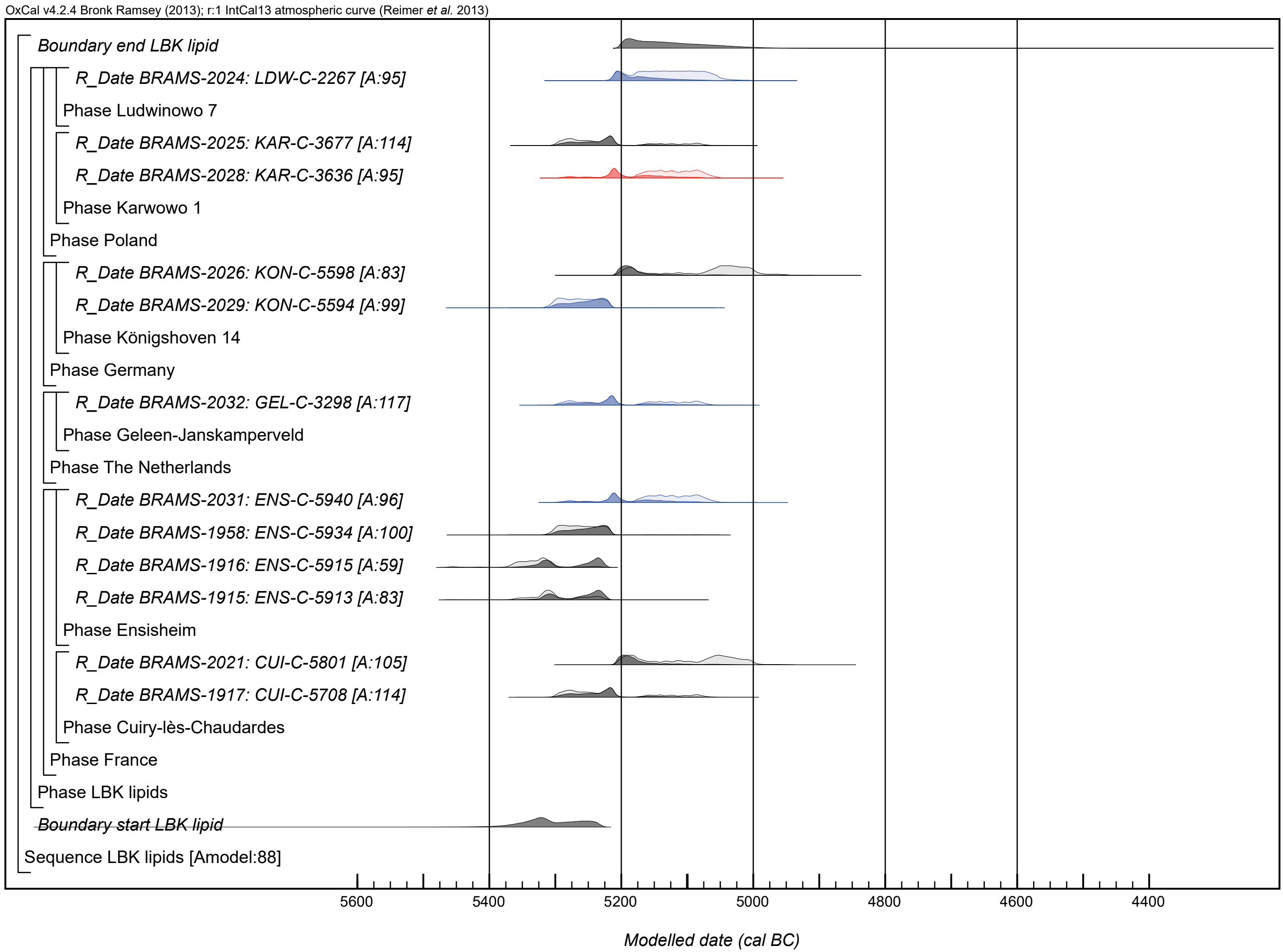
OxCal v4.2.4 Bronk Ramsey (2013); r:1 IntCal13 atmospheric curve (Reimer et al. 2013)
Boundary end LBK lipid
R_Date BRAMS-2024: LDW-C-2267 [A:95]
Phase Ludwinowo 7
R_Date BRAMS-2025: KAR-C-3677 [A:114]
R_Date BRAMS-2028: KAR-C-3636 [A:95]
Phase Karwowo 1
Phase Poland
R_Date BRAMS-2026: KON-C-5598 [A:83]
R_Date BRAMS-2029: KON-C-5594 [A:99]
Phase Königshoven 14
Phase Germany
R_Date BRAMS-2032: GEL-C-3298 [A:117]
Phase Geleen-Janskamperveld
Phase The Netherlands
R_Date BRAMS-2031: ENS-C-5940 [A:96]
R_Date BRAMS-1958: ENS-C-5934 [A:100]
R_Date BRAMS-1916: ENS-C-5915 [A:59]
R_Date BRAMS-1915: ENS-C-5913 [A:83]
Phase Ensisheim
R_Date BRAMS-2021: CUI-C-5801 [A:105]
R_Date BRAMS-1917: CUI-C-5708 [A:114]
Phase Cuiry-lès-Chaudardes
Phase France
Phase LBK lipids
Boundary start LBK lipid
Sequence LBK lipids [Amodel:88]
5600
5400
5200
5000
4800
4600
4400
Modelled date (cal BC)

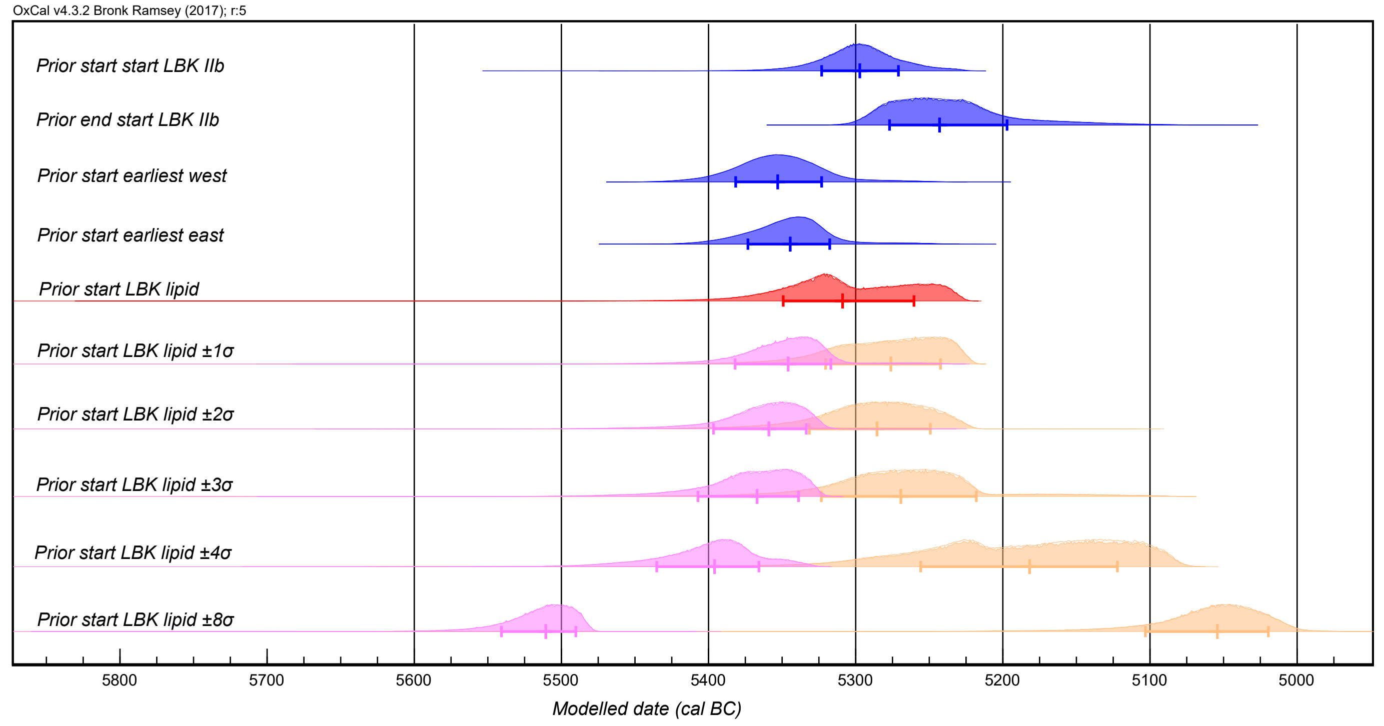

OxCal v4.3.2 Bronk Ramsey (2017); r:5
Prior start start LBK IIb
Prior end start LBK IIb
Prior start earliest west
Prior start earliest east
Prior start LBK lipid
Prior start LBK lipid ±1σ
Prior start LBK lipid ±2σ
Prior start LBK lipid ±3σ
Prior start LBK lipid ±4σ
Prior start LBK lipid ±8σ
5800
5700
5600
5500
5400
5300
5200
5100
5000
Modelled date (cal BC)

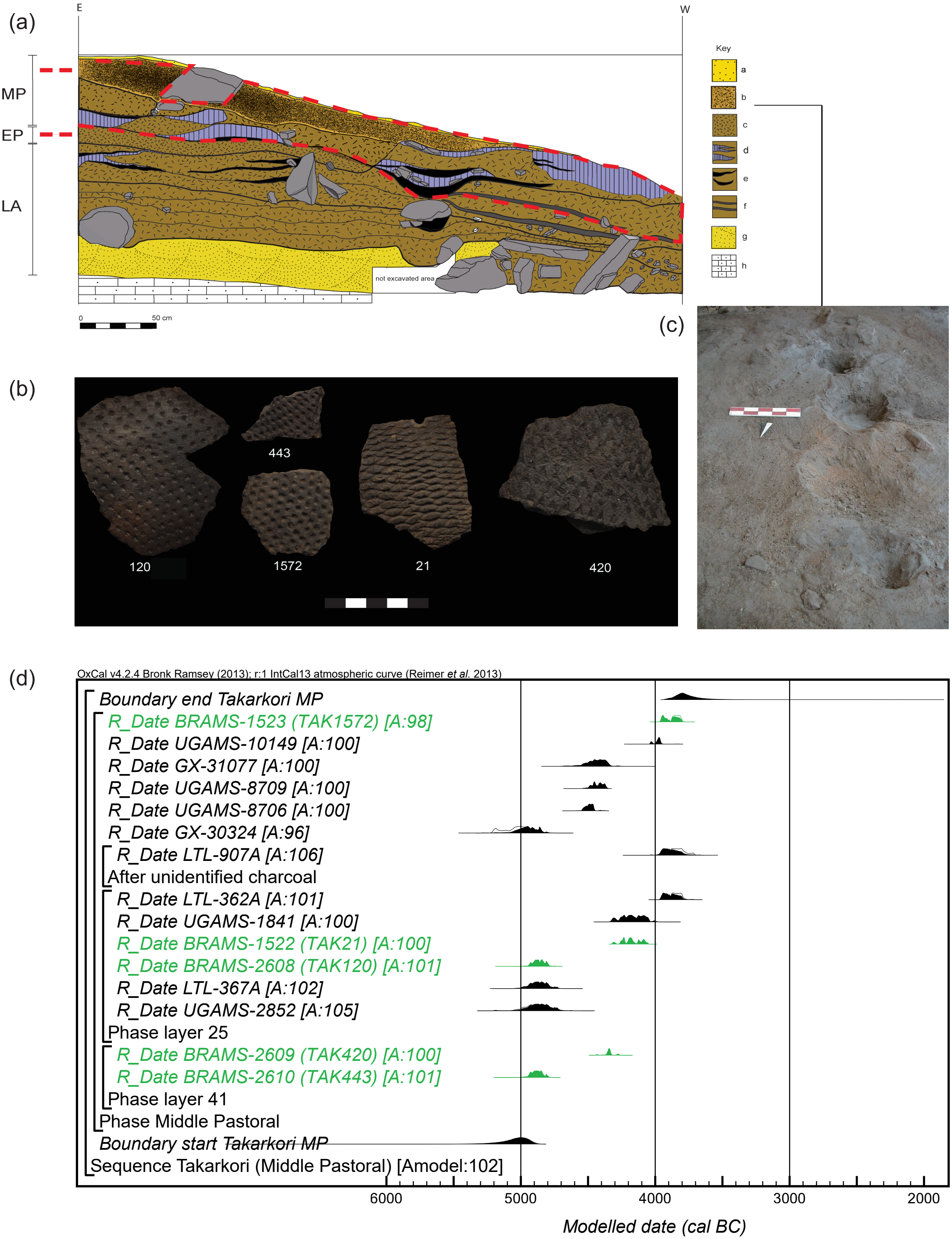
(a)
E
W
MP
EP
LA
Key
a
b
c
d
e
f
g
h
not excavated area
0
50 cm
(b)
443
120
1572
21
420
(c)
(d)
OxCal v4.2.4 Bronk Ramsey (2013); r:1 IntCal13 atmospheric curve (Reimer et al. 2013)
Boundary end Takarkori MP
R_Date BRAMS-1523 (TAK1572) [A:98]
R_Date UGAMS-10149 [A:100]
R_Date GX-31077 [A:100]
R_Date UGAMS-8709 [A:100]
R_Date UGAMS-8706 [A:100]
R_Date GX-30324 [A:96]
R_Date LTL-907A [A:106]
After unidentified charcoal
R_Date LTL-362A [A:101]
R_Date UGAMS-1841 [A:100]
R_Date BRAMS-1522 (TAK21) [A:100]
R_Date BRAMS-2608 (TAK120) [A:101]
R_Date LTL-367A [A:102]
R_Date UGAMS-2852 [A:105]
Phase layer 25
R_Date BRAMS-2609 (TAK420) [A:100]
R_Date BRAMS-2610 (TAK443) [A:101]
Phase layer 41
Phase Middle Pastoral
Boundary start Takarkori MP
Sequence Takarkori (Middle Pastoral) [Amodel:102]
6000
5000
4000
3000
2000
Modelled date (cal BC)

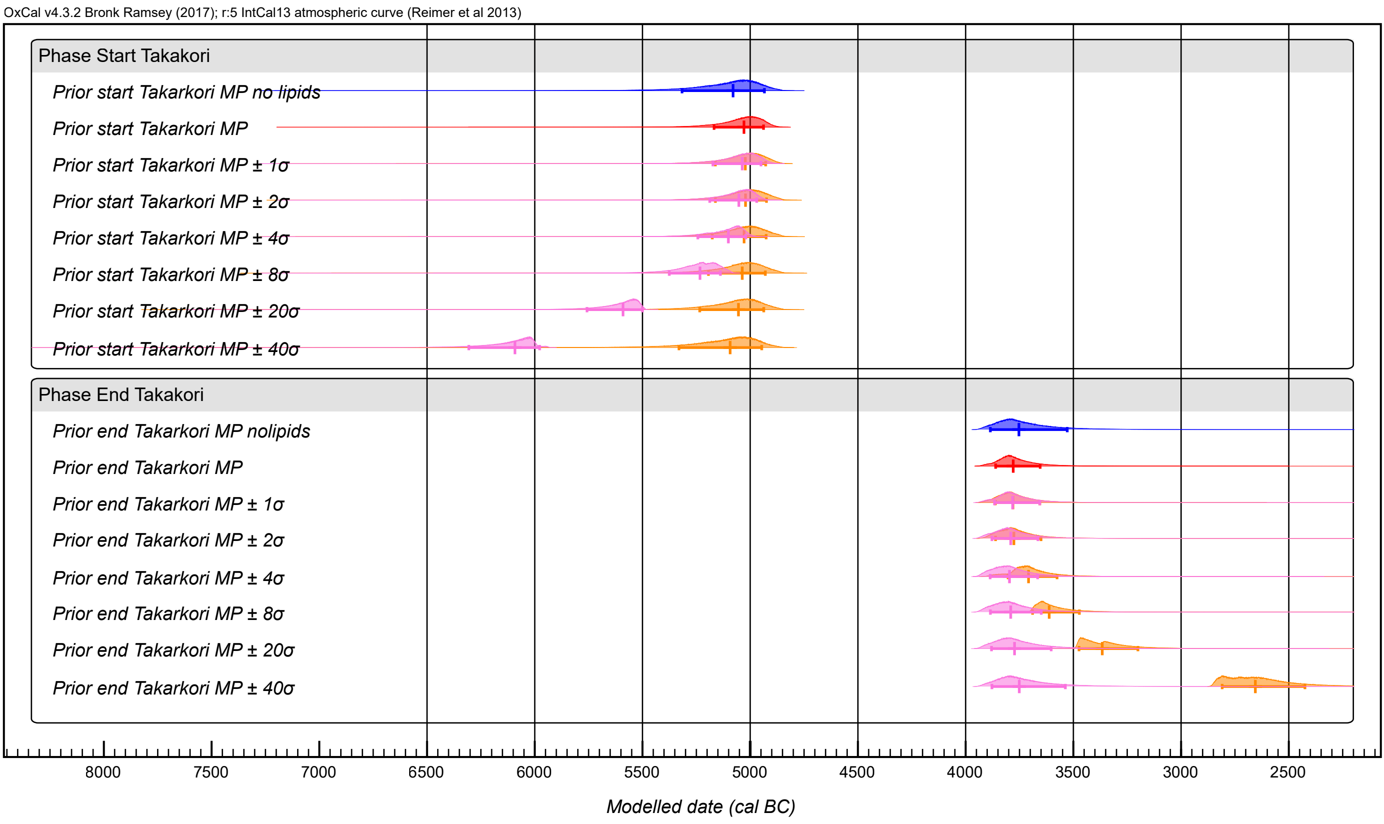

OxCal v4.3.2 Bronk Ramsey (2017); r:5 IntCal13 atmospheric curve (Reimer et al 2013)
Phase Start Takakori
Prior start Takarkori MP no lipids
Prior start Takarkori MP
Prior start Takarkori MP ± 1σ
Prior start Takarkori MP ± 2σ
Prior start Takarkori MP ± 4σ
Prior start Takarkori MP ± 8σ
Prior start Takarkori MP ± 20σ
Prior start Takarkori MP ± 40σ
Phase End Takakori
Prior end Takarkori MP nolipids
Prior end Takarkori MP
Prior end Takarkori MP ± 1σ
Prior end Takarkori MP ± 2σ
Prior end Takarkori MP ± 4σ
Prior end Takarkori MP ± 8σ
Prior end Takarkori MP ± 20σ
Prior end Takarkori MP ± 40σ
8000
7500
7000
6500
6000
5500
5000
4500
4000
3500
3000
2500
Modelled date (cal BC)

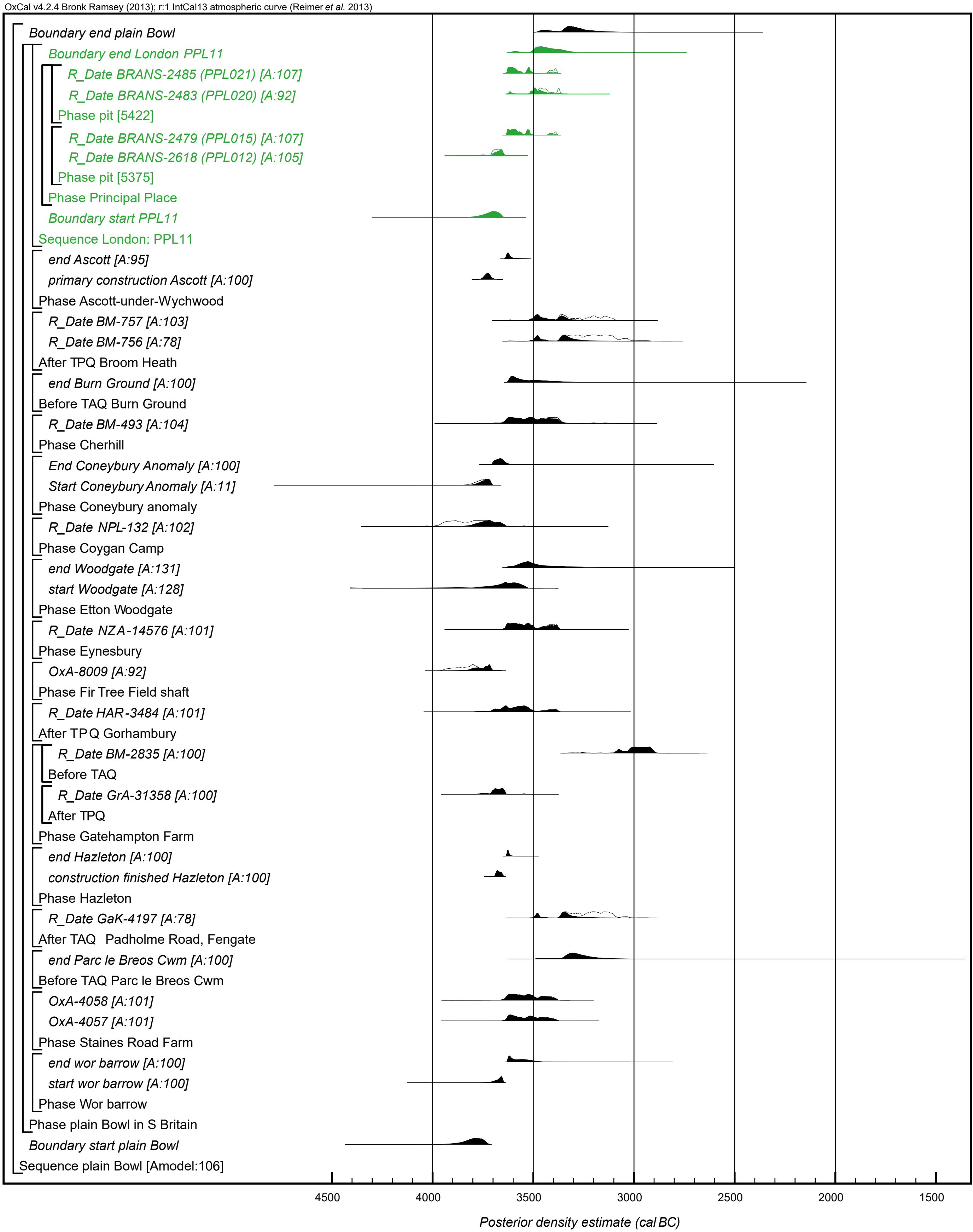
OxCal v4.2.4 Bronk Ramsey (2013); r:1 IntCal13 atmospheric curve (Reimer et al. 2013)
Boundary end plain Bowl
Boundary end London PPL11
R_Date BRANS-2485 (PPL021) [A:107]
R_Date BRANS-2483 (PPL020) [A:92]
Phase pit [5422]
R_Date BRANS-2479 (PPL015) [A:107]
R_Date BRANS-2618 (PPL012) [A:105]
Phase pit [5375]
Phase Principal Place
Boundary start PPL11
Sequence London: PPL11
end Ascott [A:95]
primary construction Ascott [A:100]
Phase Ascott-under-Wychwood
R_Date BM-757 [A:103]
R_Date BM-756 [A:78]
After TPQ Broom Heath
end Burn Ground [A:100]
Before TAQ Burn Ground
R_Date BM-493 [A:104]
Phase Cherhill
End Coneybury Anomaly [A:100]
Start Coneybury Anomaly [A:11]
Phase Coneybury anomaly
R_Date NPL-132 [A:102]
Phase Coygan Camp
end Woodgate [A:131]
start Woodgate [A:128]
Phase Etton Woodgate
R_Date NZA-14576 [A:101]
Phase Eynesbury
OxA-8009 [A:92]
Phase Fir Tree Field shaft
R_Date HAR-3484 [A:101]
After TPQ Gorhambury
R_Date BM-2835 [A:100]
Before TAQ
R_Date GrA-31358 [A:100]
After TPQ
Phase Gatehampton Farm
end Hazleton [A:100]
construction finished Hazleton [A:100]
Phase Hazleton
R_Date GaK-4197 [A:78]
After TAQ Padholme Road, Fengate
end Parc le Breos Cwm [A:100]
Before TAQ Parc le Breos Cwm
OxA-4058 [A:101]
OxA-4057 [A:101]
Phase Staines Road Farm
end wor barrow [A:100]
start wor barrow [A:100]
Phase Wor barrow
Phase plain Bowl in S Britain
Boundary start plain Bowl
Sequence plain Bowl [Amodel:106]
4500
4000
3500
3000
2500
2000
1500
Posterior density estimate (cal BC)

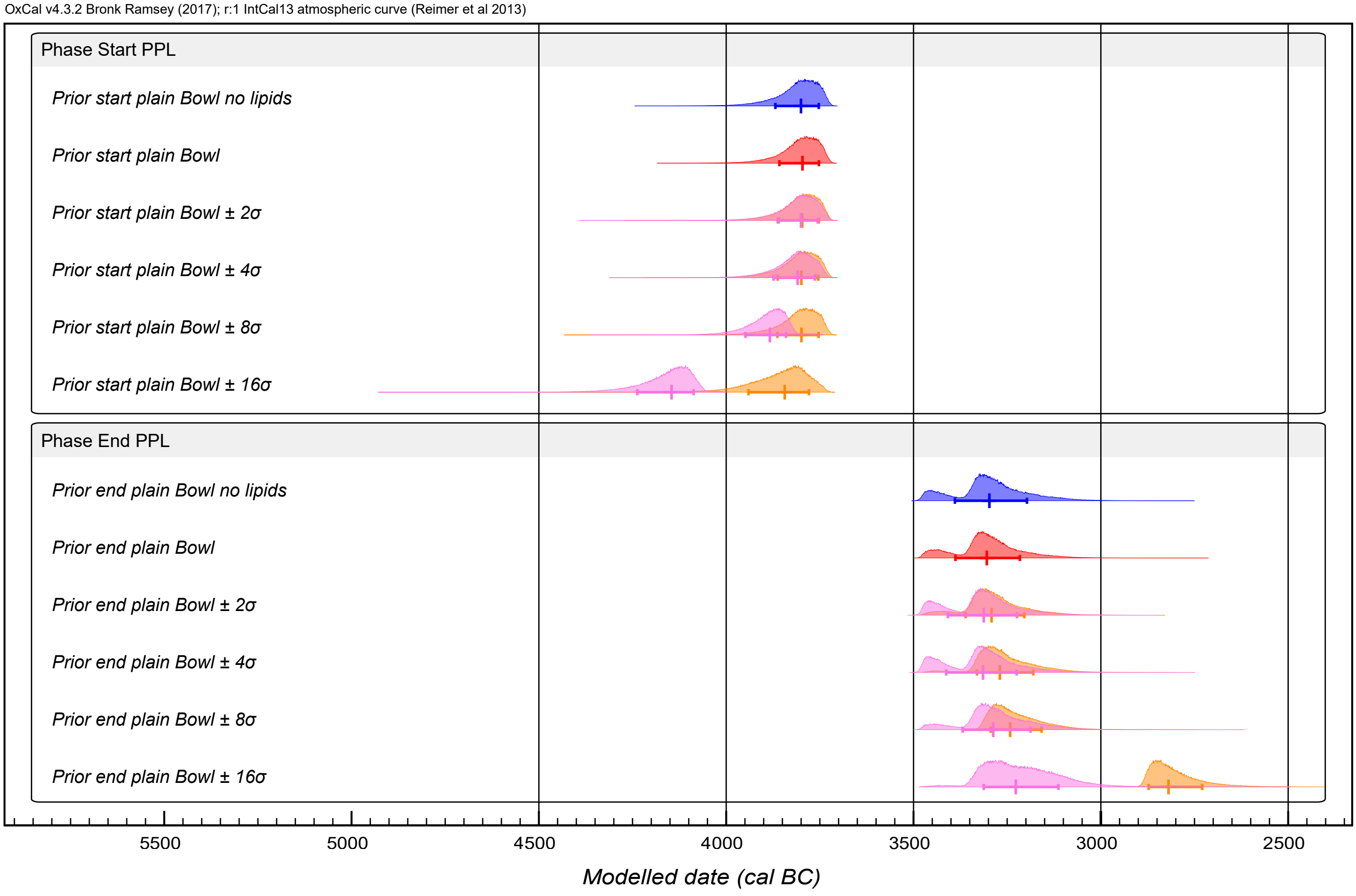

OxCal v4.3.2 Bronk Ramsey (2017); r:1 IntCal13 atmospheric curve (Reimer et al 2013)
Phase Start PPL
Prior start plain Bowl no lipids
Prior start plain Bowl
Prior start plain Bowl ± 2σ
Prior start plain Bowl ± 4σ
Prior start plain Bowl ± 8σ
Prior start plain Bowl ± 16σ
Phase End PPL
Prior end plain Bowl no lipids
Prior end plain Bowl
Prior end plain Bowl ± 2σ
Prior end plain Bowl ± 4σ
Prior end plain Bowl ± 8σ
Prior end plain Bowl ± 16σ
5500
5000
4500
4000
3500
3000
2500
Modelled date (cal BC)

SI guides

Accurate compound-specific ^{14}C dating of archaeological pottery vessels

Emmanuelle Casanova[1], Timothy D.J. Knowles[1,2], Alex Bayliss[3,4], Julie Dunne[1], Marek Z. Barański[5], Anthony Denaire[6], Philippe Lefranc[7], Savino di Lernia[8,9], Mélanie Roffet-Salque[1], Jessica Smyth[1,10], Alistair Barclay[11], Toby Gillard[1], Erich Claβen[12], Bryony Coles[13], Michael Ilett[14], Christian Jeunesse[15], Marta Krueger[16], Arkadiusz Marciniak[16], Steve Minnitt[17], Rocco Rotunno[8], Pieter van de Velde[18], Ivo van Wijk[19], MOLA[20] and Richard P. Evershed[1,2]

[1]Organic Geochemistry unit, School of chemistry, University of Bristol, Cantock's Close Bristol BS8 1TS, UK

[2] Bristol Radiocarbon Accelerator Mass Spectrometer, 43 Woodland Road, University of Bristol, Bristol BS8 1UU, UK

[3]Scientific Dating, Historic England, Cannon Bridge House, 25 Dowgate Hill, London, EC4R 2YA, UK

[4]Biological & Environmental Sciences, University of Stirling, FK9 4LA, Stirling, UK

[5]Academy of Fine Arts in Gdańsk, Faculty of Architecture and Design, ul. Targ Węglowy 6, Gdańsk, Poland

[6]University of Burgundy/UMR 6298 ARTEHIS, Bâtiment Sciences Gabriel, 6 Boulevard Gabriel, 21000 Dijon, France

[7]University of Strasbourg UMR 7044/INRAP, 10 rue Altkirch, 67100 Strasbourg, France

[8]Dipartimento di Scienze dell'Antichità, Sapienza, Università di Roma, Via dei Volsci, 122 – 00185 Roma, Italy

[9]GAES, University of the Witwatersrand, Johannesburg, South Africa

[10]School of Archaeology, University College Dublin, Belfield, D04F6X4, Ireland

[11]Cotswold Archaeology, Building 11, Keble Enterprise Park, Kemble, Cirencester GL7 6BQ, UK

[12]LVR-State Service for Archaeological Heritage, Endenicher Str. 133, 53115 Bonn, Germany

[13]Department of Archaeology, University of Exeter, Laver Building, North Park Road, Exeter, Devon, 27 EX4 4QE, UK

[14]Université Paris 1 Panthéon-Sorbonne, UMR 8215 TRAJECTOIRES, 21 allée de l'université, 92023 Nanterre, France

[15]University of Strasbourg, UMR7044, Misha, 5 allé du général Rouvillois, 67083 Strasbourg, France

[16]Institute of Archaeology, Adam Mickiewicz University, 61-614 Poznan, Poland

[17]Somerset County Museum, Taunton Castle, Castle Green, Taunton, TA1 1AA, UK

[18]Archaeological Research Leiden, Einsteinweg 2, 2333 CC Leiden, The Netherlands

[19]Faculty of Archaeology, Leiden University, Einsteinweg 2, 2333 CC Leiden, The Netherlands

[20]MOLA (Museum of London Archaeology), 46 Eagle Wharf Road, London N1 7ED

List of supplementary materials:

Comparison of radiocarbon dates of absorbed lipids with other chronological information (pdf)
This file contains the details on the methods employed (SI 1) as well as the discussion of the results for every case study presented in the paper (SI 2-7) and conclusions of the analyses (SI 8).

Sorted Table (text document)
This file contains the matrix of the correspondence analysis based on decorative motifs of main and secondary motifs during the Middle Neolithic in Alsace (SI 4).

Sweet_Track_OxCal_Model (OXCAL file)
This file is the OxCal code used for evaluation of the accurate dating of pottery vessels associated with the Sweet Track, Somerset levels, UK (SI 2).

TP_OxCal_Model (OXCAL file)
This file is the OxCal code used for evaluation of the accurate dating of pottery vessels from the TP area at Çatalhöyük East, Turkey (SI 3).

Alsace_Middle_Neolithic_OxCal_Model (OXCAL file)
This file is the OxCal code used for evaluation of the accurate dating of pottery vessels from the Alsatian Middle Neolithic, France (SI 4).

LBK_lipids_OxCal_Model (OXCAL file)
This file is the OxCal code used for evaluation of the accurate dating of pottery vessels from the LBK sites in Central Europe (SI 5).

Takarkori_Middle_Pastoral_OxCal_Model (OXCAL file)
This file is the OxCal code used for evaluation of the accurate dating of pottery vessels from the Middle Pastoral period at Takarkori, Libya (SI 6).

Plain_Bowl_OxCal_Model (OXCAL file)
This file is the OxCal code used for evaluation of the accurate dating of pottery vessels from Principal Place, London, UK (SI 7).

Comparison of radiocarbon dates of absorbed lipids with other chronological information

SI 1. Methodological information

In this paper we evaluated the compatibility of the first radiocarbon dates measured on archaeological pot lipid residues, obtained using the methods presented by Casanova *et al.*[5,6], with pre-existing chronological information. In order to test the accuracy of the reported radiocarbon ages on absorbed fatty residues, we carefully selected samples from sites that already had robust and precise chronologies from a variety of sources. It is extremely difficult to obtain datable pottery that is of known age or paired with other organic material that is certainly contemporaneous. Chronologies produced by combining scientific dating with archaeological prior information can, however, produce robust and precise chronologies for the deposits from which pottery has been dated. The accuracy of the ^{14}C dates on absorbed fatty acids can therefore be assessed by comparison with the date estimated for the parent context from the chronological model.

This has been done in three ways:

1) by comparing posterior density estimates for key parameters from a model with equivalent archaeological date estimates, or the age known from dendrochronology (inaccuracies in ^{14}C measurements would be identified when the posterior density for key parameters deviate significantly from the equivalent archaeological date estimates),
2) using the individual and model indices of agreement (Bronk Ramsey[34], p429; Bronk Ramsey[18], p357) when the measurements on absorbed fatty acids are included in the relevant chronological model (inaccuracies in ^{14}C measurements would be identified when the indices of agreement fall below the critical value of 60),
3) by comparing posterior density estimates for key parameters from a model including the ^{14}C dates on absorbed fatty acids with the equivalent parameters from the model that does not include the new data (inaccuracies in ^{14}C measurements would be identified when the posterior density for key parameters deviate significantly from the equivalent parameters in the existing model).

As Bayesian chronological models are context specific, the power of these tests will vary (based on the amount of prior chronological information and nature of the Bayesian model), but in cases where the prior information is extremely informative (for example, tree-ring wiggle-matching), they can be very sensitive to inaccuracies in the data (cf Bayliss *et al.*[36], tables 5-6 and fig 8). We illustrate the sensitivity of each case study using simulations. All modelling has been undertaken using the radiocarbon ages reported for the combined measurements on the $C_{16:0}$ and $C_{18:0}$ fractions using OxCal v4.2 and v4.3[18] and the currently internationally agreed radiocarbon calibration curve for the northern hemisphere, IntCal13[26]. These compatibility assessments within pre-existing chronological frameworks provide the most rigorous compatibility tests of pot lipid dates.

The construction of the Sweet Track, Somerset, UK has been dated by dendrochronology[10]. The other sites have Bayesian chronological models that incorporate series of radiocarbon dates on traditional sample types with a variety of prior archaeological information: stratigraphy (Çatalhöyük East, Turkey), seriation of closed ceramic assemblages by correspondence analysis (the Middle Neolithic sequence in Lower Alsace, France/Germany), and cultural phases (*Linearbandkeramik* in Northern and Western Europe, the Middle Pastoral Neolithic at Takarkori in south-west Libya, and plain Bowl pottery in Southern Britain).

These sites were previously subject to extensive organic residue analysis (ORA), which allowed us to select the most suitable pottery vessels for compound-specific radiocarbon analyses (CSRA). All sherds sampled for CSRA had previously been sampled for ORA. The number of analyses undertaken was:

1) Sweet Track: 13 potsherds for ORA, 2 for CSRA;
2) Çatalhöyük East: 87 potsherds for ORA, 15 for CSRA;
3) Middle Neolithic sequence in Lower Alsace: 86 potsherds for ORA, 8 for CSRA;
4) *Linearbandkeramik* in Northern and Western Europe: over 3000 potsherds for ORA, 22 for CSRA;
5) Takarkori: 81 potsherds for ORA, 5 for CSRA;
6) Principal Place London: 31 potsherds for ORA, 5 for CSRA.

These numbers illustrate the proportion of sherds that would be suitable for dating to answer a particular research question currently (e.g. at Takarkori we focussed on dairy residues only).

The potsherds were carefully selected to contain lipid residues that had been identified as fats from terrestrial animals (ruminant carcass fats and ruminant dairy fats[7,28,37]) in order to avoid any radiocarbon reservoir effects arising from the processing of aquatic products from marine or freshwater environments. The terrestrial animal fats are dominated by $C_{16:0}$ and $C_{18:0}$ fatty acids, compounds which also occur in nature from other sources (e.g. vegetation or soil bacteria). For this reason, we excluded potsherds with lipid profiles indicating additional compounds (e.g. *n*-alkanes) which could suggest that the fatty acids derived partly from a source other than terrestrial animal fats (see manuscript Fig. 1b). We targeted potsherds with lipid concentrations that allowed the extraction of a minimum of 200 µg of both fatty acids when 1–10g of sherd was sampled. The available size of sherds, but also inhomogeneity in lipid distribution within the vessel wall, affected the extraction yield during the second sampling for radiocarbon analyses (e.g. Çatalhöyük East, Turkey).

The $C_{16:0}$ and $C_{18:0}$ fatty acids (FAs) extracted from the pottery sherds derive from animal fats absorbed by the vessel during its period of use. Both compounds should therefore give radiocarbon ages that are identical within error[6]. The contribution of the methyl group of fossil origin added during the simultaneous extraction and derivatization of the FAs into fatty acid methyl esters (FAMEs) was corrected by mass balance[6,21]. We consider that the corrected measurements on the two FAs extracted from the same pot are compatible when they are not statistically significantly different at the 5% significance level (according to Ward and Wilson[33]).

Where the radiocarbon measurements on the individual FAs from a potsherd are outside these limits, the results are thought not to provide a reliable date for the sherd as one or both of the FA samples may have been contaminated by exogenous carbon during processing. As we have no way to estimate which of the radiocarbon results reflects the true age of vessel use, in such cases neither measurement has been included in the statistical modelling. Samples where the $C_{16:0}$ and $C_{18:0}$ FAs were isolated together in the same trap (to obtain sufficient C for dating) were also excluded from the modelling exercise.

The radiocarbon measurements on the $C_{16:0}$ and $C_{18:0}$ FAs that were not statistically significantly different at the 5% significance level were combined for the statistical modelling. As these were extracted from the same vessel during the same pcGC run, any additional uncertainties introduced as a result of sample preparation procedures are not entirely statistically independent. Therefore, the errors for the radiocarbon ages reported for the combined fractions were calculated using the following equation:

$$\sigma_f = \sqrt{\sigma_{wm}^2 + \sigma_{ss}^2}$$

Where σ_f is the final overall uncertainty associated with the combined measurements of the FAs, σ_{wm} is the combined (reduced) uncertainty from the weighted mean of measurements using only the AMS uncertainty (equivalent to $\sigma_{\langle Rmol,bl,f\rangle}$ in Wacker *et al.*[31]), and σ_{ss} is the sample scatter factor to account for additional uncertainties associated with sample preparation (equivalent to σ_{ex} in Wacker *et al.*[31]). A value of 0.0025 was used in this study which was determined by calculating the value required to obtain a right-tailed P value of close to 0.5 from a χ^2 test of over 150 pot lipid dates (normalised such that the weighted mean of the $C_{16:0}$ and $C_{18:0}$ FA dates was 1 after removal of outliers outside the 1.5 IQR range). A σ_{ss} value of 0.0025 yielded a right-tailed P value of 0.585.

Readers wishing to utilise radiocarbon measurements reported in this paper should use the corrected and combined radiocarbon results e.g. BRAMS-1520 (5110 ± 25 BP) is the conventional radiocarbon age for pot SW1 (or SWD1299) from the Sweet Track.

SI 2. Sweet Track, Somerset, UK

The Sweet Track is an elevated wooden trackway, c. 2.1km in length, which crossed the Somerset Levels in south-west England between the Polden Hills and Westhay Island[38]. Dendrochronology has determined that it was constructed between the winter of 3807/6 BC and the spring of 3806 BC, with evidence of repair between 3804 and 3800 BC[10]. It has been suggested that the track may only have been used for about a decade, before it became unusable as a result of flooding in the winter and summer reed growth[38] (Coles 1999[39], p164).

These precise dates for the construction and use of the Sweet Track can be applied to the artefacts (e.g. pottery, flints and tools) recovered adjacent to the track, although we do not know that they are precisely contemporary. The pottery vessels may include lipids accumulated over the use life of the vessels, the duration of which is unknown, and we do not know when within the use life of the trackway the pottery vessels were deposited. But this association, which is probably within a few years, represents the best archaeological situation available. The pottery assemblage consisted entirely of fine wares of the early Neolithic Bowl tradition. Thirteen potsherds (SW1–SW13) from nine vessels were sampled for organic residue analysis (Berstan *et al.*[23], table 1), most of which were recovered from near the southern end of the trackway[9,40].

Two of these sherds, SW1 (vessel SWD 1299) and SW2 (vessel SWC 124), were analysed as part of this project (Table s1). Each sherd produced statistically consistent radiocarbon measurements on the $C_{16:0}$ and $C_{18:0}$ fatty acids (Table s1; T'=0.0, T'(5%)=3.8, ν=1 for both[33]). The combined results on the lipids are statistically indistinguishable from those included in IntCal13 for the relevant decade (UB-1198, 5020±23 BP; GrN-9024, 5058±18 BP; QL-11528, 5083±17 BP with total errors estimated using the multipliers suggested by Reimer *et al.*[41] (table 1); T'=9.0, T'(5%)=9.5, ν=4), and also with the interpolated value for 5755 cal BP (3806 BC) from IntCal13 (T'=4.1, T'(5%)=6.0, ν=2).

But these are not replicate measurements on the same material, so we combine the dates on the decadal and bi-decadal blocks of wood included in IntCal13 with the measurements on the lipids (see manuscript Fig. 2c). Although the dates are in agreement with the interpretation of these samples as contemporaneous (Acomb: 50.9; An: 31.6; n: 5), in this model *UB-1198* has poor individual agreement (A: 29), probably because of the bi-decadal bandwidth of this sample. It is clear however, that the combined results on the lipids are compatible with the dendrochronological date on the timbers of the trackway (see manuscript Fig. 2c).

Table s1. Lipid concentration, stable isotope ratios (measured by gas chromatography-combustion-stable isotope ratio mass spectrometry[37]), conventional radiocarbon ages (as defined by Stuiver and Polach[32] and calculated according to Wacker *et al.*[31]) and statistical consistency (χ^2 test, n=2 independent ^{14}C ages) on lipids extracted from pottery vessels associated with the Sweet Track.

Pot#	Description	Lipid C° (μg/g)	$AreaC_{16:0}$/ $AreaC_{18:0}$	$\delta^{13}C_{16:0}$ (‰)	$\delta^{13}C_{18:0}$ (‰)	$\Delta^{13}C$ (‰)	Assignment	Compound dated	Laboratory #	Conventional radiocarbon age (BP)	Statistical consistency
SW1	Complete refitted profile of a carinated bowl (SWD1299, 130/1986/2453)	13806	0.9	-30.1	-32.8	-2.7	Ruminant adipose fats	$C_{16:0}$ $C_{18:0}$ **Combined**	BRAMS-1520.1.1 BRAMS-1520.1.2 **BRAMS-1520**	5,105 ± 33 5,114 ± 32 **5,110 ± 25**	* T′=0.0, T′(5%)=3.8, ν=1
SW2	Complete refitted profile of a carinated bowl (SWC124, 130/1986/2452)	4900	0.9	-28.8	-33.6	-4.8	Dairy fats	$C_{16:0}$ $C_{18:0}$ **Combined**	BRAMS-1521.1.1 BRAMS-1521.1.2 **BRAMS-1521**	5,089 ± 38 5,094 ± 32 **5,092 ± 23**	* T′=0.0, T′(5%)=3.8, ν=1

* $C_{16:0}$ and $C_{18:0}$ conventional radiocarbon age statistically identical at the 5% significant level[33]

SI 3. Çatalhöyük East, Turkey

Marcinak *et al.*[11] present a Bayesian chronological model for late Neolithic deposits in the TP Area of the east mound at Çatalhöyük, Turkey. Fifty of the 56 radiocarbon measurements from this area of the site are incorporated in this model with the recorded stratigraphic sequence in this part of the mound (Marcinak *et al.* [11], figs 2–3 and table 1).

As part of this study, radiocarbon measurements were obtained on $C_{16:0}$ and $C_{18:0}$ fatty acids extracted from 15 pottery sherds from this sequence (Table s2). Four of the dated sherds come from units that have already produced radiocarbon dates, and the rest come from units that can be placed within the stratigraphic sequence of dated deposits (ED Fig. 1).

The measurements on only four sherds meet the quality assurance criteria employed in this study. For the remaining potsherds, one failed the internal criteria, one had combined $C_{16:0}$ and $C_{18:0}$ in the same trap (thus there was no possible quality criterion) and the nine remaining had a small amount of extracted C (<100 µg) for at least one of the targets could not. For this study 200 µg blanks were prepared, and so these small targets could not be reliably blank corrected using them. They were measured and reported in Table s2, however, to assess whether the 100 µg cut-off was appropriate. This issue likely came from the small sherd sizes available for sampling and potential inhomogeneous lipid distribution within them.

When the four dates which passed the quality control are included the model for the Neolithic deposits in the TP Area (cf. Marciniak *et al.*[11], fig 2), the model has poor overall agreement (Amodel: 53; model not shown). Two dates have poor individual agreement: *BRAMS-1703* (*TP.P13*) (A: 16) and *UCIAMS-96506* (A: 21). The stratigraphic position of this sherd is clearly forcing the posterior distribution of *BRAMS-1703* (*TP.P13*) in this model to be much later than the radiocarbon date itself would suggest. Since the two dates on samples of refitting sherds have good individual agreement in this model (*BRAMS-1699* (*TP.N10*), A: 115; *BRAMS-1546* (*TP.O23*), A: 140), it seems likely that TP.P13 is reworked in the midden from which it was recovered.

When this interpretation is included in a revised model for the Neolithic deposits in the TP Area, with TP.P13 included as a *terminus post quem* for unit 13522, the model has good overall agreement (Amodel: 69; ED Fig. 2) and all four dates on absorbed residues have good individual agreement (*BRAMS-1699* (*TP.N10*), A: 115; *BRAMS-1703* (*TP.P13*), A: 112; *BRAMS-1546* (*TP.O23*), A: 141; and *BRAMS-1654* (*TP.M17*), A: 83).

BRAMS-1546 is on a residue from three refitting sherds and was found in the same midden deposit as an articulating sheep left humerus and radius that has also been dated (Poz-40796, 7310 ± 50 BP). These measurements are again statistically consistent at the 5% significance level ($T'=0.0$, $T'(5\%)=3.8$, $\nu=1$), although again there are archaeological uncertainties about the duration of midden accumulation and the time width of the sampled material (although both are likely to amount to a few decades at most).

We have investigated how far the reported results on the absorbed lipids would have to change before the indices of agreement in the model shown in ED Fig. 2 would identify them as inaccurate, by deliberately biasing each measurement to varying degrees (e.g. a 1 sigma bias younger for BRAMS-1654 = 7351 ± 31 BP). The results are summarised in Table s3. For BRAMS-1546 we also report the statistical consistency of the deliberately biased measurement with Poz-40796 ($T'(5\%)=3.8$, $\nu=1$ for all).

Table s2. Lipid concentration, stable isotope ratios (measured by gas chromatography-combustion-stable isotope ratio mass spectrometry[37]), conventional radiocarbon ages (as defined by Stuiver and Polach32 and calculated according to Wacker *et al.*[31]) and statistical consistency (χ^2 test, n=2 independent ^{14}C ages on the $C_{16:0}$ and $C_{18:0}$ FAs) on lipids extracted from pottery vessels from Çatalhöyük East, TP area.

Pot#	Description	Lipid C° (µg/g)	AreaC$_{16:0}$/ AreaC$_{18:0}$	$\delta^{13}C_{16:0}$ (‰)	$\delta^{13}C_{18:0}$ (‰)	$\Delta^{13}C$ (‰)	Assignment	Compound dated	Laboratory #	Conventional radiocarbon age (BP)	Statistical consistency
TP.M12	Single sherd (S1) of a bowl from midden 17670, in Sp.420, level M	115	0.3	-28.4	-28.8	-0.4	Ruminant adipose fats	$C_{16:0}$/$C_{18:0}$	BRAMS-1698.1.1	7,154 ± 35	
TP.M17	Single sherd (S5) of a holemouth/deep jar from midden 17670 in Sp.420, level M	393	0.2	-24.1	-24.5	-0.4	Ruminant adipose fats	$C_{16:0}$ $C_{18:0}$ **Combined**	BRAMS-1654.1.1 BRAMS-1654.1.2 **BRAMS-1654**	7,338 ± 42 7,416 ± 39 **7,382 ± 31**	* T′=1.9, T′(5%)=3.8, v=1
TP.M24	Single sherd (S8) of a bowl from midden 17617 in Sp.420, level M	992	0.4	-25.9	-26.5	-0.6	Ruminant adipose fats	◊$C_{16:0}$ ◊$C_{18:0}$	BRAMS-1657.1.1	7,234 ± 46	
TP.N02	Two refitting sherds (S3) of a bowl from cluster 17809 in B.103, level N	362	0.5	-25.2	-26.6	-1.3	Ruminant adipose fats	◊$C_{16:0}$ $C_{18:0}$	BRAMS-1658.1.1 BRAMS-1658.1.2	6,963 ± 47 7,292 ± 43	X T′=26.7, T′(5%)=3.8, v=1
TP.N10	Two refitting sherds (S2) of a holemouth/deep jar from cluster 17809 in B.103, level N	575	0.5	-25.3	-27.0	-1.7	Ruminant adipose fats	$C_{16:0}$ $C_{18:0}$ **Combined**	BRAMS-1699.1.1 BRAMS-1699.1.2 **BRAMS-1699**	7,318 ± 29 7,378 ± 30 **7,348 ± 25**	* T′=2.7, T′(5%)=3.8, v=1
TP.O09	Two refitting sherds (S3) of a bowl from fill 17630 of pit F.6015 in B.72, level O	310	0.3	-25.3	-26.3	-1.0	Ruminant adipose fats	◊$C_{16:0}$ $C_{18:0}$	BRAMS-1656.1.1 BRAMS-1656.1.2	7,099 ± 65 7,239 ± 43	* T′=3.2, T′(5%)=3.8, v=1
TP.O15	Single sherd (S12) of a holemouth/deep jar from layer 15839 in Sp.327, level O	327	0.3	-24.3	-25.5	-1.2	Ruminant adipose fats	◊$C_{16:0}$ ◊$C_{18:0}$	BRAMS-1655.1.1	7,354 ± 51	
TP.O23	Three refitting sherds (S30) of a holemouth/deep jar from fill 17630 of pit F.6017 in B.72, level O	1390	0.3	-25.2	-27.0	-1.8	Ruminant adipose fats	$C_{16:0}$ $C_{18:0}$ **Combined**	BRAMS-1546.1.1 BRAMS-1546.1.2 **BRAMS-1546**	7,290 ± 36 7,375 ± 32 **7,340 ± 27**	* T′=3.1, T′(5%)=3.8, v=1
TP.P07	Single sherd (S40) of a holemouth/deep jar from infill 13522 in B.73, level P	640	0.7	-25.0	-27.8	-2.8	Ruminant adipose fats	◊$C_{16:0}$ $C_{18:0}$	- BRAMS-1701.1.2	- 7,230 ± 35	
TP.P13	Single sherd (S23) of a holemouth/deep jar from infill 13522 in B.73, level P	362	0.6	-22.3	-24.3	-2.1	Ruminant adipose fats	$C_{16:0}$ $C_{18:0}$ **Combined**	BRAMS-1703.1.1 BRAMS-1703.1.2 **BRAMS-1703**	7,328 ± 31 7,394 ± 29 **7,364 ± 25**	* T′=2.4, T′(5%)=3.8, v=1
TP.P14	Single sherd (S5) of a holemouth/deep jar from infill 13522 in B.73, level P	715	0.4	-22.6	-25.9	-3.3	Ruminant adipose fats	◊$C_{16:0}$ $C_{18:0}$	BRAMS-1591.1.1 BRAMS-1591.1.2	7,021 ± 70 7,271 ± 32	X T′=10.6, T′(5%)=3.8, v=1
TP.Q05	Single sherd (S13) of a holemouth/deep jar from midden 7841 in Sp.414, level Q	915	0.8	-27.7	-26.7	-2.0	Ruminant adipose fats	◊$C_{16:0}$ ◊$C_{18:0}$	BRAMS-1545.1.1 BRAMS-1545.1.2	6,717 ± 55 6,712 ± 43	* T′=0.0, T′(5%)=3.8, v=1
TP.Q06	Single sherd (S2) of a holemouth/deep jar from midden 7841 in Sp.414, level Q	331	0.3	-25.5	-27.4	-1.9	Ruminant adipose fats	◊$C_{16:0}$ $C_{18:0}$	BRAMS-1702.1.2	7,223 ± 32	
TP.Q07	Single sherd (S6) of a holemouth/deep jar from midden 7841 in Sp.414, level Q	471	0.5	-24.3	-25.8	-1.5	Ruminant adipose fats	◊$C_{16:0}$ $C_{18:0}$	BRAMS-1700.1.2	7,072 ± 36	
TP.R09	Single sherd (S1) of a holemouth/deep jar from midden 7867 in Sp.412, level R	989	0.3	-25.2	-26.5	-1.3	Ruminant adipose fats	$C_{16:0}$ $C_{18:0}$	BRAMS-1592.1.1 BRAMS-1592.1.2	7,012 ± 39 7,299 ± 38	X T′=27.8, T′(5%)=3.8, v=1

* $C_{16:0}$ and $C_{18:0}$ conventional radiocarbon age statistically identical at the 5% significant level[33]

X $C_{16:0}$ and $C_{18:0}$ conventional radiocarbon age statistically different at the 5% significant level[33]

◊ refers to compound that generated target with a mass of C below 100 µg. For this study 200 µg blanks were prepared, and so these small targets cannot be reliably blank-corrected using them. They were measured, however, to assess whether the 100 µg cut-off was appropriate.

On this basis we consider that this model is likely to have identified inaccuracies in the lipid dates at least as effectively as measurements on paired materials. It appears to be particularly sensitive to younger bias in BRAMS-1654.

Table s3. Agreement indices and χ^2 test (n=2 independent ^{14}C ages) for the combined lipid measurements deliberately biased as described in the text for Çatalhöyük East, TP area (form of model illustrated in ED Fig. 2); orange denotes poor agreement/statistically inconsistent at more than the 5% significance level.

	Amodel	A / T'		
		BRAMS-1699	BRAMS-1546	BRAMS-1654
1 sigma bias younger	56	105	105 / 0.0	26
1 sigma bias older	71	115	142 / 1.0	108
2 sigma bias younger	40	103	96 / 0.2	2
2 sigma bias older	68	108	113 / 2.2	107
3 sigma bias younger	26	104	91 / 0.8	0
3 sigma bias older	63	102	98 / 3.8	81
4 sigma bias younger	15	87	48 / 1.9	0
4 sigma bias older	53	102	100 / 5.8	27

SI 4. Middle Neolithic ceramic sequence, Lower Alsace, France/Germany

Denaire *et al.*[12] (fig 10 and electronic supplementary material matrix 2) present a seriation of the presence of 208 decorative motifs in 190 assemblages of Middle Neolithic pottery from pits and graves in Lower Alsace. The correspondence analysis was partitioned into four phases, which are interpreted as showing a temporal sequence which can be equated with the classically defined Hinkelstein, Grossgartach, Planig-Friedberg, and Rössen typological stages. The model incorporates this sequence, and the successive Bischheim and Bruebach-Oberbergen typological stages and, finally, two of the three phases of *Bischheim Occidental du Rhin Supérieur* (BORS) pottery identified by a second correspondence analysis (Denaire *et al.*[12], fig 13 and electronic supplementary material matrix 3) that produced datable material.

A total of ninety-five radiocarbon measurements are available from 84 samples from this sequence, along with two tree-ring dates from wells at Dambach. In order to ensure that the dated sample was the same age as the closed ceramic context from which it was recovered, samples of articulated human or animal bone (n=55), articulating animal bone (n=4), animal bone with refitting unfused epiphyses (n=6), paired bones judged to be from the same animal (n=2), and visible residues on pottery sherds (n=3) were targeted for dating. Measurements on seven disarticulated animal bones, three samples of cereal grain, and four samples of unidentified charcoal were inherited from previous work. Replicate measurements from two laboratories were obtained on nine samples, six of which were statistically consistent at the 5% significance level, with one other consistent at 1% significance level, and two divergent at more than this level of significance (Denaire *et al.*[12], table 2). These dates were combined with the sequence of ceramic phases derived from the correspondence analyses and typological study in the Bayesian statistical model presented in Denaire *et al.*[12] (figs 15 and 16).

Radiocarbon measurements have been obtained on $C_{16:0}$ and $C_{18:0}$ fatty acids extracted from eight pottery sherds from four features containing diagnostic assemblages of Middle Neolithic pottery from Lower Alsace (Table s4). The results on four sherds pass the quality assurance criteria used in this study, coming from three pits. Two of these features have been included in a revised correspondence analysis (manuscript Fig. 3a,b and supplementary text document "Sorted table"), although pit 50 at Rosheim-Sandgrube can only be assigned to the Grossgartach phase on typological grounds as it is a large pit complex (19m x 11m) that is clearly not a closed assemblage.

Table s4: Lipid concentration, stable isotope ratios (measured by gas chromatography-combustion-stable isotope ratio mass spectrometry[37]) conventional radiocarbon ages (as defined by Stuiver and Polach[32] and calculated according to Wacker *et al.*[31]) and statistical consistency (χ^2 test, n=2 independent ^{14}C ages on the $C_{16:0}$ and $C_{18:0}$ FAs) on lipids extracted from pottery vessels of the Grossgartach and Rössen ceramic phases.

Pot#	Description	Lipid C° (μg/g)	AreaC16:0/ AreaC18:0	$\delta^{13}C_{16:0}$ (‰)	$\delta^{13}C_{18:0}$ (‰)	$\Delta^{13}C$ (‰)	Assignment	Compound dated	Laboratory #	Conventional radiocarbon Age (BP) (mean ± 1SD)	Statistical consistency (χ^2 test, n=2 independent ^{14}C ages)
ROS-C-4644	Single sherd of a fine kumpf from pit 50, square H4, Rosheim "Sandgrube", Grossgartach	6064	0.4	-26.5	-28.9	-2.4	Ruminant adipose fats	$C_{16:0}$ $C_{18:0}$ **Combined**	BRAMS-1525.1.1 BRAMS-1525.1.2 **BRAMS-1525**	5,937 ± 33 5,926 ± 30 **5,931 ± 26**	* T′=0.0, T′(5%)=3.8, v=1
ROS-C-4648	Five refitted sherds of a coarse kumpf from pit 50, square J7, Rosheim "Sangrube", Grossgartach	1001	0.7	-27.0	-24.6	2.4	Ruminant adipose fats	$C_{16:0}$ ◊$C_{18:0}$	BRAMS-1544.1.1	5,815 ± 39	
ROS-C-4649	Single sherd of a coarse kumpf from pit 50, square K8, Rosheim "Sandgrube", Grossgartach	2596	1.1	-26.1	-28.6	-2.5	Ruminant adipose fats	$C_{16:0}/C_{18:0}$ $C_{16:0}$ $C_{18:0}$	BRAMS-1528.1.1 BRAMS-1534.1.1 BRAMS-1534.1.2	5,879 ± 35 5,702 ± 34 5,914 ± 41	X T′=20.1, T′(5%)=6.0, v=2
ROS-C-4657	Single sherds of a coarse kumpf from pit 50, Rosheim "Sandgrube", Grossgartach	1914	0.6	-26.8	-28.7	-0.8	Ruminant adipose fats	$C_{16:0}/C_{18:0}$ $C_{16:0}$ $C_{18:0}$ **Combined**	BRAMS-1524.1.1 BRAMS-1524.2.1 BRAMS-1524.2.2 **BRAMS-1524**	5,892 ± 32 5,855 ± 37 5,934 ± 34 **5,912 ± 28**	* T′=1.7, T′(5%)=6.0, v=2
ROS-C-4596	Single sherds of a coarse kumpf from pit 122, Rosheim "Laser", Grossgartach	973	1.2	-26.9	-29.6	-2.6	Ruminant adipose fats	$C_{16:0}$ $C_{18:0}$ **Combined**	BRAMS-1526.1.1 BRAMS-1526.1.2 **BRAMS-1526**	5,810 ± 30 5,798 ± 30 **5,804 ± 25**	* T′=0.1, T′(5%)=3.8, v=1
ROS-C-4600	Two refitted sherds of a coarse kumpf from pit 63, square 23 Rosheim "Mittelweg", Grossgartach	4163	0.7	-27.1	-29.4	-2.3	Ruminant adipose fats	$C_{16:0}$ $C_{18:0}$ **Combined**	BRAMS-1527.3.1 BRAMS-1527.3.2 **BRAMS-1527**	5,897 ± 36 5,909 ± 35 **5,904 ± 28**	* T′=0.1, T′(5%)=3.8, v=1
ROS-C-4622	Single sherds of a coarse kumpf from pit 200, square 25, Rosheim "Mittelweg", Rössen	1183	0.7	-27.8	-32.6	-4.8	Dairy fats	$C_{16:0}/C_{18:0}$	BRAMS-1529.1.1	5,809 ± 32	
ROS-C-4629	Two refitted sherds of a coarse kumpf from pit 200, square 6, Rosheim "Mittelweg", Rössen	2032	0.3	-28.9	-32.2	-3.2	Dairy fats	$C_{16:0}/C_{18:0}$	BRAMS-1533.1.1	5,763 ± 35	

* $C_{16:0}$ and $C_{18:0}$ conventional radiocarbon age statistically identical at the 5% significant level[33]

X $C_{16:0}$ and $C_{18:0}$ conventional radiocarbon age statistically different at the 5% significant level[33]

◊ refers to compound that generated target with a mass of C below 100 μg. For this study 200 μg blanks were prepared, and so these small targets cannot be reliably blank-corrected using them. They were measured, however, to assess whether the 100 μg cut-off was appropriate.

Fig. 3c of the manuscript shows the first part of a chronological model which combines the available radiocarbon dates with the revised seriation illustrated in Fig. 3b (main manuscript). This part of the model is equivalent to that defined by Denaire *et al.*[12] (fig 15), the second part of the model is identical to that shown in Denaire *et al.*[12] (fig 16). The revised model has good overall agreement (Amodel: 100). Three of the dates on absorbed lipids have good individual agreement in this model (*BRAMS-1527* (*Ros.MW63*), A: 98; *BRAMS-1526* (*Ros.L122*), A: 112; and *BRAMS-1524* (*Ros.S50)*, A: 90), although the fourth has slightly poor individual agreement (*BRAMS-1525* (*Ros.S50*), A: 46). It is possible that this single sherd is residual, although it could simply be a statistical outlier.

We have again investigated how far the reported results on the absorbed lipids would have to change before the indices of agreement in the model illustrated in manuscript Fig. 3c would identify them as inaccurate, by deliberately biasing each measurement to varying degrees. The results are summarised in Table s5.

On this basis we consider that it is likely that this model would identify any substantive inaccuracies in the new measurements, and that it is likely to be more sensitive to small biases than paired measurements on associated materials.

Table s5. Agreement indices for the combined lipid measurements deliberately biased as described in the text for the Middle Neolithic in Alsace (form of model illustrated in manuscript Fig. 3c); orange denotes poor agreement.

	Amodel	A			
		BRAMS-1524	BRAMS-1525	BRAMS-1526	BRAMS-1527
1 sigma bias younger	107	96	90	102	99
1 sigma bias older	72	34	10	122	50
2 sigma bias younger	103	115	88	73	126
2 sigma bias older	40	6	1	113	11
3 sigma bias younger	94	135	119	31	130
3 sigma bias older	30	4	1	105	6
4 sigma bias younger	77	112	136	6	108
4 sigma bias older	23	6	2	107	10

SI 5. Linearbandkeramik pottery in NW Europe

Radiocarbon measurements have been made on absorbed $C_{16:0}$ and $C_{18:0}$ fatty acids from 22 sherds of *Linearbandkeramik* (LBK) pottery (Meier-Arendt[42], Table s6). These come from sixteen features from nine sites which lay across the northern and western parts of the LBK oecumene. Twelve sherds produced results that pass the quality assurance criteria used in this study.

A model which simply incorporates the information that all these samples date to within the period of use of LBK ceramics is shown in ED Fig. 3. It has good overall agreement (Amodel: 88). It suggests that LBK pottery began to be used in *5385–5225 cal BC* (*95% probability; start LBK lipid*; ED Fig. 3), probably in *5350–5300 cal BC* (*38% probability*) or *5285–5235 cal BC* (*30% probability*), and that its use ended in *5210–5010 cal BC* (*95% probability; end LBK lipid*; ED Fig. 3), probably in *5205–5100 cal BC* (*68% probability*).

Formal chronological models are currently available for only some aspects of LBK pottery. Jakucs *et al.*[13] present three alternative models for the appearance of Formative and earliest (*älteste*) LBK ceramics in the western part of its distribution. The sherds sampled for absorbed lipids come from the Western and Eastern areas defined by Jakucs *et al.*[13] for their Model 3, and all belong to the period when LBK pottery occurred over wide areas of NW Europe. No sherds have been dated that are assigned to the Formative typological phase. We therefore compare the parameter *start LBK lipid* (ED Fig. 3) with the estimated dates for the start of the earliest (*älteste*) LBK ceramics in the Western area (*start earliest west:* ED Fig. 4) and Eastern area (*start earliest east:* ED Fig. 4) from Jakucs *et al.*[13] (Model 3). The dates on absorbed fatty acids have clearly provided comparable results, although the sherds sampled for fatty acids have not been restricted to those that can be allocated by typology to the earliest phase of LBK pottery, and so it is not unexpected that the estimated start date for the period when the lipids accumulated is generally a few decades later than the date estimates for the appearance of the first LBK ceramics in these regions. For the lipid analysis and dating, the samples have been taken from the earliest LBK ceramics (with dairy residues) on the sites sampled, whereas Jakucs *et al.*[13] confine their modelling to the earliest (*älteste*) typological phase of LBK pottery. The two models are not estimating the start of exactly the same period of past activity.

This is illustrated further by comparison with the estimated dates for the first LBK ceramics in Lower Alsace, where pottery of the earliest (*älteste)* typological phase does not occur, that have been derived from a model which combines the available radiocarbon dates with the seriation by correspondence analysis of the associated ceramic assemblages (Denaire *et al.*[12], figs 5, 8, and electronic supplementary material matrix 1). This model allows for a gradual appearance of LBK ceramics in Lower Alsace (using a flexible trapezium distribution[43]), so two parameters are relevant: *start start LBK IIb*, which estimates the date when the very first LBK pottery appeared in Alsace, and *end start LBK IIb*, which estimates the date when the tradition became fully established. These date estimates are again, clearly comparable with the date estimate for the first LBK pottery calculated only from the radiocarbon dates on fatty acids absorbed in sherds (ED Fig. 4).

These formal chronological models are so far available only for the LBK sequence in Lower Alsace[12], and for the first appearance of this pottery type in some areas of Northern Europe[13]. For this reason, currently it is not possible to compare the dates on the absorbed fatty acids with the dating of this pottery in the Paris Basin, in the Lower Rhineland, or in north-western Poland.

For this model we have investigated how far the reported results on the absorbed lipids would have to change before the key parameters discussed above differ substantively. Again, we have deliberately biased each measurement on absorbed lipids by varying degrees. In this case we examine the overlap of key parameters (ED Fig. 4). This application is, unsurprisingly, more sensitive to an older bias in the measurements, with the median of *start LBK lipid* (ED Fig. 4) falling earlier than the medians of the other comparable parameters considered here when ages are biased by 2σ. In contrast the median of this parameter does not fall after all the medians of the comparable parameters until ages are biased by 4σ (ED Fig. 4).

Table s6. Lipid concentration, stable isotope ratios (measured by gas chromatography-combustion-stable isotope ratio mass spectrometry[37]), conventional radiocarbon ages (as defined by Stuiver and Polach[32] and calculated according to Wacker *et al.*[31]) and statistical consistency (χ^2 test, n=2 independent ^{14}C ages on the $C_{16:0}$ and $C_{18:0}$ FAs) on lipids extracted from LBK pottery sherds. The assigned phases are from classic scheme LBK chronology (Meier-Arend[42]), Ensisheim “Ratfeld” (ENS, Alsace, France), Cuiry-lès-Chaudardes “Les Fontinettes” (CUI, Aisne, France), Königshoven 14 (KON, Rhineland, Germany), Geleen-Janskamperveld (GEL, Graetheide, The Netherlands), Maastricht-Klinkers (MAK, Heeswater, The Netherlands), Karwowo 1 (KAR, West Pomerania, Poland) and Ludwinowo 7 (LDW, Kuyavia, Poland).

Pot#	Description	Lipid C° (µg/g)	$AreaC_{16:0}$/ $AreaC_{18:0}$	$\delta^{13}C_{16:0}$ (‰)	$\delta^{13}C_{18:0}$ (‰)	$\Delta^{13}C$ (‰)	Assignment	Compound dated	Laboratory #	Conventional radiocarbon Age (BP)	Statistical consistency
ENS-C-5913	Single sherd (1106-TRC-9-4) of a coarse kumpf from pit 9, early LBK, ENS	1177	0.6	-27.3	-30.9	-3.6	Dairy fats	$C_{16:0}$ $C_{18:0}$ **Combined**	BRAMS-1915.1.1 BRAMS-1915.1.2 **BRAMS-1915**	6,345 ± 31 6,303 ± 31 **6,324 ± 26**	* T′=1.0, T′(5%)=3.8, v=1
ENS-C-5915	Single sherd (1106-TRC-9-11) of a coarse kumpf from pit 9, early LBK, ENS	771	0.8	-26.4	-29.6	-3.2	Dairy fats	$C_{16:0}$ $C_{18:0}$ **Combined**	BRAMS-1916.1.1 BRAMS-1916.1.2 **BRAMS-1916**	6,383 ± 32 6,314 ± 33 **6,348 ± 26**	* T′=2.3, T′(5%)=3.8, v=1
ENS-C-5934	Single sherd (1106-TRC-28-12) of a coarse kumpf from pit 28, early LBK, ENS	1647	1.0	-26.2	-29.7	-3.5	Dairy fats	$C_{16:0}$ $C_{18:0}$ **Combined**	BRAMS-1958.1.1 BRAMS-1958.1.2 **BRAMS-1958**	6,282 ± 30 6,258 ± 30 **6,270 ± 25**	* T′=0.3, T′(5%)=3.8, v=1
ENS-C-5940	Single sherd (1106-TRC-28-25) of a coarse kumpf from pit 28, early LBK, ENS	2082	0.6	-28.7	-30.9	-2.2	Ruminant adipose fats	$C_{16:0}$ $C_{18:0}$ **Combined**	BRAMS-2031.1.1 BRAMS-2031.1.2 **BRAMS-2031**	6,162 ± 33 6,239 ± 30 **6,206 ± 26**	* T′=3.0, T′(5%)=3.8, v=1
CUI-C-5708	Single sherd (158, 3847) of a coarse bowl from loam pit 25, final LBK, CUI	881	1.1	-26.6	-32.5	-5.9	Dairy fats	$C_{16:0}$ $C_{18:0}$ **Combined**	BRAMS-1917.1.1 BRAMS-1917.1.2 **BRAMS-1917**	6,252 ± 34 6,218 ± 36 **6,236 ± 27**	* T′=0.5, T′(5%)=3.8, v=1
CUI-C-5776	Single sherd (1119, 26888) of a coarse bowl from loam pit 378, final LBK, CUI	3531	0.6	-30.2	-33.6	-3.4	Dairy fats	$C_{16:0}C_{18:0}$	BRAMS-2020.1.1	6,142 ± 32	
CUI-C-5801	Single sherd (1247, 29295) of a coarse bowl from loam pit 386, final LBK, CUI	9886	0.8	-28.2	-33.3	-5.0	Dairy fats	$C_{16:0}$ $C_{18:0}$ **Combined**	BRAMS-2021.1.1 BRAMS-2021.1.2 **BRAMS-2021**	6,138 ± 30 6,134 ± 30 **6,136 ± 25**	* T′=0.0, T′(5%)=3.8, v=1
CUI-C-5735	Three refitted sherds (529, 13823) of a coarse bowl from loam pit 241, final LBK, CUI	3417	1.0	-29.1	-33.9	-4.8	Dairy fats	$C_{16:0}$ ◊$C_{18:0}$	BRAMS-1918.1.1 BRAMS-1918.1.2	6,138 ± 37	
KON-C-5594	Single sherd (77.162, 522-2) of a coarse kumpf from pit complex 522, late LBK, KON	531	0.6	-32.0	-34.4	-2.4	Ruminant adipose fats	$C_{16:0}$ $C_{18:0}$ **Combined**	BRAMS-2029.1.1 BRAMS-2029.1.2 **BRAMS-2029**	6,253 ± 29 6,298 ± 29 **6,276 ± 24**	* T′=1.2, T′(5%)=3.8, v=1
KON-C-5598	Single sherd (77.162, 522-2) of a coarse kumpf from pit complex 522, late LBK, KON	1023	0.8	-31.0	-35.1	-4.1	Dairy fats	$C_{16:0}$ $C_{18:0}$ **Combined**	BRAMS-2026.1.1 BRAMS-2026.1.2 **BRAMS-2026**	6,106 ± 34 6,139 ± 34 **6,123 ± 27**	* T′=0.5, T′(5%)=3.8, v=1
KON-C-5617	Single sherd of a coarse kumpf from pit 522, late LBK, KON	679	0.4	-28.5	-31.9	-3.4	Dairy fats	$C_{16:0}$ $C_{18:0}$	BRAMS-2023.1.1 BRAMS-2023.1.2	6,078 ± 39 6,213 ± 30	X T′=7.5, T′(5%)=3.8, v=1
GEL-C-3271	Single sherd of a fine kumpf (box 21) from pit 49015, early LBK, GEL	1260	0.5	-30.4	-33.5	-3.2	Dairy fats	$C_{16:0}$ ◊$C_{18:0}$	BRAMS-2027.1.1 BRAMS-2027.1.2	6,500 ± 33	
GEL-C-3276	Single sherd of a coarse kumpf (box 45) from loam pit 49015, early LBK, GEL	339	0.8	-31.8	-35.2	-3.4	Dairy fats	$C_{16:0}C_{18:0}$	BRAMS-1923.1.1	6,142 ± 33	
GEL-C-3298	Single sherd of a coarse kumpf (box 41) from pit 53010.04, early LBK, GEL	577	0.5	-29.0	-31.8	-2.8	Ruminant adipose fats	$C_{16:0}$ $C_{18:0}$ **Combined**	BRAMS-2032.1.1 BRAMS-2032.1.2 **BRAMS-2032**	6,188 ± 31 6,253 ± 29 **6,224 ± 25**	* T′=2.3, T′(5%)=3.8, v=1
GEL-C-3299	Single sherd of a coarse kumpf (box 41) from pit 53010.05, early LBK, GEL	2743	0.4	-30.0	-33.1	-3.1	Dairy fats	$C_{16:0}$ $C_{18:0}$	BRAMS-1924.1.1 BRAMS-1924.1.2	6,304 ± 32 6,444 ± 30	X T′=10.2, T′(5%)=3.8, v=1
MAK-C-3094	Single sherd (501) of a fine kumpf from pit 207, final LBK, MAK	7672	0.4	-27.8	-27.5	0.4	Non-ruminant adipose fats	$C_{16:0}$ $C_{18:0}$	BRAMS-2022.1.1 BRAMS-2022.1.2	6,002 ± 30 6,251 ± 29	X T′=35.6, T′(5%)=3.8, v=1
MAK-C-3099	Single sherd (501) of a coarse bowl from pit 207, final LBK, MAK	494	0.6	-29.0	-32.4	-3.4	Dairy fats	$C_{16:0}C_{18:0}$	BRAMS-1922.1.1	6,300 ± 37	
KAR-C-3636	Single sherd of a coarse kumpf from pit 47, trench 2A, LBK, KAR	3316	0.9	-26.0	-26.9	-0.9	Non-ruminant adipose fats	$C_{16:0}$ $C_{18:0}$ **Combined**	BRAMS-2028.1.1 BRAMS-2028.1.2 **BRAMS-2028**	6,176 ± 30 6,230 ± 30 **6,204 ± 25**	* T′=1.6, T′(5%)=3.8, v=1
KAR-C-3677	Two refitted sherds of a coarse kumpf from pit 43, LBK, KAR	1900	1.3	-26.4	-30.7	-4.3	Dairy fats	$C_{16:0}$ $C_{18:0}$ **Combined**	BRAMS-2025.1.1 BRAMS-2025.1.2 **BRAMS-2025**	6,255 ± 30 6,214 ± 32 **6,236 ± 26**	* T′=0.9, T′(5%)=3.8, v=1

KOP-C-2949	Full profile of a fine kumpf (242), pit 25B, LBK, KOP	548	2.4	-25.5	-29.4	-3.9	Dairy fats	◊$C_{16:0}$	BRAMS-1920.1.1	-	
LDW-C-2267	Single sherd (A/484) of a coarse kumpf from pit A49, middle LBK, LDW	323	0.5	-26.6	-29.2	-2.6	Non-ruminant adipose fats	$C_{16:0}$ $C_{18:0}$ **Combined**	BRAMS-2024.1.1 BRAMS-2024.1.2 **BRAMS-2024**	6,173 ± 36 6,179 ± 30 **6,177 ± 26**	* T′=0.0, T′(5%)=3.8, v=1
LDW-C-2272	Single sherd (A/26) of a coarse vessel from loam pit A49, middle LBK, LDW	1628	0.2	-25.7	-29.7	-4.0	Dairy fats	$C_{16:0}$ $C_{18:0}$	BRAMS-1919.1.1 BRAMS-1919.1.2	6,150 ± 33 6,283 ± 32	X T′=8.4, T′(5%)=3.8, v=1

* $C_{16:0}$ and $C_{18:0}$ conventional radiocarbon age statistically identical at the 5% significant level[33]

X $C_{16:0}$ and $C_{18:0}$ conventional radiocarbon age statistically different at the 5% significant level[33]

◊ refers to compound that generated target with a mass of C below 100 µg. For this study 200 µg blanks were prepared, and so these small targets cannot be reliably blank-corrected using them. They were measured, however, to assess whether the 100 µg cut-off was appropriate.

SI 6. Middle Pastoral Neolithic occupation at Takarkori rockshelter, Libya

The Takarkori rock shelter is an early to middle Holocene site in the Tadrart Acacus Mountains, SW Libya (ED Fig. 5).

The archaeological deposit is the result of repeated occupation of the most protected part of the shelter, a roughly rectangular surface c. 26 x 15 m (~400 m^2) of a settled area that must have reached over 2000 m[2; 14,44]. The stratigraphy is highly disturbed by recent Tuareg occupation[45] and by sin-depositional and ancient post-depositional phenomena, including the repeated use of the internal area of the shelter as burial site. A basic distinction between archaeological layers, can be made between those mainly represented by 'matrix' and those that are 'fixture' (*sensu* Biagetti and di Lernia 2013[14]), whose depositional histories differ strongly. Given the high rate of disturbance and the 'matrix' nature of the dominant type of layer called "organic sands" – incoherent loose sediments made of quartz grains and abundant organic material (e.g., plant remains, charcoal, bones) – the stratigraphic control of the archaeological features has been confirmed by a series of radiocarbon dates[14,29]. In particular, a series of samples have been dated associated with the Middle Pastoral occupation at Takarkori (Table s7).

The sherds analysed for this study all come from organic sands and show typical Middle Pastoral decoration (ED Fig. 6b)[46]: most usually APS (Alternate Pivoting Stamp) in the 'return' technique variant (TAK120, TAK443, and TAK1572), the APS impression with triangular dots (TAK420) and a sherd with rocker plain edge impression resulting in the fishnet pattern (TAK21). All the specimens are medium/thin walled (4 to 7 mm maximum thickness) with a general convex profile, probably deriving from simple globular/rounded bowls. Typologically the decorations outlined are all compatible with the chronological horizon of the long Middle Pastoral, and analogous specimens (for instance to TAK21 (rocker-plain-fishnet pattern)) all come from layers of the same chrono-cultural attribution. Decorations in the "return" technique are particularly diagnostic of this cultural period, as attested not only in the pottery assemblage from Tarkarkori, but also from other sites with similar ceramics (e.g., from the Uan Muhuggiag shelter assemblage, see Barich[47]).

Absorbed $C_{16:0}$ and $C_{18:0}$ fatty acids have been dated from five single decorated sherds of Middle Pastoral period type, all producing results that pass the quality assurance criteria adopted in this study (Table s8).

A model which incorporates these dates with those from other materials associated with the Middle Pastoral Neolithic at Takarkori has good overall agreement (Amodel: 102; ED Fig. 6d), and all five dates on absorbed fatty acids have good individual agreement (*BRAMS-2610* (*TAK443*), A: 101; *BRAMS-2609* (*TAK420*), A:100; *BRAMS-2608* (*TAK120*), A: 101; *BRAMS-1522* (*TAK21*), A: 100; and *BRAMS-1523* (*TAK1572*), A:98). It suggests that the Middle Pastoral period began there in *5290–4875 cal BC (95% probability; start Takarkori MP*; ED Fig. 6d), probably in *5105–4925 cal BC* (*68% probability*). This cultural period ended at Takarkori in *3930–3545 cal BC* (*95% probability; end Takarkori MP*: ED Fig. 6d), probably in *3865–3705 cal BC* (*68% probability).* The Middle Pastoral period on the site lasted for well over 1000 years (*1025–1645 years* (*95% probability; use Takarkori MP*; distribution not shown), probably for *1115–1385 years* (*68% probability*)).

Table s7. Reference conventional radiocarbon measurements (n=10) for the Middle Pastoral Neolithic at Takarkori.

Type of material	Context	Type of archaeological deposit	Laboratory #	Conventional radiocarbon age (BP)	$\delta^{13}C$ (‰)
charcoal	T-U23, FP 22	fixture (ash dump)	LTL-907A	5064 ± 55	-23.40
skin (sheep/goat)	Q-R28-29, layer 25	matrix (organic sands)	LTL-362A	5070 ± 35	-25.20
dung relict	R-S15-16, layer 330	matrix (organic sands)	UGAMS-10149	5170 ± 25	-23.10
bone collagen	U26, layer 25	matrix (organic sands)	UGAMS-01841	5340 ± 50	-7.60
bone collagen	V-Z25-26; layer 142	burial (human remains)	GX-31077	5600 ± 70	-12.80
seeds	SPOT 6715	matrix (organic sands)	UGAMS-8709	5610 ± 30	-11.40
seeds	SPOT 8126	matrix (organic sands)	UGAMS-8706	5660 ± 25	-11.20
coprolites	Q30, layer 25	matrix (organic sands)	LTL-367A	5980 ± 50	-26.00
enamel bioapatite (sheep/goat)	T27, layer 25	matrix (organic sands)	UGAMS-2852	5980 ± 70	-12.27
bone	V-Z25-26; layer 142	burial (human remain, H1)	GX-30324 (AMS)	6090 ± 60	-11.40

Table s8. Lipid concentration, stable isotope ratios (measured by gas chromatography-combustion-stable isotope ratio mass spectrometry[73]), conventional radiocarbon ages (as defined by Stuiver and Polach[32] and calculated according to Wacker *et al.*[31]) and statistical consistency (χ^2 test, n=2 independent ^{14}C ages on the $C_{16:0}$ and $C_{18:0}$ FAs) on lipids extracted from pottery vessels from Middle Pastoral Neolithic at Takarkori.

Pot#	Description	Lipid C° (µg/g)	$AreaC_{16:0}$/ $AreaC_{18:0}$	$\delta^{13}C_{16:0}$ (‰)	$\delta^{13}C_{18:0}$ (‰)	$\Delta^{13}C$ (‰)	Assignment	Compound dated	Laboratory #	Conventional radiocarbon age (BP)	Statistical consistency
TAK21	Single sherd with plain edge fishnet decoration (21) from layer 25, square T23, Middle Pastoral Neolithic	5830	1.6	-14.7	-20.5	-5.8	Dairy fats	$C_{16:0}$ $C_{18:0}$ **Combined**	BRAMS-1522.1.1 BRAMS-1522.1.2 **BRAMS-1522**	5,362 ± 33 5,331 ± 32 **5,348 ± 24**	* T′=0.5, T′(5%)=3.8, ν=1
TAK1572	Single sherd with APS return decorations (1572) from layer 245, square S33, Middle Pastoral Neolithic	3149	1.2	-23.7	-28.2	-4.5	Dairy fats	$C_{16:0}$ $C_{18:0}$ **Combined**	BRAMS-1523.1.1 BRAMS-1523.1.2 **BRAMS-1523**	5,099 ± 38 5,071 ± 32 **5,085 ± 24**	* T′=0.3, T′(5%)=3.8, ν=1
TAK120	Refitted sherds with APS return decorations (120) from layer 25, square U27, Middle Pastoral Neolithic	5593	1.5	-15.2	-18.7	-3.5	Dairy fats	$C_{16:0}$ $C_{18:0}$ **Combined**	BRAMS-2608.2.1 BRAMS-2608.2.2 **BRAMS-2608**	6,008 ± 35 5,949 ± 35 **5,979 ± 28**	* T′=1.4, T′(5%)=3.8, ν=1
TAK420	Single sherd with APS-triangles decoration (420) from layer 41, square T25, Middle Pastoral Neolithic	1119	0.6	-18.3	-21.5	-3.2	Dairy fats	$C_{16:0}$ $C_{18:0}$ **Combined**	BRAMS-2609.1.1 BRAMS-2609.1.2 **BRAMS-2609**	5,487 ± 34 5,498 ± 35 **5,493 ± 28**	* T′=0.1, T′(5%)=3.8, ν=1
TAK443	Single sherd with APS return decorations (443) from layer 41, square T29, Middle Pastoral Neolithic	17217	1.4	-16.9	-23.7	-6.8	Dairy fats	$C_{16:0}$ $C_{18:0}$ **Combined**	BRAMS-2610.1.1 BRAMS-2610.1.2 **BRAMS-2610**	6,021 ± 35 5,962 ± 35 **5,993 ± 28**	* T′=1.4, T′(5%)=3.8, ν=1

* $C_{16:0}$ and $C_{18:0}$ conventional radiocarbon age statistically identical at the 5% significant level[33]

APS: Alternate Pivoting Stamp

Sherd TAK1572, dates to the first quarter of the fourth millennium cal BC (*3960–3890 cal BC* (*42% probability; BRAMS-1523* (*TAK1572*) or *3880–3800 cal BC* (*53% probability*), probably to *3955–3925 cal BC* (*23% probability*) or *3875–3815 cal BC* (*45% probability*); ED Fig. 6d), and so falls almost at the end of the Middle Pastoral Neolithic occupation at Takarkori. This demonstrates the long duration of the "return" technique and exemplifies the utility of dating pottery directly using absorbed fatty acids. It also supports the need for more refined typological definitions to be obtained for such long lasting but culturally diagnostic types.

The compatibility of the dates on absorbed lipids with the dates on other samples types (Table s7) is illustrated in ED Fig. 7. The posterior density estimates for the start and end of Middle Pastoral ceramics at Takarkori clearly overlap, although the new dates refine the pre-existing model. We have again investigated how far the reported results on the absorbed lipids would have to change before these key parameters change substantively by deliberately biasing each measurement on absorbed residues to varying degrees. In this case we examine the overlap of key parameters (ED Fig. 7). As a test of accuracy, this case study is weak, as the number of dates in the model is very small given the duration of archaeological phase under consideration. The median value of *start Takarkori MP* only becomes earlier than those of the model calculated with the quoted errors (and without the lipid dates) when the lipid results are biased to older ages by 4σ. Similarly, *end Takarkori MP* only become later than the equivalent parameters when the lipid measurements are biased to younger ages by 4σ. This disparity is clearly visible on ED Fig. 7. This example does, however, demonstrate the feasibility of dating absorbed lipids in extremely arid and hot environments.

SI 7. Principal Place, Worship Street, London, UK

Excavations by Museum of London Archaeology at Principal Place, Worship Street, London Borough of Hackney (site code: PPL11) recovered four small, shallow, bowl-shaped pits [5371], [5375], [5377], and [5422]. A total of 298 sherds (weighing 6.1kg) of early Neolithic Plain Bowl and Decorated Bowl was recovered from these features, along with a further 50 sherds (weighing 325g) redeposited in a late Roman cremation burial [5373]. At least 28 separate vessels are represented. Ceramic analysis indicates that there are direct sherd linkages between pottery recovered from pits [5371] and [5377].

Absorbed $C_{16:0}$ and $C_{18:0}$ fatty acids have been dated from five sherds of Plain Bowl and one sherd from a plain cup, of which four vessels have provided results that pass the quality assurance criteria adopted in this study (Table s9). Two of these sherds (PPL012 and PPL015) come from pit [5375]. The combined results on these two sherds are not statistically consistent ($T'=23.6$, $T'(5\%)=3.8$, $\nu=1$[33]). The other two sherds (PPL020 and PPL021) come from pit [5422]. The combined results on these two sherds are also not statistically consistent ($T'=5.6$, $T'(5\%)=3.8$, $\nu=1$[33]). In pit [5422] the later date comes from the group of refitting sherds (PPL020), which suggests that at least some of the single sherds dated are reworked in the deposit from which they were recovered.

Whether the dated samples were reworked in the context from which they were recovered or not, all are on typologically distinctive vessels in the Plain Bowl tradition. The accuracy of the results on the absorbed fatty acids can therefore be assessed in relation to the currency of this type of ceramic in Southern Britain. A chronological model for this pottery is presented by Whittle *et al.*[15] (fig. 14.90), based upon the typological assessment of the ceramic assemblages presented in Whittle *et al.*[15] (table 14. 8).

Table s9: Lipid concentration, stable isotope ratios (measured by gas chromatography-combustion-stable isotope ratio mass spectrometry[73]), conventional radiocarbon ages (as defined by Stuiver and Polach[32] and calculated according to Wacker *et al.*[31]) and statistical consistency (χ^2 test, n=2 independent ^{14}C ages on the $C_{16:0}$ and $C_{18:0}$ FAs) on lipids extracted from pottery vessels from Principal Place (PPL11), London.

Pot#	Description	Lipid C° (µg/g)	$AreaC_{16:0}$/ $AreaC_{18:0}$	$\delta^{13}C_{16:0}$ (‰)	$\delta^{13}C_{18:0}$ (‰)	$\Delta^{13}C$ (‰)	Assignment	Compound dated	Laboratory #	Conventional radiocarbon Age (BP)	Statistical consistency (χ^2 test, n=2 independent ^{14}C ages)
PPL005	Single sherd of a plain bowl <P3> from pit 5370	4101	0.2	-28.9	-31.2	-5.0	Ruminant adipose fat	$C_{16:0}$	BRAMS-2477.1.1	4,624 ± 34	X
								$C_{18:0}$	BRAMS-2478.1.1	4,765 ± 30	T′=9.7, T′(5%)=3.8, v=1
PPL010	Two refitting rim sherds of a plain bowl <P11> from pit 5376	5127	0.3	-27.8	-28.1	-0.3	Non ruminant/ ruminant adipose fat	$C_{16:0}$	BRAMS-2616.1.1	4,716 ± 37	X
								$C_{18:0}$	BRAMS-2617.1.1	4,858 ± 33	T′=8.2, T′(5%)=3.8, v=1
PPL012	Single sherd of a plain bowl <P6> from pit 5374	713	0.6	-28.8	-31.1	-2.2	Ruminant adipose fat	$C_{16:0}$	BRAMS-2618.1.1	4,894 ± 34	*
								$C_{18:0}$	BRAMS-2619.1.1	4,928 ± 33	T′=0.5, T′(5%)=3.8, v=1
								Combined	**BRAMS-2618**	**4,911 ± 27**	
PPL015	Single sherd of a plain bowl (1845) from pit 5374	1999	0.3	+29.5	-31.4	-1.9	Ruminant adipose	$C_{16:0}$	BRAMS-2479.1.1	4,708 ± 33	*
								$C_{18:0}$	BRAMS-2480.1.1	4,771 ± 30	T′=2.0, T′(5%)=3.8, v=1
								Combined	**BRAMS-2479**	**4,742 ± 22**	
PPL020	Multiple refitting sherds of a plain bowl <P12> from pit 5421	3660	0.6	-30.0	-34.6	-4.6	Dairy fats	$C_{16:0}$	BRAMS-2483.1.1	4,628 ± 40	*
								$C_{18:0}$	BRAMS-2484.1.1	4,670 ± 34	T′=0.6, T′(5%)=3.8, v=1
								Combined	**BRAMS-2483**	**4,652 ± 26**	
PPL021	Single sherd of a plain cup <P13> from pit 5421	2985	0.2	-30.1	-32.9	-2.8	Ruminant adipose fat	$C_{16:0}$	BRAMS-2485.1.1	4,732 ± 32	*
								$C_{18:0}$	BRAMS-2486.1.1	4,734 ± 30	T′=0.0, T′(5%)=3.8, v=1
								Combined	**BRAMS-2485**	**4,733 ± 22**	

* $C_{16:0}$ and $C_{18:0}$ conventional radiocarbon age statistically identical at the 5% significant level[33]

X $C_{16:0}$ and $C_{18:0}$ conventional radiocarbon age statistically different at the 5% significant level[33]

ED Fig. 8 illustrates an updated version of this model, adding the results on the absorbed lipid samples from Principal Place. The prior distributions for Fir Tree Field Shaft (Whittle *et al.*[15], fig. 4.21), Etton Woodgate (Whittle *et al.*[15], fig. 6.36), Burn Ground (Whittle *et al*[15], fig. 9.25), Parc le Breos Cwm (Whittle *et al.*[15], fig. 11.13), Hazleton[48], and Ascott-under-Wychwood[49] have been recalculated by re-programming the models in OxCal v4.2[15] (and re-calculating them using IntCal13[26]. New dating programmes have been undertaken for Wor Barrow and the Coneybury Anomaly since the previous analysis, so for these sites the radiocarbon dates available in 2011 have been replaced by appropriate key parameters from the chronological models for those sites (Allen *et al.*[50], fig 12a for Wor Barrow, and Barclay *et al.*[51], fig 5 for the Coneybury Anomaly).

The recalculated model has good overall agreement (Amodel: 106; ED Fig. 8), and all four dates on absorbed lipids have good individual agreement (*BRAMS-2618* (*PPL012)*, A: 105; *BRAMS-2479 (PPL015)*, A: 107; *BRAMS-2483 (PPL020)*, A: 92; and *BRAMS-2485 (PPL021)*, A: 107).

The compatibility of the dates on absorbed lipids with the dates on other samples types (Table s9) is illustrated in ED Fig. 9. The posterior density estimates for the start and end of Plain Bowl ceramics in Southern Britain from the models including, or not including, the dates on absorbed lipids clearly overlap, although in this case the lipid dates do little to refine the pre-existing model. We have again investigated how far the reported results on the absorbed lipids would have to change before these key parameters change substantively by deliberately biasing each measurement on absorbed residues to varying degrees. In this case we examine the overlap of key parameters (ED Fig. 9) with visible disparity only when the lipid measurements are biased by 8σ. Clearly, as a test of accuracy, this case study is very weak, but it does demonstrate the utility of dating absorbed lipids residues in situations where no other datable material has been recovered.

SI 8. Conclusions

This study has considered the accuracy of 116 measurements on $C_{16:0}$ and $C_{18:0}$ fatty acids from 58 pottery vessels (Table s10). We have reported all the data generated for each case study, showing both the samples that were reliably dated and the ones which were not reliably dated to highlight the current limits of the method presented in this paper.

Table s10: Summary of ^{14}C results on absorbed fatty acids (n=116) considered in this study (statistically consistency has been assessed using the χ^2 test of Ward and Wilson[33] at a 5% significance level)

Site	Consistent groups	Inconsistent groups	Insufficient data	Failures
Somerset Levels	2	0	0	0
Çatalhöyük East	4	1	10	0
Alsace Middle Neolithic	4	1	3	0
LBK in NW Europe	12	4	5	1
Takarkori	5	0	0	0
Principal Place London	4	2	0	0

Statistically consistent replicate measurements were obtained on the $C_{16:0}$ fatty acids and the $C_{18:0}$ fatty acids separately from 31 vessels (Tables s1, 2, 4, 6, 8 and 9). The combined measurement on both fractions for each of these vessels has been compared to the other chronological information available for these archaeological sites using formal statistical methods. In all cases the results are compatible with the comparative information, although in four cases single sherds are likely to have been redeposited in the context from which they were recovered. This highlights the need to sample refitting groups of sherds wherever possible.

Statistically inconsistent results were obtained on the $C_{16:0}$ fatty acids and the $C_{18:0}$ fatty acids separately from eight vessels. We believe that this issue either arises from contamination after isolation (e.g. dust capture in the glass wool, graphite from the ferrule falling in the traps) or that one of the FA dates is simply a statistical outlier. Replicate radiocarbon measurements from the same vessel would probably resolve most of these issues, if they did not, then the disparity would probably be sample related (e.g. multiple source of C for the FAs; one having a reservoir effect).

Radiocarbon results could only be obtained from either the $C_{16:0}$ fatty acids, or the $C_{18:0}$ fatty acids, or both compounds combined from 18 vessels. We have no technical data to assess the accuracy of these individual measurements. In cases where one fatty acid produced less than 100 µg C, we considered the blank corrections to be unreliable due to differing sample and blank sizes (200 µg C blanks were analysed alongside samples in this study), and so there is effectively no second measurement by which the accuracy of the first may be assessed.

One vessel failed to produce sufficient fatty acid C ($C_{16:0}$ and $C_{18:0}$) for radiocarbon measurement.

We therefore highlight lipid concentration and size of sherds of being an important parameter for the success of the CSRA method. When size was not an issue 80% of the vessels that produced measurements on both fatty acids with amounts >100 µg C, successfully passed our internal criteria.

The compatibility assessments of ^{14}C measurements on pot lipids within existing chronologies revealed that the data generated is equivalent to more traditional dating methods in all of our case studies which supports the suitability of the methods presented in Casanova *et al.*[6] for the radiocarbon dating of archaeological pot lipids.

References

5 Casanova, E., Knowles, T. D. J., Williams, C., Crump, M. P. & Evershed, R. P. Use of a 700 MHz NMR microcryoprobe for the identification and quantification of exogenous carbon in compounds purified by preparative capillary gas chromatography for radiocarbon determinations. *Anal. Chem.* **89**, 7090-7098 (2017).

6 Casanova, E., Knowles, T. D. J., Williams, C., Crump, M. P. & Evershed, R. P. Practical considerations in high precision compound-specific radiocarbon dating: Eliminating the effects of solvent and sample cross-contamination on accuracy and precision. *Anal. Chem.* **90**, 11025-11032 (2018).

7 Evershed, R. P. et al. Chemistry of archaeological animal fats. *Accounts Chem. Res.* **35**, 660-668 (2002).

9 Coles, J. M. & Orme, B. J. Ten excavations along the Sweet Track (3200 BC). *Somerset Lev. Pap.* **10**, 45 (1984).

10 Hillam, J. et al. Dendrochronology of the English Neolithic. *Antiquity* **64**, 210-220 (1990).

11 Marciniak, A. et al. Fragmenting times: Interpreting a Bayesian chronology for the late Neolithic occupation of Çatalhöyük East, Turkey. *Antiquity.* **89**, 154-176 (2015).

12 Denaire, A. et al. The cultural project: Formal chronological modelling of the early and middle Neolithic sequence in Lower Alsace. *J. Archaeol. Method Th.* **24**, 1072-1149 (2017).

13 Jakucs, J. et al. Between the Vinča and Linearbandkeramik worlds: The diversity of practices and identities in the 54th–53rd centuries cal BC in Southwest Hungary and beyond. *J. World Prehist.* **29**, 267-336 (2016).

14 Biagetti, S. & di Lernia, S. Holocene deposits of Saharan Rock Shelters: The case of Takarkori and other sites from the Tadrart Acacus Mountains (southwest Libya). *Afr. Archaeol. Review.* **30**, 305-338 (2013).

15 Whittle, A. W. R., Healy, F. M. A. & Bayliss, A. *Gathering Time: dating the early Neolithic Enclosures of Southern Britain and Ireland.* (Oxbow Books, Oxford, 2011).

18 Bronk Ramsey, C. Bayesian analysis of radiocarbon dates. *Radiocarbon* **51**, 337-360 (2009).

21 Stott, A. W. et al. Radiocarbon dating of single compounds isolated from pottery cooking vessel residues. *Radiocarbon.* **43**, 191-197 (2001).

23 Berstan, R. et al. Direct dating of pottery from its organic residues: new precision using compound-specific carbon isotopes. *Antiquity.* **82**, 702-713 (2008).

26 Reimer, P. J. et al. IntCal13 and Marine13 radiocarbon age calibration curves 0–50,000 years cal BP. *Radiocarbon.* **55**, 1869-1887 (2013).

28 Dunne, J. et al. First dairying in green Saharan Africa in the fifth millennium BC. *Nature.* **486**, 390-394 (2012).

29 Cherkinsky, A. & di Lernia, S. Bayesian approach to ^{14}C dates for estimation of long-term archaeological sequences in arid environments: The Holocene site of Takarkori Rockshelter, Southwest Libya. *Radiocarbon.* **55**, 771-782 (2013).

31 Wacker, L, et al. Bats: A new tool for AMS data reduction, *Nucl. Instrum. Meth. B*, **268**, 976–979 (2010)

32 Stuiver, M., Polach, H.A., Discussion reporting of ^{14}C data, *Radiocarbon,* **19**, 355-363 (1977).

33 Ward, G K, and Wilson, S R. Procedures for comparing and combining radiocarbon age determinations: a critique, *Archaeometry*, **20**, 19–31 (1978)

34 Bronk Ramsey, C, Radiocarbon calibration and analysis of stratigraphy: the OxCal program, *Radiocarbon*, **36**, 425–30 (1995)

35 Stuiver, M, and Reimer, P J. Extended ^{14}C data base and revised CALIB 3.0 ^{14}C age calibration program, *Radiocarbon*, **35**, 215–230 (1993)

36 Bayliss, A, et al. Informing conservation: towards ^{14}C wiggle-matching of short tree-ring sequences from medieval buildings in England, *Radiocarbon*, **59**, 985–1007 (2017)

37 Copley, M S, et al. Direct chemical evidence for widespread dairying in prehistoric Britain, *P. Natl. Acad. Sci. USA.* **100 (4)**, 1524–1529 (2003)

38 Coles, B, and Coles, J, *Sweet Track to Glastonbury: the Somerset Levels in Prehistory*, (Thames and Hudson, London, 1986)

39 Coles, B, Somerset and the Sweet conundrum, in *Experiment and Design: Archaeological Studies in Honour of John Coles* (ed A F Harding), 163–9, (Oxbow, Oxford, 1999)

40 Smith, I F, The pottery, *Somerset Levels Papers*, **2**, 63–64 (1976)

41 Reimer, P J, et al. IntCal04 Terrestrial Radiocarbon Age Calibration, 0–26 cal kyr BP, *Radiocarbon*, **46**, 1029–58 (2004)

42 Meier-Arendt, W. *Die bandkeramische Kultur im Untermaingebiet* (Verein von Altertumsfreunden im Regierungsbezirk Darmstadt e. V., 1966).

43 Lee, S, and Bronk Ramsey, C, Development and application of the trapezoidal model for archaeological chronologies, *Radiocarbon*, **54**, 107–122 (2012)

44 Biagetti, S, et al. Decoding an Early Holocene Saharan stratified site: ceramic dispersion and site formation processes in the Takarkori rockshelter (Acacus Mountains, Libya), *J African Archaeol*, **2**, 3–21(2004)

45 di Lernia, S, and Tafuri, M A, Persistent deathplaces and mobile landmarks. The Holocene mortuary and isotopic record from Wadi Takarkori (SW Libya), *J Anthropological Archaeol.* **32**, 1–15 (2013)

46 Caneva, I. Pottery decoration in prehistoric Sahara and Upper Nile: a new perspective. In Barich, B.E. (ed.), *Archaeology and Environment in the Libyan Sahara. The Excavations in the Tadrart Acacus, 1978–1983* (British Archaeological Reports International Series 368, Oxford, 231–254, 1987).

47 Barich, B E, The Uan Muhuggiag rock shelter, in *Archaeology and Environment in the Libyan Sahara. The excavations in the Tadrart Acacus, 1978–1983* (ed B E Barich, BAR Int Ser, **368**, 97–112, Oxford (BAR) 1987)

48 Meadows, J, Barclay, A, and Bayliss, A. A short passage of time: the dating of the Hazleton long cairn revisited**,** *Cantab. Archaeol. J.* **17**, 45–64 (2007)

49 Bayliss, A, et al. One thing after another: the date of the Ascott-under-Wychwood long barrow, *Cantab Archaeol J*, **17**, 29–44 (2007)

50 Allen, M J, S. et al. *World Barrow, Cranborne Chase, Dorset: chronological modelling,* Historic England Research Report, **9/2016** (ISSN 2059-4453 Online, 2016)

51 Barclay, A, et al. *Dating the earliest Neolithic ceramics of Wessex,* Historic England Research Report, **63/2018** (2018)

```
Options()
 {
  Resolution=1;
  kIterations=20000;
 };
 Plot()
 {
  R_Combine("Sweet Track (3807/6 BC)")
  {
   R_Date("SW1: combined", 5110, 25);
   R_Date("SW2: combined", 5092, 26);
   R_Date("IntCal13: UB-1198", 5020, 23);
   R_Date("IntCal13: GrN-9024", 5058, 18);
   R_Date("IntCal13: QL-11528", 5083, 17);
  };
 };
```

```
Options()
 {
  Resolution=1;
  ConvergenceData=TRUE;
  kIterations=20000;
 };
 Phase()
 {
  Sequence( "TP Neolithic")
  {
   Boundary( "start TP Neolithic");
   Phase( "TP Neolithic")
   {
    Sequence( "TP spine")
    {
     Phase("B.81")
     {
      R_Date("UCIAMS-96505", 7430, 25);
     };
     Date("end B.81/start Sp.420");
     Sequence("Sp.420")
     {
      R_Date("Poz-40795", 7380, 60)
      {
      };
      R_Date("TP.M17", 7382, 31)
      {
       color="red";
      };
     };
     Date("end Sp.420/start B.74");
     After( "B.74")
     {
      R_Date("Poz-19000", 7539, 47)
      {
      };
      R_Date( "Poz-24010", 7790, 50)
      {
      };
      R_Date( "Poz-24011", 7090, 70)
      {
       Outlier();
      };
     };
     Date("end B.74/start B.72");
     Phase("B.72")
     {
      After("F.2867")
```

```
{
 R_Date( "Poz-24012", 7270, 50)
 {
 };
};
Sequence("")
{
 Phase("F.2888")
 {
  R_Date("Poz-40782", 7360, 50);
  R_Date("UCIAMS-96506", 7350, 25);
 };
 Phase()
 {
  Phase("17630")
  {
   R_Date("Poz-40796", 7310, 50)
   {
   };
   R_Date("TP.O23", 7340, 27)
   {
    color="red";
   };
  };
  Sequence()
  {
   Phase()
   {
    Phase("F.3182")
    {
     R_Date("Poz-40784", 7450, 50);
     R_Date("UCIAMS-96508", 7405, 25);
    };
    After("F.3141; unidentified charcoal")
    {
     R_Date("Poz-24009", 7700, 50)
     {
     };
    };
   };
   Phase( "F.1940")
   {
    R_Date("Poz-40785", 7410, 50);
    R_Date( "Poz-19007", 7440, 50);
    R_Date("UCIAMS-96509", 7430, 30);
   };
  };
 };
```

```
 };
};
Date("end B.72/start Sp.327");
Phase("Sp.327")
{
 R_Date("Poz-40793", 7250, 50)
 {
 };
 R_Date("Poz-40794", 7250, 50)
 {
 };
};
Date("end Sp.327/start B.73");
Sequence("B.73")
{
 After("residual")
 {
  R_Date("TP.P13", 7364, 25)
  {
   color="red";
  };
 };
 Phase("")
 {
  Phase("F.2854")
  {
   R_Date("UCIAMS-96507", 7310, 35);
   After("residual")
   {
    R_Date("Poz-40783", 7460, 50)
    {
    };
   };
  };
  R_Date("UCIAMS-96510", 7335, 25);
 };
};
Date("end B.73/start B.62");
After( "B.62")
{
 R_Date( "Poz-19006", 7280, 50)
 {
 };
 R_Date("UCIAMS-96511", 7445, 30)
 {
 };
 R_Date( "Poz-19005", 7460, 50)
 {
```

```
 };
};
Date("end B.62/start B.61");
Sequence( "B.61.1")
{
 After( "F.3132; unidentified charcoal")
 {
  R_Date( "Poz-13573", 7620, 50)
  {
  };
  R_Date( "Poz-19004", 7450, 50)
  {
  };
 };
 After("unidentified charcoal")
 {
  R_Date( "Poz-19001", 7430, 50)
  {
  };
 };
 Phase("F.1938")
 {
  R_Date("UCIAMS-96512", 7295, 25);
  After("residual")
  {
   R_Date("Poz-40789", 7450, 50)
   {
   };
  };
 };
};
Sequence( "B.61.3")
{
 After( "F.3135; unidentified charcoal")
 {
  R_Date( "Poz-13571", 7390, 40)
  {
  };
  R_Date( "Poz-19002", 7460, 70)
  {
  };
 };
 Phase()
 {
  After("F.1916; unidentified charcoal")
  {
   R_Date("Poz-13696", 7530, 50)
   {
```

```
    color="green";
   };
  };
  Phase("F.1918")
  {
   R_Date("Poz-40790", 7290, 50);
   R_Date("UCIAMS-96513", 7300, 25);
   R_Date("Poz-40792", 7270, 50);
   R_Date("UCIAMS-96514", 7335, 30);
  };
 };
};
Date("end B.61/start Sp.248");
Phase("Sp.248")
{
 R_Date( "Poz-13700", 7150, 50);
 Phase("articulated")
 {
  R_Date("UCIAMS-113462", 7025, 20);
  R_Date("UCIAMS-113461", 7175, 20);
 };
 After( "disarticulated")
 {
  R_Date( "Poz-13659", 7090, 50)
  {
  };
  R_Date( "Poz-19104", 6990, 40)
  {
  };
  R_Date( "Poz-19075", 7180, 40)
  {
  };
 };
};
Date("end Sp.248");
};
Sequence( "TP 2nd string")
{
Phase("B.103")
{
 R_Date("TP.N10", 7348, 25)
 {
  color="red";
 };
};
Phase("Sp.439")
{
 R_Date("UCIAMS-113459", 7265, 25)
```

```
    {
    };
   };
   After("Sp.431")
   {
    R_Date("Poz-18999", 7183, 55)
    {
    };
   };
   After("Sp.414")
   {
    R_Date("Poz-7451", 7190, 40)
    {
    };
    R_Date("Poz-7452", 7360, 50)
    {
    };
   };
   Phase("Sp.412")
   {
    R_Date("UCIAMS-113460", 7130, 20);
   };
   Date("end Sp.412/start B.33");
   Phase( "B33")
   {
    R_Combine("7878")
    {
     R_Date( "Poz-7449", 7100, 50);
     R_Date("UCIAMS-113463", 7145, 20);
    };
    After( "unidentified charcoal")
    {
     R_Date( "Poz-7450", 7210, 50)
     {
     };
    };
   };
   Date("end B.33");
  };
 };
 Boundary( "end East Mound occupation");
 Phase("Sp. 410")
 {
  R_Date("Poz-40788", 6870, 50);
  R_Date("Poz-40786", 6720, 40);
 };
};
Page( );
```

```
 Phase("summary")
 {
  Date("=end B.81/start Sp.420");
  Date("=end Sp.420/start B.74");
  Date("=end B.74/start B.72");
  Date("=end B.72/start Sp.327");
  Date("=end Sp.327/start B.73");
  Date("=end B.73/start B.62");
  Date("=end B.62/start B.61");
  Date("=end B.61/start Sp.248");
  Date("=end Sp.248");
  Date("=end Sp.412/start B.33");
  Date("=end B.33");
  Date("=end East Mound occupation");
 };
 Page( );
 Phase("durations")
 {
  Difference("use B.74", "end B.74/start B.72", "end Sp.420/start B.74");
  Difference("use B.72", "end B.72/start Sp.327", "end B.74/start B.72");
  Difference("use Sp.327", "end Sp.327/start B.73", "end B.72/start Sp.327");
  Difference("use B.73", "end B.73/start B.62", "end Sp.327/start B.73");
  Difference("use B.62", "end B.62/start B.61", "end B.73/start B.62");
  Difference("use B.61", "end B.61/start Sp.248", "end B.62/start B.61");
  Difference("use Sp.248", "end Sp.248", "end B.61/start Sp.248");
  Difference("use B.33", "end B.33", "end Sp.412/start B.33");
  Difference("gap B.33/Sp.248", "end Sp.248", "end B.33");
  Difference("gap B.81/B.61", "end B.62/start B.61", "end B.81/start Sp.420");
  Difference("gap Sp.327/Sp.248", "end B.61/start Sp.248", "end Sp.327/start B.73");
  Difference("gap fire continuity", "Poz-40792", "Poz-40784");
 };
 Order()
 {
  Date("=end B.33");
  Date("=end Sp.248");
 };
};
```

```
Options()
 {
  Resolution=1;
  kIterations=20000;
 };
 Phase()
 {
  Sequence("Alsace Middle Neolithic")
  {
   Boundary("start of HK")
   {
    Transition("duration start HK");
    Start("start start HK");
    End("end start HK");
   };
   Phase("Hinkelstein")
   {
    R_Date("Poz-33546 (Erst.2)", 5880, 40);
    R_Date("Poz-34074 (Entz.7056)", 5940, 35);
    R_Date("SUERC-60027 (Aldingen 2)", 5827, 29);
    R_Date("SUERC-60026 (Aldingen 7)", 5904, 29);
    Span("span HK");
   };
   Boundary("end HK/start GG");
   Phase("Grossgartach 2-5")
   {
    R_Date("OxA-27810 (Ling.42)", 5870, 32);
    R_Date("SUERC-46273 (Erst.7)", 5795, 31);
    R_Date("SUERC-46274 (Ros.85)", 5822, 31);
    R_Date("Poz-34077 (Entz.7105)", 5870, 40);
    R_Date("Poz-34091 (Entz.7112)", 5770, 40);
    R_Date("Poz-34073 (Entz.7043)", 5870, 40);
    R_Date("Poz-34083 (Entz.7126)", 5750, 40);
    R_Date("Poz-34081 (Entz.7121)", 5790, 50);
    Phase("KV.656")
    {
     R_Date("OxA-27811", 5848, 31);
     R_Date("SUERC-46517", 5786, 34);
    };
    R_Combine("Ros.45")
    {
     R_Date("OxA-27814", 5833, 29);
     R_Date("SUERC-46277", 5813, 31);
    };
    R_Combine("Ros.76")
    {
     R_Date("SUERC-46275", 5750, 28);
     R_Date("OxA-27812", 5865, 31);
```

```
 };
 R_Date("SUERC-46276 (Ros.89)", 5715, 31);
 R_Date("OxA-27813 (Ros.112)", 5845, 33);
 R_Date("Poz-34079 (Entz.7114)", 5920, 40);
 R_Date("Poz-34092 (Entz.7117)", 5890, 40);
 R_Date("Poz-34080 (Entz.7119)", 5790, 50);
 R_Date("Poz-34076 (Entz.7103)", 5810, 40);
 R_Date("Poz-34072 (Entz.7007)", 5840, 40);
 R_Date("Poz-34093 (Entz.7125)", 5760, 50);
 R_Date("ROSC4600", 5904, 28)
 {
 };
 R_Date("OxA-27816 (Ros.83)", 5898, 29);
 R_Date("SUERC-42679 (Ros.88)", 5775, 31);
 R_Date("OxA-27815 (Ros.91)", 5812, 30);
 R_Date("OxA-27817 (Ros.95)", 5847, 30);
 R_Date("SUERC-46283 (Ros.100)", 5772, 31);
 R_Date("SUERC-46278 (Ros.108)", 5769, 31);
 R_Date("Poz-34094 (Entz.7157)", 5830, 40);
 R_Date("Poz-34086 (Entz.7162)", 5800, 40);
 R_Date("SUERC-46435 (Ros.82)", 5802, 28);
 R_Date("OxA-27818 (Ros.87)", 5885, 31);
 R_Date("SUERC-46284 (Ros.111)", 5774, 31);
 R_Combine("Erst.19")
 {
  R_Date("OxA-27819", 5823, 30);
  R_Date("SUERC-46436", 5820, 33);
 };
 R_Date("OxA-27820 (Erst.28)", 5888, 31);
 R_Date("SUERC-46440 (Ling.37)", 5755, 31);
 R_Date("ROSC4596", 5804, 25);
 Phase("Grossgartach unknown")
 {
  Phase("Rosheim-Sandgrube, pit 50")
  {
   R_Date("ROSC4644", 5931, 26)
   {
   };
   R_Date("ROSC4657", 5912, 28)
   {
   };
  };
 };
 Span("span GG");
};
Boundary("end GG/start P-F");
Phase("Planig-Friedberg")
{
```

```
 R_Combine("Ros.5")
 {
  R_Date("OxA-27821", 5800, 31);
  R_Date("SUERC-46441", 5800, 30);
 };
 R_Date("SUERC-46442 (Ros.42)", 5762, 33);
 R_Date("OxA-30277 (Ober.4008)", 5809, 33);
 R_Date("SUERC-52378 (Ober.4015)", 5743, 30);
 R_Date("OxA-30278 (Ober.4022)", 5744, 33);
 R_Date("Poz-50940 (Gue.39", 5730, 50);
 Span("span P-F");
};
Boundary("end P-F/start RS");
Phase("Rossen")
{
 R_Date("SUERC-46443 (Ros.36)", 5753, 33);
 R_Combine("Ros.50")
 {
  R_Date("OxA-27973", 5803, 32);
  R_Date("OxA-27972", 5772, 35);
  R_Date("SUERC-46444", 5735, 32);
 };
 R_Combine("Ros.55")
 {
  R_Date("OxA-27822", 5804, 30);
  R_Date("SUERC-46445", 5731, 30);
 };
 R_Date("SUERC-52377 (Ober.4106)", 5697, 32);
 Combine("Entz.Tdc.17")
 {
  R_Date("GrA-45953", 5665, 40);
  R_Date("GrA-45797", 5660, 40);
 };
 Phase("Meist.116")
 {
  R_Date("SUERC-46450", 5649, 32);
  R_Combine("TOTL_RL_028")
  {
   R_Date("OxA-27823", 5749, 29);
   R_Date("SUERC-46446", 5686, 30);
  };
  After("possibly residual")
  {
   R_Date("Poz-32444", 5750, 70);
   R_Date("Poz-32445", 5690, 40);
   R_Date("Poz-32446", 5780, 50);
  };
 };
```

```
 After("Meist.113 (possibly residual)")
 {
  R_Date("Poz-33544", 5680, 50);
 };
 Span("span RS");
};
Boundary("end RS/start BI");
Phase("Bischheim & Brubach-Oberbergen")
{
 Phase("Bischheim (North Alsace)")
 {
  R_Combine("Schwin.10")
  {
   R_Date("OxA-30279", 5530, 32);
   R_Date("SUERC-52370", 5487, 32);
  };
  R_Date("SUERC-52371 (Schwin.552)", 5395, 29);
  Phase("Schwin.875")
  {
   R_Date("SUERC-52375", 5392, 32);
   R_Combine("TOTL_RL_80")
   {
    R_Date("OxA-30280", 5350, 32);
    R_Date("SUERC-52376", 5489, 31);
    R_Date("UBA-27378", 5307, 53);
   };
  };
 };
 Sequence("Lower Alsace")
 {
  Phase("Bischheim")
  {
   R_Date("SUERC-52397 (Entz.Tdc.722)", 5649, 30);
   Sequence("Ober.Schul.142")
   {
    After("Meist.113 (possibly old wood)")
    {
     R_Date("Poz-45620", 5610, 40);
    };
    R_Date("Poz-45612", 5600, 40);
    R_Date("Poz-45609", 5610, 40);
   };
  };
  date("end BI (Lower Alsace)/start B-O");
  Phase("Bruebach-Oberbergen")
  {
   R_Date("OxA-30019 (Duntz.3175)", 5430, 31);
   Phase("Duntz.3176")
```

```
  {
   R_Date("OxA-30053", 5536, 31);
   R_Date("OxA-30020", 5426, 33);
  };
  R_Date("SUERC-52398 (Vend.107)", 5524, 32);
  R_Date("SUERC-55323 (KV.509)", 5415, 31);
  After("Ober.Schul.27")
  {
   R_Date("Poz-45610", 5550, 40);
   R_Date("Poz-45614", 5630, 40);
   R_Date("Poz-45618", 5630, 35);
  };
  After("Ober.Schul.121")
  {
   R_Date("Poz-45611", 5640, 40);
   R_Date("Poz-45615", 5660, 40);
   R_Date("Poz-45762", 5640, 40);
  };
  After("Ober.Schul.167")
  {
   R_Date("Poz-45616", 5590, 40);
   R_Date("Poz-45621", 5610, 50);
  };
  Span("span B-O");
 };
 };
};
Boundary("end B-O/start BORS I");
Phase("BORS I")
{
 R_Date("OxA-30281 (Bisch.RdS.10)", 5338, 32);
 Phase("Bisch.RdS.12")
 {
  R_Date("SUERC-52399", 5277, 28);
  R_Combine("TOTL_RL_089")
  {
   R_Date("OxA-30282", 5273, 34);
   R_Date("SUERC-52400", 5391, 32);
  };
 };
 R_Date("SUERC-55321 (Bisch.RdS.31", 5274, 33);
 R_Date("SUERC-55322 (Bisch.RdS.38", 5361, 31);
 C_Date("Dambach 404", -4128, 5);
 C_Date("Dambach 556", -4147, 0.1);
 Span("span BORS I");
};
Boundary("end BORS I/start BORS II");
Phase("BORS II")
```

```
  {
   Phase("Geisp.14")
   {
    R_Date("UBA-27377", 5208, 52);
    R_Date("Poz-46043", 5260, 40);
   };
   Span("span BORS II");
  };
  Boundary("end of BORS")
  {
   Transition("duration end BORS II");
   Start("start end BORS II");
   End("end end BORS II");
  };
 };
 Difference("span BI (Lower Alsace)", "end BI (Lower Alsace)/start B-O", "end RS/start BI");
};
```

```
Options()
 {
  Resolution=1;
  kIterations=20000;
 };
 Plot()
 {
  Sequence("LBK lipids")
  {
   Boundary("start LBK lipid");
   Phase("LBK lipids")
   {
    Phase("France")
    {
     Phase("Cuiry-les-Chaudardes")
     {
      R_Date("CUI-C-5708", 6236, 27);
      R_Date("CUI-C-5801", 6136, 25);
     };
     Phase("Ensisheim")
     {
      R_Date("ENS-C-5913", 6324, 26);
      R_Date("ENS-C-5915", 6348, 26);
      R_Date("ENS-C-5934", 6270, 25);
      R_Date("ENS-C-5940", 6206, 26)
      {
       color="blue";
      };
     };
    };
    Phase("The Netherlands")
    {
     Phase("Geleen-Janskamperveld")
     {
      R_Date("GEL-C-3298", 6224, 25)
      {
       color="blue";
      };
     };
    };
    Phase("Germany")
    {
     Phase("Konigshoven 14")
     {
      R_Date("KON-C-5594", 6276, 24)
      {
       color="blue";
      };
```

```
    R_Date("KON-C-5598", 6123, 27);
   };
  };
  Phase("Poland")
  {
   Phase("Karwowo 1")
   {
    R_Date("KAR-C-3636", 6204, 25)
    {
     color="red";
    };
    R_Date("KAR-C-3677", 6236, 26);
   };
   Phase("Ludwinowo 7")
   {
    R_Date("LDW-C-2267", 6177, 26)
    {
     color="blue";
    };
   };
  };
 };
 Boundary("end LBK lipid");
};
Page( );
Order("invoke priors")
{
 Prior("start earliest east","/Model_3_start_earliest_east.prior");
 Prior("start earliest west","/Model_3_start_earliest_west.prior");
 Prior("end formative","/Model_3_end_formative.prior");
 Prior("start formative","/Model_3_start_formative.prior");
 Prior("Model_2_formative_earliest","/Model_2_formative_earliest.prior");
 Prior("start earliest south east","/Model_3_start_earliest_south_east.prior");
 Prior("Model_2_start_formative","/Model_2_start_formative.prior");
 Prior("Model_1_start_LBK","/Model_1_start_LBK.prior");
 Prior("end start LBK IIb","/end_start_LBK_IIb.prior");
 Prior("start start LBK IIb","/start_start_LBK_IIb.prior");
};
Page( );
Phase("earliest LBK")
{
 Phase("formative and earliest LBK in central Europe")
 {
  Phase("Model 1")
  {
   Date("=Model_1_start_LBK");
  };
  Phase("Model 2")
```

```
  {
   Date("=Model_2_start_formative");
   Date("=Model_2_formative_earliest");
  };
  Phase("Model 3")
  {
   Date("=start formative");
   Date("=end formative");
   Date("=start earliest south east");
   Date("=start earliest east");
   Date("=start earliest west");
  };
 };
 Phase("start LBK in Lower Alsace")
 {
  Date("=start start LBK IIb");
  Date("=end start LBK IIb");
 };
 Phase("LBK lipids")
 {
  Date("=start LBK lipid");
  Date("=end LBK lipid");
 };
};
};
```

```
Options()
 {
  Resolution=1;
  kIterations=20000;
 };
 Plot()
 {
  Sequence("Takarkori (Middle Pastoral)")
  {
   Boundary("start Takarkori MP");
   Phase("Middle Pastoral")
   {
    Phase("layer 41")
    {
     R_Date("BRAMS-2610 (TAK443)", 5993, 28);
     R_Date("BRAMS-2609 (TAK420)", 5493, 28);
    };
    Phase("layer 25")
    {
     R_Date("UGAMS-2852", 5980, 70);
     R_Date("LTL-367A", 5980, 50);
     R_Date("BRAMS-2608 (TAK120)", 5979, 28);
     R_Date("BRAMS-1522 (TAK21)", 5348, 24);
     R_Date("UGAMS-1841", 5340, 50);
     R_Date("LTL-362A", 5070, 35);
    };
    After("unidentified charcoal")
    {
     R_Date("LTL-907A", 5064, 55);
    };
    R_Date("GX-30324", 6090, 60);
    R_Date("UGAMS-8706", 5660, 25);
    R_Date("UGAMS-8709", 5610, 30);
    R_Date("GX-31077", 5600, 70);
    R_Date("UGAMS-10149", 5170, 25);
    R_Date("BRAMS-1523 (TAK1572)", 5085, 24);
   };
   Boundary("end Takarkori MP");
   Span("duration Takarkori MP");
  };
 };
```

```
Options()
 {
  Resolution=1;
  kIterations=20000;
 };
 Plot()
 {
  Sequence("plain Bowl")
  {
   Boundary("start plain Bowl");
   Phase("plain Bowl in S Britain")
   {
    Phase("Wor barrow")
    {
     Prior("start_wor_barrow","/start_wor_barrow.prior");
     Prior("end_wor_barrow","/end_wor_barrow.prior");
    };
    Phase("Staines Road Farm")
    {
     Prior("OxA_4057","/OxA_4057.prior");
     Prior("OxA_4058","/OxA_4058.prior");
    };
    Before("TAQ Parc le Breos Cwm")
    {
     Prior("end_Parc_le_Breos_Cwm","/end_Parc_le_Breos_Cwm.prior");
    };
    After("TAQ Padholme Road, Fengate")
    {
     R_Date("GaK-4197", 4527, 50);
    };
    Phase("Hazleton")
    {
     Prior("construction_finished_Hazleton","/construction_finished_Hazleton.prior");
     Prior("end_Hazleton","/end_Hazleton.prior");
    };
    Phase("Gatehampton Farm")
    {
     After("TPQ")
     {
      R_Date("GrA-31358", 4890, 40);
     };
     Before("TAQ")
     {
      R_Date("BM-2835", 4360, 45);
     };
    };
    After("TPQ Gorhambury")
    {
```

```
 R_Date("HAR-3484", 4810, 80);
};
Phase("Fir Tree Field shaft")
{
 Prior("OxA_8009","/OxA_8009.prior");
};
Phase("Eynesbury")
{
 R_Date("NZA-14576", 4743, 60);
};
Phase("Etton Woodgate")
{
 Prior("start_Woodgate","/start_Woodgate.prior");
 Prior("end_Woodgate","/end_Woodgate.prior");
};
Phase("Coygan Camp")
{
 R_Date("NPL-132", 5000, 95);
};
Phase("Coneybury anomaly")
{
 Prior("Start_Coneybury_Anomaly","/Start_Coneybury_Anomaly.prior");
 Prior("End_Coneybury_Anomaly","/End_Coneybury_Anomaly.prior");
};
Phase("Cherhill")
{
 R_Date("BM-493", 4715, 90);
};
Before("TAQ Burn Ground")
{
 Prior("end_Burn_Ground","/end_Burn_Ground.prior");
};
After("TPQ Broom Heath")
{
 R_Date("BM-756", 4523, 67);
 R_Date("BM-757", 4579, 65);
};
Phase("Ascott-under-Wychwood")
{
 Prior("primary_construction_Ascott","/primary_construction_Ascott.prior");
 Prior("end_Ascott","/end_Ascott.prior");
};
Sequence("London: PPL11")
{
 Boundary("start PPL11");
 Phase("Principal Place")
 {
  Phase("pit [5375]")
```

```
     {
      R_Date("PPL012", 4911, 27);
      R_Date("PPL015", 4742, 22);
     };
     Phase("pit [5422]")
     {
      R_Date("PPL020", 4652, 26);
      R_Date("PPL021", 4733, 22);
     };
    };
    Boundary("end London PPL11");
   };
  };
  Boundary("end plain Bowl");
 };
};
```

	S001a05	M092	S001a2b	S003a2c	SA02	S072a38	I001a2c	M095	M068	M094	I009a7a	M093	ES02a04	SA21	S003a9a	M063
H02	1	1														
H100	1	1			1							1			1	
H03	1	1	1	1	1			1								
G35lb						1		1						1		
G31t33																
G13							1									
G76d				1	1			1							1	
G88a					1			1	1			1			1	
G14st11														1		
G37t48								1								
Oberschaef310		1			1			1		1		1				1
G101t52												1				
G100t7126																
G48f1912																
G46t085																
G02								1	1					1		
G46MA77											1			1		
G43st508								1					1			1
G16t07																
G46SGE																1
G35I												1				
G35b13																
G100t7112												1				
G08A		1										1		1		
G100t7043																
G100t7121																
G35bIV																
G31t42																

G46SG50D																
G32st08A																
G30ptl																
G31t12																
G43st498								1								
G100t7174																
G32st64															1	
G24f02																1
G42t1																
G43st494												1				
G100t7114																
G100t7105																
G43f132B																
G32g1A																
G16fd1																
G46SG93																
G32st15												1				
G32st27A																
G46t098																
G100t7125																
G46t117																
G32g1B																
G20																
G43st398																
G31t28																
G46G50B																
G46t107																
G31t06																
G31t09																

G46G50C																
G31t13																
G46Hstah																
G46SG50F																
G46t112																
G46MA63																
G46t084																
G32st12															1	
G46t003																
G46pt02																
G31t44																
G56st54A														1		
G12ptIV																
G46t025																
G46t039																
G46t058																
G46t105															1	
G55A																
G100t7117																
G46t044																
G46t076																
G100t7007																
G32st24																
G100t7119																
G46t102																
G18ptIII																
G31t05																
G46t089																
G46t068																

G46t078																
G31t17																
G32st44																
G31t36																
G46t007																
G46t045																
G100t7103																
G46t002																
G46t090																
G46t095																
G46t119																
G46t088																
G46t026																
G46t115																
G46t091																
G46t008																
G46pt06																
G46t108																
G46t092																
G46t200																
G100t7157																
G16t03																
G46SG50A																
G46SG50I																
G46t028																
G16t22																
G100t7162																
G09																
G55C																

G46t110																
G46t083																
G33ssind																
G46t034																
G46pt01																
G46t118																
G46t027																
G16t05																
G46t024																
G46t114																
G46t099																
G46t113																
G46t073																
G46t062																
G46t074																
G46SG50G																
G46t100																
G46t101																
G46t077																
G16t28																
G46t116																
G46pt05																
G46t023																
G46t081																
G46L172																
G46t067																
G46t059																
G46t087																
G46t009																

G46L122																
G31t37																
G46pt04																
G46t082																
G46t063																
G46t071																
G46t043																
G37ptl																
G46t202																
G17																
G28																
G46t111																
G46t28																
G100t7179																
G100t7049																
G16t01																
G46t096																
G16t19																
Ober422																
G46R303																
G74																
G65st55																
Ober4008																
G46t042																
G101t35																
G81C																
G101t39																
Ober4015																
G81D																

G46t005																
R08																
R05																
R15MB300																
R100st114																
R10																
R15t55																
R15L4																
R100st116																
R16																
R03																
R100st113																
R15L59																
R15t36																
R04																
R15MB200																
R100st200																

I105a57	EM35	EM31	M098	M072d	SA05	M091	SB25	S009a03	M052	EM29a55	M103	S006a01	SA26	SB09	SA25	I009a10	EM02a2a	M100
	1									1			1					
1		1								1								
	1	1			1													
	1			1								1						
	1		1							1								
1	1	1			1					1								
		1		1	1					1								
			1		1					1			1					
			1							1				1				
			1															
										1								
	1		1							1								
		1	1				1											
			1							1								
					1			1					1					
	1	1	1							1								
	1					1				1			1			1		
	1		1				1			1	1							
													1					
					1		1											
						1				1								
			1	1	1				1				1					
													1					
	1	1	1							1								
		1					1			1					1	1		1
		1																

													1					
													1					
		1	1		1						1							
		1		1														
					1	1		1										
															1			
			1														1	
		1	1						1	1				1	1	1		1
							1						1					
										1								
										1								1
		1																
										1								
				1														
	1	1	1								1		1					
						1		1										
		1								1								
													1					

				1														
										1								
		1			1													
	1															1		
					1					1								
														1				
													1					
	1																	
													1					
							1											
	1									1								
					1					1								
					1													
										1								
										1								

										1								
	1																	
												1						
													1					
													1					

1

1																		
			1															
										1								

M050	SB01a55	M040	I004a2b	EM02a2b	M009	S009a10	SA09	EM37	SB10	M001	EM03a09	F001	M045	EM17	S003a04	M102	EM39
										1							
								1									
							1										
				1													
												1					
					1												
				1		1											
															1		1
										1							
								1							1		
								1							1		
1								1							1		
			1												1		
	1											1					
															1		
		1		1				1							1		
	1			1				1			1						
					1			1							1		
1	1	1						1							1		1
								1									
								1				1	1				
1	1																

								1							1		
											1			1	1		
						1											
1	1			1				1	1								
								1	1			1			1		
								1									
1	1	1												1	1		
	1						1										
								1							1		
														1	1		
								1		1					1		
1																	
															1		
	1																
								1									
								1		1					1		
1									1								
								1									
																1	
															1		1
					1										1		
1				1			1	1							1		
															1		
	1						1										
							1								1		
				1				1	1								
													1		1		

	1																
								1									1
					1			1							1		
	1			1				1									
												1					
								1		1					1		
							1										
			1												1		
1															1		
															1		
								1									
							1					1					
								1									
					1					1							
		1															
															1		1
															1		
														1			
															1		
											1						
															1		
								1									

															1		
								1							1		
																	1
								1									
															1		
						1											
															1		

												1					
								1									

				1													
										1							

M083	EM09-014	ES17	SA10	I003a08	SB01a59	SB26	I105a55	M047	SB11	M057	M024	I003a03	EM16a2b	M034	M041	M003	S004a04
							1										
				1													
			1														
1																	
			1						1								
				1								1					
						1											
												1					
1	1			1									1				
1																1	
			1	1												1	
1			1	1								1					
1	1																
												1					

1																	
		1		1													
	1												1				
	1		1									1				1	
1																	
				1						1							
1	1																
				1													
1																	
1						1											
																1	
1			1														
1	1											1					
																1	
				1													
				1	1	1							1				1
				1				1									
				1													
1			1														
1			1	1									1				
												1				1	

					1						1						
														1	1		
	1												1	1	1	1	
			1					1									
	1									1						1	
		1	1														
1			1	1													
						1											
												1					
1																	
1						1											
																1	
1																	
1																	
	1															1	
1																	
			1	1						1							
						1											
												1	1				

				1			1										
			1														
																	1
							1						1				
													1				
						1											
1																	
1																	
				1													
	1																
			1														
															1		

													1				
									1							1	
												1					
				1													
			1	1													

																1	
				1			1										
												1					

F005	I105a59	EM29a63	SA07	EM02a04	I003a9a	I002a2b	SA27	I004a9a	SB27	M042a25	M211	M084	SB28	SA28	M005	EF16	SA11	EM05
					1	1												
					1													
				1	1													
					1													
					1													
					1													
						1												
					1	1												
					1		1						1	1				
						1		1										
					1													
						1							1					
								1										
	1				1		1											
1		1			1	1	1										1	
						1												
1					1	1	1											
						1								1			1	

					1													
			1						1									
					1	1												1
					1				1					1			1	1
					1	1								1			1	1
					1													1
					1				1									1
		1			1									1				
					1													
					1	1												
					1													
									1					1				
					1												1	
													1					
						1								1				
					1													
																		1
					1				1									
					1													
					1													
						1												
	1				1													
				1	1		1		1	1				1			1	
					1	1		1					1					
					1	1								1	1			
					1													
														1				
													1	1				
				1														1

					1													
					1													
					1								1	1				1
1								1				1		1				
					1			1										1
					1				1				1	1	1			
	1			1	1				1				1				1	
					1		1		1								1	
							1											
					1		1		1				1	1				1
1					1								1	1			1	
					1													
							1									1		
						1	1		1				1					
					1		1						1	1				
1																		
					1													
					1									1				
			1			1						1	1	1	1	1		
									1								1	1
			1		1	1												
					1						1							1
1								1	1				1	1				
					1	1			1					1			1	
							1											
					1								1					
					1							1						

							1											
					1													1
					1		1											
								1										1
					1							1	1					
					1				1				1	1				1
					1											1		
						1												
					1													
					1													
					1								1					
					1				1					1				
			1			1												
					1				1					1	1			
							1											
					1													
																		1
																	1	
															1		1	
										1							1	1
													1	1			1	
								1										
					1													
					1	1												

					1	1												
					1									1				
														1				
													1					
								1									1	
					1													
					1		1							1				
					1								1	1				
					1								1					
																	1	
1					1												1	
					1													
														1				
	1				1	1	1		1									
					1													
						1								1				

					1	1	1	1	1					1				1
					1													1
					1				1									
					1	1												
																	1	
					1	1												
		1			1	1												1
					1	1												1
					1								1	1				
				1														
						1												

M085	I001a03	F003	M042a14	S005a03	M046	I007a9a	S003a2b	S005a04	F037a13	S005a2b	I009a9a	EM01a63	SA29	M077	S007a04
				1											
							1								
							1								1
							1								
				1			1			1					
							1								
															1
	1														
								1							
	1														
	1														
								1							
								1							
							1								
				1		1	1	1							
								1							

															1
								1			1				
		1													
										1					
								1							
	1	1	1					1		1					1
								1							
				1											
		1						1							
								1							
	1														
								1							
								1							
								1							
1															
		1	1	1			1	1		1			1		
				1											
								1							
		1													1
		1					1								

								1							
								1							
													1		
								1			1				
1							1	1					1		1
				1			1	1							
								1							
						1	1	1		1	1		1		
		1			1			1							
							1								
		1	1	1			1	1			1		1		
								1					1		
		1						1							
1															
			1				1								
								1				1			
		1					1	1					1		
								1							
		1						1							
							1	1					1		
		1		1				1					1		
								1					1	1	
				1						1					
				1				1			1				
						1									
		1	1									1	1		
								1	1				1		

										1					
			1					1			1		1		
								1							
	1						1	1							
		1						1							
								1					1		
								1							
				1					1			1			
1															
													1		
				1								1		1	
		1						1							1
								1					1		
								1	1						
					1										
								1							
				1											
								1					1		
															1
								1							
								1							
								1					1		
															1
								1					1		
				1											
								1							

		1						1							
							1						1		
								1			1				
								1							
													1		
										1					
				1											
													1	1	
								1							
										1					
								1							
						1									
							1						1		
1				1				1					1		
								1							
										1					
				1							1		1		
								1							1
	1							1							
			1					1					1		1
															1
				1											
				1											1
	1							1							
				1				1				1			
								1					1		
								1							

	1	1	1	1		1		1					1		1
								1							
															1
								1							
															1
											1				
				1				1					1		
										1					
								1			1				1
		1						1							
		1													1
								1							
	1														

										1					
							1								
							1								
							1								
							1								
								1							

M044a32	S007a2b	M044a25	M007	EM30	M087	SA30	EI16	I001a2b	S003a03	EF02	I002a2a	S005a9a	S006a04	EM02a03	EM20	F037a15
									1							
														1		
									1							
												1				
														1		
														1		
			1			1							1	1		
									1							
								1								

														1		
					1											
									1				1			
										1						
								1					1	1		
														1		
									1							
									1							
	1															
							1									
													1			
							1							1		
														1		
														1		
					1									1		
													1	1		
													1			
													1			
								1							1	

													1	1		
								1						1		
														1	1	
														1		
				1				1						1		
1						1			1							
			1													
														1		
		1														
						1										
									1					1		
							1							1		
														1		
															1	
														1		
		1				1								1		
									1					1		
														1		
			1									1		1		
														1		
						1							1			

									1					1		
							1									
														1		
														1		
1						1					1		1	1		
					1											
						1				1				1		1
														1		
									1					1		
					1								1			
												1		1		
						1										
														1		
														1		
												1		1		
						1										
		1												1	1	
														1		
														1		
						1								1		

														1		
														1	1	
						1										
						1								1		
		1														
								1								
														1		
														1		
								1								
		1				1										
													1	1		
															1	
								1								
														1		
							1							1		
						1								1		
													1	1		
															1	
														1		
						1							1	1	1	
						1								1		
														1		
	1	1				1										
	1					1								1		
			1											1		
														1		
1						1								1		
						1	1									

						1					1			1	1	
														1	1	
								1						1		1
						1								1		
				1												
									1					1		
								1						1		
					1					1				1		
									1					1		
										1				1		
												1		1	1	
														1		
			1		1							1		1		
														1		
							1							1		

													1			
									1					1		
									1				1			
														1		
								1						1		
														1		
													1			
									1							

EM24	M037a14	SB29	EM16a03	EM19	F002	I001a04	I005a04	SB30	I003a10	I005a9a	M037a32	S005a01	I004a03	F009	EM02a2c	M044a14
			1													
									1							
						1										
						1										

	1															
			1			1				1						
	1			1												
															1	
															1	
			1								1					
			1													
			1													
															1	
	1		1													
	1															

															1	
	1															
	1			1												
								1								
	1		1												1	
			1							1						
							1								1	
															1	
	1		1			1									1	
					1										1	
										1					1	1
															1	
															1	
	1		1													
		1		1				1		1					1	
	1			1												
	1									1					1	
	1			1		1										
1										1	1					
	1			1						1						1
	1		1													
					1											

																1
	1					1										
											1				1	
	1			1												
	1															
	1															1
															1	
						1										
			1												1	
	1			1											1	
	1			1												
	1															1
	1															
	1		1	1											1	
			1													
	1														1	
	1			1												
		1		1							1				1	
				1						1					1	
			1												1	1
	1			1												
	1	1						1								
			1												1	1
	1															

				1											1	1
															1	
															1	1
	1												1			
	1															
										1						
	1														1	
			1													
	1															
	1			1											1	
	1		1		1										1	
											1					
	1															
	1											1			1	1
	1	1													1	
	1		1			1								1		
	1	1						1		1			1		1	
			1													1
	1				1										1	1
			1													1
	1			1				1							1	1
	1	1	1					1		1						1
	1		1													
1	1		1												1	
	1		1	1									1		1	
	1														1	
								1							1	
	1	1	1	1											1	
	1		1													

1	1	1	1	1			1	1							1	1
	1			1											1	
	1															
	1															
	1															1
	1				1						1				1	
															1	
			1	1											1	
	1		1	1												
	1			1		1	1			1					1	1
	1		1	1												1
				1	1											1
	1														1	
	1			1												
				1				1								1
				1											1	1
	1									1					1	
															1	
										1						
										1						
									1						1	

	1		1												1	
						1					1					
															1	
	1		1													
						1										
			1													
															1	

M037a30	I003a2b	I002a03	SB32	S011a03	EI02	I001a2a	M105	I002a04	EM03a07	S007a9a	F037a14	SB40	SA32	EM16a2c	SA40	EM06
	1															
						1										

	1															

		1						1								
																1
														1		
								1								
														1		
				1												
														1		
																1
						1										
													1			
								1						1		
		1														

														1		
			1								1					
													1	1		
1						1										
		1								1			1			
			1							1						
													1			
								1								
													1			
								1								
								1								
														1		
						1										

													1	1		
1																
		1														
		1														
			1													
								1						1		
	1													1		
			1										1			
		1														
														1		
				1								1		1		
					1											
			1	1									1			
1																
		1											1			
													1			
			1				1						1	1		
				1					1				1			
		1														
	1														1	1
		1				1		1					1			1
		1	1			1							1	1		
			1										1			
				1								1	1			
			1		1				1							

1		1					1	1	1	1		1			1	
		1														
			1									1	1			
						1										
			1	1									1			
						1						1	1			
				1									1	1		
		1		1		1		1			1		1	1	1	
1						1										
		1									1		1			
			1										1			
													1			
		1														
								1								
								1		1			1			
													1			
								1								

														1		
														1		
														1		
						1										1
	1															

EM01a55	EM01a68	M044a15	F027	S007a03	I007a03	S011a2b	I005a03	S001a01	Es02a2b	M044a13	S037a15	M037a13	I003a04	I013

								1						
							1							

											1			
												1		
											1			

												1		
											1			
							1							
									1					

				1									1	
				1										
							1							
									1					
				1										
							1							
							1							
									1					
			1											
				1						1				
				1						1	1			
											1			
												1		
													1	

1	1			1			1				1	1		
							1							
				1										
		1												
							1	1						
				1			1					1		
									1					
1	1	1		1	1		1				1	1	1	
						1								1
			1											
												1		1
												1		
							1							
									1					
				1										
										1	1	1		
											1			
												1		
													1	

				1					1		1	1		
											1			
							1	1						
							1							

EM03a03	S001a04	S013a9a	F004	S011a04	ES16a2b	I007a04	EM16a04	ES16a03	I004a04	M037a16	S013a04	M081	ES16a2c	M011	S013a03

									1						
												1			
									1						

						1									

		1						1							
								1							
1															
					1										
1										1					
1															
					1				1						
							1				1				
												1			

			1										1		
		1			1										
									1						
								1							
				1											
															1
								1							
						1					1			1	
								1							1
								1					1		
															1
	1	1			1										
									1			1			
											1				1
							1								
														1	1
		1	1	1					1				1	1	
1															1
					1										1
		1						1		1					1
							1							1	
								1		1					
													1		
													1		
									1			1			1

												1			1
1															
												1			
						1		1							
					1										
											1				
									1						
								1							
									1						

M013	S037a14	S037a30	M037a36	S037a22	ES02a03	M037a25	M037a22	M059	ES02a2c	S008a04	M037a24	M072a	I006a04	M060	S037a36

						1									
						1									
													1		

					1	1					1				
	1														
					1										
						1									1
			1		1										
					1										
	1				1				1						
					1										
						1									
										1					
1															
												1			
	1	1						1	1			1			
					1										
					1										
					1										
	1				1										
				1					1						
				1			1		1						

					1							1		1	
						1									
						1						1		1	
					1										
			1		1	1				1				1	
						1				1			1	1	
					1	1		1	1					1	1
	1				1	1			1				1	1	
									1		1				1
												1			
					1	1				1		1	1	1	1
												1			
					1						1				1
					1	1								1	1
					1	1							1		

M075	M076	M073	S037a13	I005a2b

	1			
		1		
1				
			1	
1				
			1	
	1	1	1	
1				
	1		1	
		1	1	
				1
1	1	1	1	1
			1	